

AD-A069 070

BARBER-NICHOLS ENGINEERING CO ARVADA COLO

F/G 21/3

MECHANICAL INTERFACE FOR AN ELECTRIC PROPULSION TEST BED.(U)

FEB 79 R W BLAKEMORE

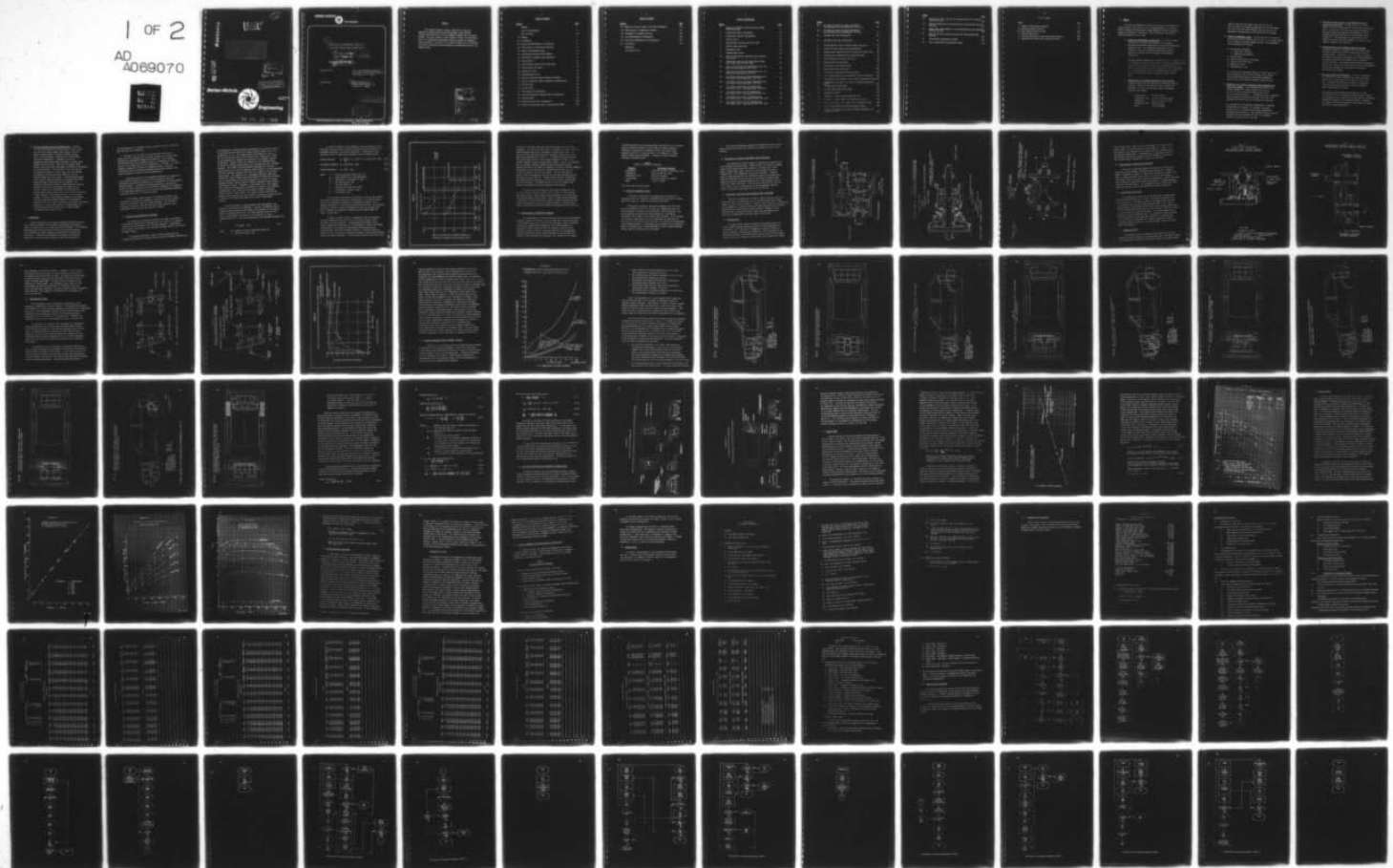
DAAK70-78-C-0055

UNCLASSIFIED

NL

1 OF 2

AD
A069070



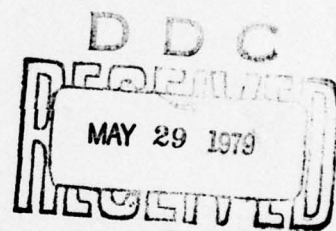
AD A069070

LEVEL *#*

12



DDC FILE COPY



Sp A

DISTRIBUTION STATEMENT A
Approved for public release
Distribution Unlimited

Barber-Nichols



Engineering

79 04 25 106

BARBER-NICHOLS



ENGINEERING Co.

6
MECHANICAL INTERFACE FOR AN
ELECTRIC PROPULSION TEST BED,

9
FINAL REPORT,

11 February 1979

12 166p.

15
Contract DAAK-78-78-C-0055

Prepared For:

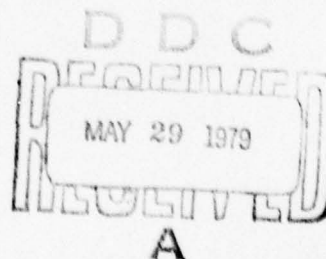
U. S. Army Mobility Equipment
Research & Development Command
Fort Belvoir, VA 22060

Prepared By:

10
Ralph W./Blakemore
Barber-Nichols Engr. Co.
Arvada, CO 80002

DISTRIBUTION STATEMENT A

Approved for public release
Distribution Unlimited



PREFACE

This report contains a summary compilation of the work performed by Barber-Nichols Engineering Company under MERADCOM contract DAAK70-78-C-0055, for which EBERHART REIMERS was the project officer. The author wishes to thank Thomas E. Weitzel for the development of the computerized performance modeling program and subsequent study and Robert G. Olander for his technical support and for providing the electric propulsion system mathematical representation used in the computer model.

ADDITION BY	
DTIC	DTIC SECTION <input checked="" type="checkbox"/>
DOC	DOC SECTION <input type="checkbox"/>
ORIGINATOR	
JANUARY 1979	
<i>File on file</i>	
BY	
DISTRIBUTION AVAILABILITY STATE	
Dist.	AVAIL. AND IN STOCK
A	

79 04 25 106

TABLE OF CONTENTS

<u>Section</u>	<u>Page</u>
Preface	i
List of Illustrations	iv
List of Tables	vii
1.0 Summary	1
2.0 Introduction	4
3.0 Review and Establishment of Guidelines	5
4.0 Establishment of Performance Standards	9
5.0 Review of Transmission Types	10
5.1 Conventional Automobile Type (Manual)	11
5.2 Conventional Automobile Type (Automatic)	11
5.3 Traction Drive	11
5.4 Custom Design (Involute Gear Tooth Form)	15
5.5 Variable Ratio Belt Drive	15
5.6 Hydrostatic Drive	15
5.7 Hydromechanical Drive	18
6.0 Electric Propulsion System Component Packaging	22
7.0 Electric Propulsion System Mathematical Representation	35
7.1 Battery Model	40
7.2 DC Motor Model	45
7.3 Motor-Controller Performance	49
8.0 Test Bed Performance Computer Model & Optimization	51
8.1 Computer Model	52
8.2 Mechanical Drive Train Optimization	123
8.3 Effect of Acceleration Path on Driving Cycle Range	135

TABLE OF CONTENTS

<u>Section</u>	<u>Page</u>
8.4 Effect of Battery Voltage on Test Bed Performance	135
8.5 Effectiveness of Regenerative Braking	139
8.6 Performance of Advanced Test Bed	139
9.0 Test Bed Mechanical Configuration	150
10.0 Test Bed Instrumentation and Accessories	151
11.0 Conclusions	151
References	
Distribution List	

LIST OF ILLUSTRATIONS

<u>Figure</u>		<u>Page</u>
1	Percent of Available Volume and Battery Weight Versus Wheel Base	8
2	Conventional Manual Transmission	12
3	Conventional Automatic Transmission	13
4	Traction Drive	14
5	Custom Design (Involute Gear Tooth Form)	16
6	Variable Ratio Belt Drive	17
7	Hydrostatic Drive	19
8	Hydromechanical Drive	20
9a	Relative Transmission Efficiency Versus Relative Motor Speed	21
9b	Transmission Watt Loss per Newton-Meter Torque Input Versus Relative Motor Speed	23
10a	Single Electric Motor and Transmission with Front Wheel Drive Differential (Side View)	24
10b	Single Electric Motor and Transmission with Front Wheel Drive Differential (Top View)	25
11a	Two Electric Motors and Single Transmission with Front Wheel Drive Differential (Side View)	26
11b	Two Electric Motors and Single Transmission with Front Wheel Drive Differential (Top View)	27
12a	Two Electric Motors with Two Transmissions Front Wheel Drive - Transverse Mount (Side View)	28
12b	Two Electric Motors and Two Transmissions Front Wheel Drive - Transverse Mount (Top View)	29
13a	Two Electric Motors with Two Transmissions Front Wheel Drive - Longitudinal Mount (Side View)	30
13b	Two Electric Motors with Two Transmissions Front Wheel Drive - Longitudinal Mount (Top View)	31

<u>Figure</u>		<u>Page</u>
14a	Two Electric Motors and Single Transmission with Rear Wheel Drive Differential (Side View)	36
14b	Two Electric Motors and Single Transmission with Rear Wheel Drive Differential (Top View)	37
15	Preferred Test Bed Configuration	38
16	Alternative Test Bed Configuration	39
17	Battery Capacity Versus Discharge Current Amplitude	42
18	Terminal Voltage Versus Current and Capacity	44
19	Torque-Current Characteristics for Bogue Motor Model 7354	46
20	Predicted Motor Performance for Bogue Model 7896	47
21	Motor Efficiency for Bogue Model 7354	48
22	Sample Listing of Input Data	57
23	Acceleration Path Specifications	119
24	Range Versus Final Drive Ratio	125
25	Acceleration Time Versus Final Drive Ratio	126
26	Test Bed Acceleration Time Versus Shift Point Motor Speed	128
27	Range Under J227a Schedule "D" for Various Transmission Types	131
28	Acceleration Time from 0 to 88 kph for Various Transmission Types	132
29	Cruising Range Versus Speed	133
30	Maximum Gradeability Versus Speed	134
31	Acceleration Paths	136
32	Schedule D Range Versus Acceleration Path	137
33	Schedule D Range Versus Test Bed Battery Voltage	140
34	Range at Constant 88 kph Versus Test Bed Battery Voltage	141
35	Test Bed Acceleration Time Versus Battery Voltage	142
36	Effects of Regenerative Braking on Driving Cycle Range for Schedules C and D	143

<u>Figure</u>		<u>Page</u>
37	Acceleration Time to 88 kph for State-of-the-Art and Projected Electric Test Bed	146
38	Maximum Gradeability for State-of-the-Art and Projected Electric Test Bed	147
39	Range Under J227a Schedule "D" for State-of-the-Art and Projected Electric Test Bed	148
40	Range at 88 kph for State-of-the-Art and Projected Electric Test Bed	149
41	Conventional Instrumentation Panel	152
42	Micro computer/LED Instrumentation Panel	153

LIST OF TABLES

TABLE	PAGE
I Summary of Performance Standards	10
II Modeling Program Objectives	51
III ERAB Program Variable Listing	112
IV Variable Definitions	117
V Test Bed Specifications With Additional Batteries	138
VI Comparative Projected Test Bed Specifications	144

1.0 SUMMARY

The study considerations affecting the selection and modification of an automobile type vehicle for use in demonstrating the U.S. Army's Mobility Research and Development Command (MERADCOM) electric propulsion system are addressed in this report. More specifically, the topical areas investigated are as follows:

- 1) Review and establishment of guidelines. This task provided the basis for the effective conversion of a currently manufactured automobile type vehicle to an electric propulsion system test bed. The guidelines established for use in selecting a test bed configuration were identified as a result of a cursory survey of automobile type commuter vehicle data.

The data reviewed inferred that a vehicle with 229 - 239 cm (90 - 94 in.) wheelbase, weighing 909 kg (2000 lb), with four occupant seating capacity should satisfy the needs of the average commuter. The effect of aerodynamic form, weight, and drive train configuration on test bed performance was also considered from the standpoint of complementing electric propulsion system performance.

- 2) Establishment of performance standards for the test bed.

A primary objective of the program was to design an electric propulsion system test bed that would meet or exceed the Department of Energy Electric-Hybrid Vehicle Performance Standards listed below:

Forward speed	80 kph (50 mph)
Acceleration time	15 sec to 50 kph (31 mph)
Gradeability	10% at 25 kph (15.5 mph)
Gradeability limit	20% for 20 sec
Range	50 km (31 miles)

Computer model results indicate that the test bed will meet or exceed all performance specifications and requirements set forth in the SAE J227a schedule D driving cycle and the Department of Energy Electric and Hybrid Vehicle Standards.

- 3) Review of transmission types. This was done for the purpose of selecting the optimum transmission for use as a motor speed reducer for the electric propulsion system test bed. The transmission types considered are outlined:

- a) Conventional automobile
 - 1. Manual gear selection
 - 2. Automatic gear selection
- b) Traction drive
- c) Custom design helical or spur gear
- d) Variable ratio belt driven
- e) Hydrostatic drive
- f) Hydromechanical drive

As a result of the reviewing process, an involute gear tooth form transmission type utilizing variable ratio solenoid shifted gearing was chosen as the optimum transmission type for use in the electric propulsion system test bed.

- 4) Packaging of the electric propulsion system components and drive train hardware. The configuration selected as the optimum consists of two rear mounted 10 hp dc motors driving a 2-speed transmission through coordinated an "electrical differential". The MERADCOM electric propulsion system components are also rear mounted, while the 6 volt batteries are divided with 12 in front and 6 in the rear.

As an alternative to the primary configuration a secondary configuration was selected. It consists of two front mounted 10 hp dc motors driving a single transmission and mechanical differential. The propulsion system electrical components are front mounted with the 6 volt batteries divided 6 in front and 12 in the rear.

- 5) Mathematical representation of the MERADCOM electrical components and batteries. In order to provide a highly refined, accurate computerized test bed performance simulation model, test bed data for a previously designed MERADCOM dc propulsion system was normalized and modified for use in mathematically describing the test bed propulsion system interaction. The representation of the system is very complete and models heretofore assumed dc propulsion system component behavior very accurately.
- 6) Computerized test bed performance simulation program. A computer program was constructed for the purpose of test bed design optimization under the conditions of SAE test procedure J227a. Schedules A, B, C, or D can be simulated. The program is extremely comprehensive and utilizes equations describing complete vehicle dynamics and dc propulsion system interaction. The program computes detailed information for the specified driving cycle along with test bed acceleration capabilities, gradeability information, and complete electrical system status.
- 7) Test bed mechanical configuration. A cursory investigation was conducted in order to identify the overall mechanical concept for a state-of-the-art dc propulsion system test bed. The design philosophy was to define a mechanically simple system so that a maximum of routine maintenance could be performed by the owner.

High capacity self-energizing drum brakes will be used in conjunction with the regenerative braking system. DeDion type suspension will be used for the drive wheels and completely independent suspension on the remaining wheels. Batteries are grouped in trays and arranged for easy access for removal from front or rear compartments.

- 8) Test bed instrumentation and accessory power. Initially the test bed instrumentation would consist of state-of-the-art solid state battery charge level sensors along with a panel of warning lights to indicate propulsion system status. Test bed speed is indicated with a conventional cable driven speedometer. Eventually, with the dc propulsion system microprocessor available, a digital speed readout would be utilized. The use of two digital speed sensors, one in each drive wheel makes it possible to incorporate an anti-skid system. A microcomputer center would provide an intermittent display of time of day, total trip mileage, and elapsed trip time upon driver command, as well as available energy from the battery. A refined battery charge level indicator that would correct for variables that affect apparent battery voltage would also be possible. The electrical accessories (lighting, windshield wipers, heater/defroster blower motor) are powered by a single 12 volt battery. However, it is preferable to utilize only one energy storage battery system which, with a 500 watt dc-chopper voltage converter, could generate the 12 volt dc accessory voltage. In place of the separate auxiliary 12 volt battery, the actual propulsion battery voltage can be increased by another 12 volts or 24 volts which would also increase the vehicle drive range. The gas heater system is located beneath the instrument panel while the fuel tank is located inboard of the rear axle at chassis level.

2.0 INTRODUCTION

With the resurgence of the electric propulsion system vehicle for use in commuter transport and the numerous configurations beginning to appear, it becomes obvious that design rationale is missing. The information presented herein has resulted from a study to provide such rationale for the MERADCOM two phase, sequentially switched dc controller dual motor drive. In addition to developing the rationale to configure a design base electric propulsion system test bed, the rationale for

optimum packaging of the MERADCOM electric propulsion system in the design base test bed is also presented.

Initially, for the purpose of quantitatively describing an optimum test bed configuration, a review of existing and proposed design guidelines and performance standards was conducted. The information collected has been used as baseline criteria for evaluating the acceptability of the design base test bed configuration. Of course, the electric propulsion system drive train has a fundamental effect on test bed acceptability from a performance standpoint and has been studied to the extent necessary to provide an optimum configuration.

A detailed discussion of the parameters affecting the optimization of the electric propulsion system test bed is presented along with performance projections made possible by a computerized test bed performance modeling program. The performance modeling program was constructed to accept test bed and propulsion system descriptive parameters for computation of the performance capabilities of the test bed while performing according to the SAE J227a A, B, C, or D driving cycles.

The conceptual approach taken in the mechanical design of the test bed was to optimize the components that were matched and therefore unique to the electric propulsion system components. As refinements are made by industry on tires and batteries, these components can be retrofitted to the test bed, and range will increase.

3.0 REVIEW AND ESTABLISHMENT OF GUIDELINES

The problem of establishing guidelines that define the geometric and mechanical configuration requirements for the selection of a commuter class test bed is discussed in the following paragraphs. Consideration must be given to such items as test bed size, seating, capacity, and overall mechanical design.

The rationale developed in order to define the geometric and mechanical configuration was based solely on potential consumer considerations.

An investigation of seating capacity requirements was conducted initially. It was found that the statistical average occupancy number for all trip purposes was 1.9 (1). This average number was bounded by 1.4 and 3.3 for "to and from work trips" and "vacation trips", respectively. Based on this information it appears that seating for two occupants would be satisfactory. However, what is not reflected in the referenced study is the use of interior seating capacity for carrying other than "occupant" payloads. Two occupants with any personal belongings in a two seat vehicle would be at a loss for adequate interior space if it were presupposed that their personal belongings would have to be carried in the occupant interior area. This appears to be a reasonable supposition since the conventional "trunk" storage area would probably be filled with batteries. Also, in consideration of long range planning for a network of battery recharge stations, vacation trips in electric propulsion system vehicles could become a reality. Therefore, it was decided that a four occupant test bed seating configuration be provided as an answer to the foregoing considerations. For "to and from work trips", personal belongings could be stored in vacant seats. For "vacation trips", there would be adequate seating capacity for four occupants, and personal belongings could be stored in a trunk-mounted carrier or in a small, light-weight trailer.

Once the question of seating capacity had been answered, the question of vehicle size was addressed. A review of fundamental vehicle geometry versus performance relationships was conducted in an attempt to define the optimum vehicle size. The power required to move the test bed at a given speed is proportional to the summation of motion resisting forces (2). This power requirement may be expressed mathematically as:

$$N = R_x V / 367 \quad (\text{kw}) \quad (3-1)$$

where R_x = summation of motion resisting forces, kg
 V = test bed velocity, kph

Of specific interest was the summation of motion resisting forces. The motion resisting forces of primary concern are rolling resistance (3), aerodynamic resistance, and inertial resistance. A mathematical representation of each of these motion resisting forces is presented below:

$$\text{Rolling Resistance} \quad R_r = \frac{T_r W}{75} [1 + 2.2 (10)^{-3} V + 4.2 (10)^{-5} V^2] \quad (\text{kg}) \quad (3-2)$$

$$\text{Aerodynamic Resistance} \quad R_a = C_a \rho A V^2 / 2g \quad (\text{kg}) \quad (3-3)$$

$$\text{Inertial Resistance} \quad R_i = W a / g \quad (\text{kg}) \quad (3-4)$$

where:

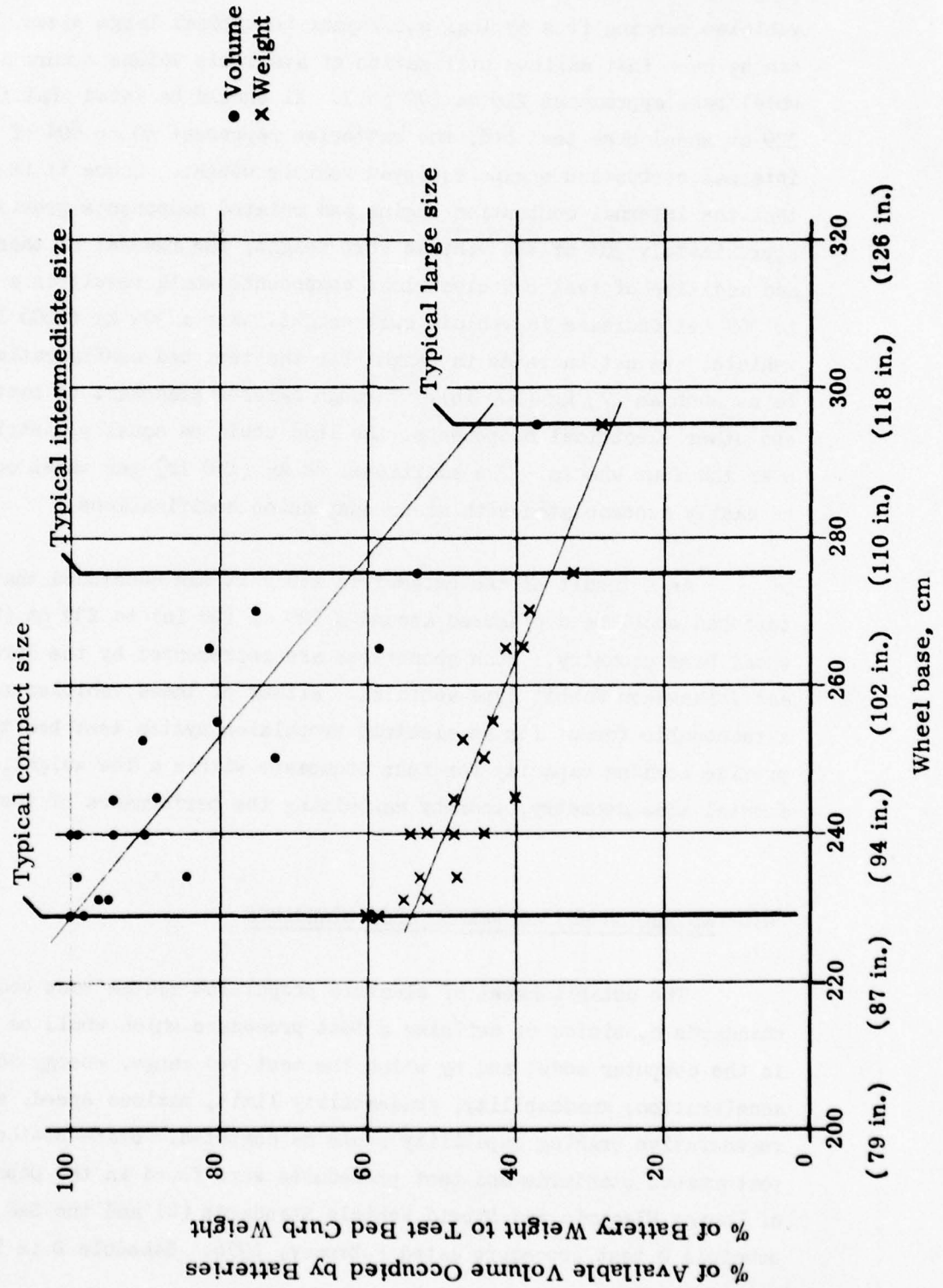
- A = test bed projected frontal area, m^2
- C_a = drag coefficient for test bed geometry
- T_r = Coefficient of resistance of tires
- V = test bed velocity, kph
- W = test bed weight, kg
- a = acceleration of test bed, m/sec^2
- g = gravitational constant, m/sec^2
- ρ = air density, kg/m^3

It can be seen by inspection of equations 3-2 and 3-4 that rolling and inertial resistance are directly proportional to the test bed weight and that the aerodynamic resistance, as expressed in equation 3-3 is directly proportional to the test bed projected frontal area. The conclusion reached as a result of these relationships was that the test bed should have a geometric and mechanical configuration that tended toward the "small" chassis sizes.

In order to quantify "small", a parametric study was conducted utilizing preliminary estimates of the total battery volume ($.22 \text{ m}^3$) and weight (507 kg) parameters. The percentage of available vehicle volume occupied by the batteries and the percentage of vehicle curb weight represented by the batteries was computed and plotted against test bed wheel base. This plot is shown in Figure 1. Available volume was defined as that volume which is typically occupied by the internal combustion engine and related components. In the conversion process these items would,

Figure 1

Percent of Available Volume and Battery Weight Versus Wheel Base



of course, be removed to make room for batteries and other electrical components. The wheel base range shown is comprised of current production vehicles ranging from typical subcompact to typical large sizes. It can be seen that maximum utilization of available volume occurs as the wheel base approaches 229 cm (90 in.). It should be noted that for the 229 cm wheel base test bed, the batteries represent 50 to 60% of the internal combustion engine equipped vehicle weight. Since it is estimated that the internal combustion engine and related components provide approximately 30% of the vehicle curb weight, the removal of these components and addition of test bed electrical components would result in a 20 to 30% net increase in vehicle curb weight. For a 909 kg (2000 lb) vehicle, the net increase in weight for the test bed configuration could be as much as 273 kg (600 lb). Through careful placement of batteries and other electrical components, the load could be equally distributed over the four wheels. The additional 68 kg (150 lb) per wheel could be easily accommodated with minor suspension modifications.

As a result of the parametric study it was concluded that the test bed would be configured around a 229 cm (90 in) to 239 cm (94 in) wheel base geometry. Such geometries are represented by the Ford Fiesta and Volkswagen Rabbit type vehicles. Either of these vehicles represent a reasonable format for an electric propulsion system test bed that would provide seating capacity for four occupants within a low weight, small frontal area geometry, thereby maximizing the performance of the test bed.

4.0 ESTABLISHMENT OF PERFORMANCE STANDARDS

The establishment of electric propulsion system test bed performance standards consisted of defining a test procedure which would be simulated in the computer model and by which the test bed range, energy consumption acceleration, gradeability, gradeability limit, maximum speed, and regenerative braking capability could be computed. State-of-the-art performance standards and test procedures were found in the Department of Energy Electric and Hybrid Vehicle Standards (4) and the SAE J227a schedule D test procedure dated February, 1976. Schedule D is intended

to simulate variable route suburban driving, and was used in the computer study to determine projected test bed range and energy consumption. Acceleration, gradeability, gradeability limit, and forward speed parameters used will be those presented in the Department of Energy Electric-Hybrid Vehicle Standards. A summary of these performance standards is presented below:

TABLE I
SUMMARY OF PERFORMANCE STANDARDS

<u>Parameter</u>	<u>Performance Standard*</u>
Acceleration	0-50 km/h (31 mph) in less than 15 sec.
Gradeability	10% @ 25 km/h (15.5 mph)
Gradeability Limit	20% for 20 seconds
Forward Speed	80 km/h (50 mph) for 5 minutes
Range	50 km (31 miles)

* SAE J227a test procedures apply.

5.0 REVIEW OF TRANSMISSION TYPES

Of primary concern during the program was the selection of a transmission for use in reducing the MERADCOM electric propulsion system drive motor speed to a useful test bed drive wheel speed.

While many transmission types were considered, most were found to be too inefficient for use in the test bed. Maximization of drive system component efficiency must be achieved in order to provide a test bed with maximum performance and range capability. Additionally, transmission size, weight, and quietness were considered. In the interest of providing a transmission that would complement the relatively low noise level of the electric motor or motors, a low noise level transmission was considered mandatory. Transmission size and weight were considered in terms of minimizing both of these parameters in order to provide maximum battery space and minimum vehicle curb weight.

The following paragraphs summarize the transmission types investigated and briefly describe their operational characteristics and salient features.

5.1 Conventional Automobile Type (Manual Ratio Selection)

This transmission type is capable of variable ratio selection by the interchange of helical gears. Various ratios are obtained by sliding a gear along a splined shaft and bringing it into mesh with a second gear on another shaft which is driven by a set of gears which are in constant mesh. This arrangement may be seen in Figure 2. Commonly three to five forward ratios are available as well as one reverse ratio. While the efficiency of any one ratio is quite good, the power losses associated with the non-meshing gears and other shaft bearings tend to reduce the overall efficiency. Noise levels are acceptably low but the size, weight, and axial configuration of this transmission type may require unreasonable compromises for use in the test bed.

5.2 Conventional Automobile Type (Automatic Ratio Selection)

This type of transmission utilizes a torque converter, usually in conjunction with a planetary gear set, to provide variable ratio change capability and is shown in Figure 3. Automatic ratio selection is accomplished by the engagement of various elements with brake bands which are activated hydraulically as speed sensing governors indicate a change of ratio. Relatively poor low speed efficiency, large size, and weight prevent this type of transmission from being used in the test bed.

5.3 Traction Drive

Of great interest during this phase of the study was the cone roller toroidal geometry traction drive such as that manufactured by Excelermatic, Inc. This type of transmission, as shown in Figure 4, provides infinitely variable ratio capability. Ratio selection can be accomplished manually or automatically by moving a conical roller between two discs such that a change of contact radius occurs between the conical

FIG. 2
CONVENTIONAL MANUAL TRANSMISSION

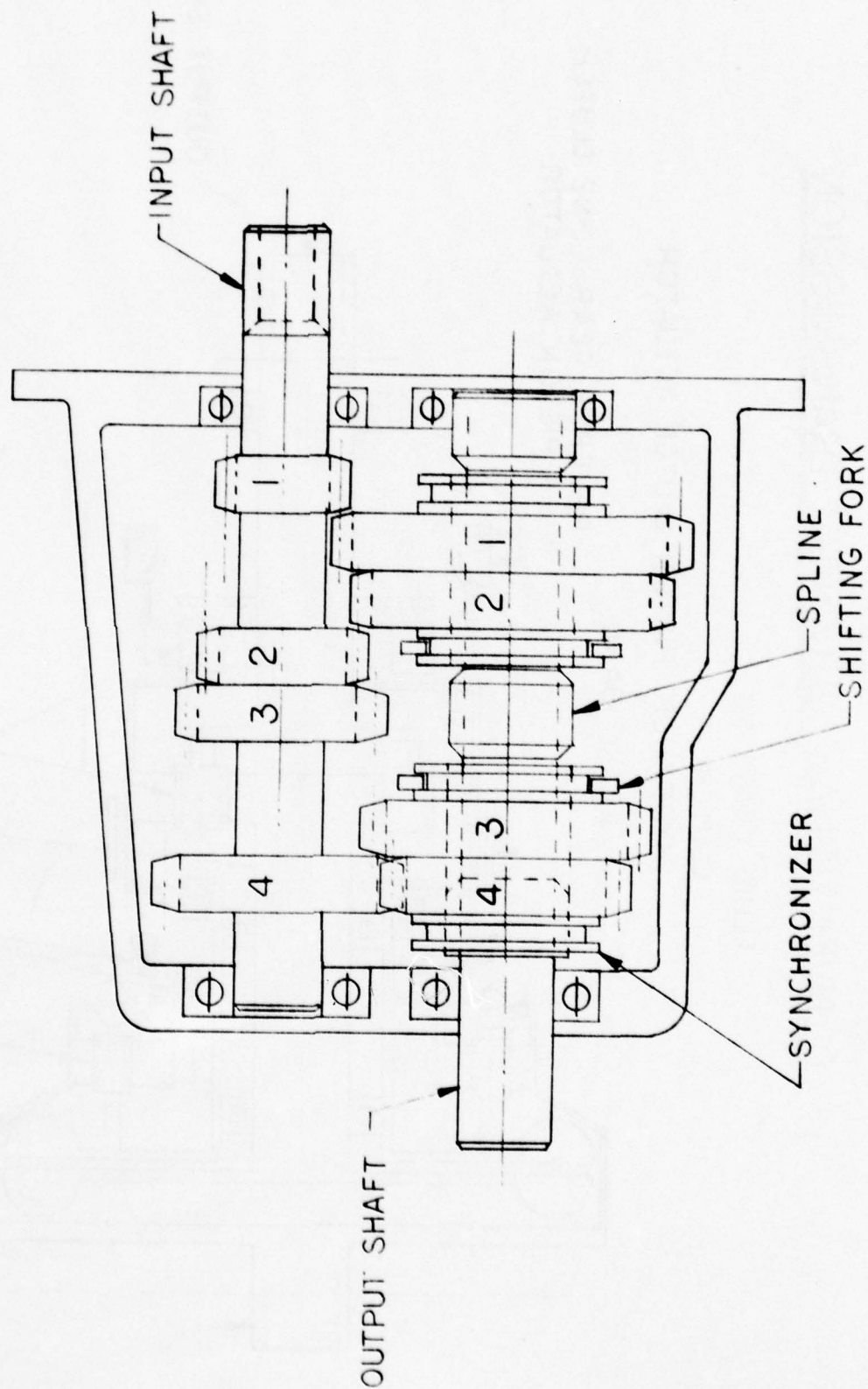


FIG. 3
CONVENTIONAL AUTOMATIC TRANSMISSION

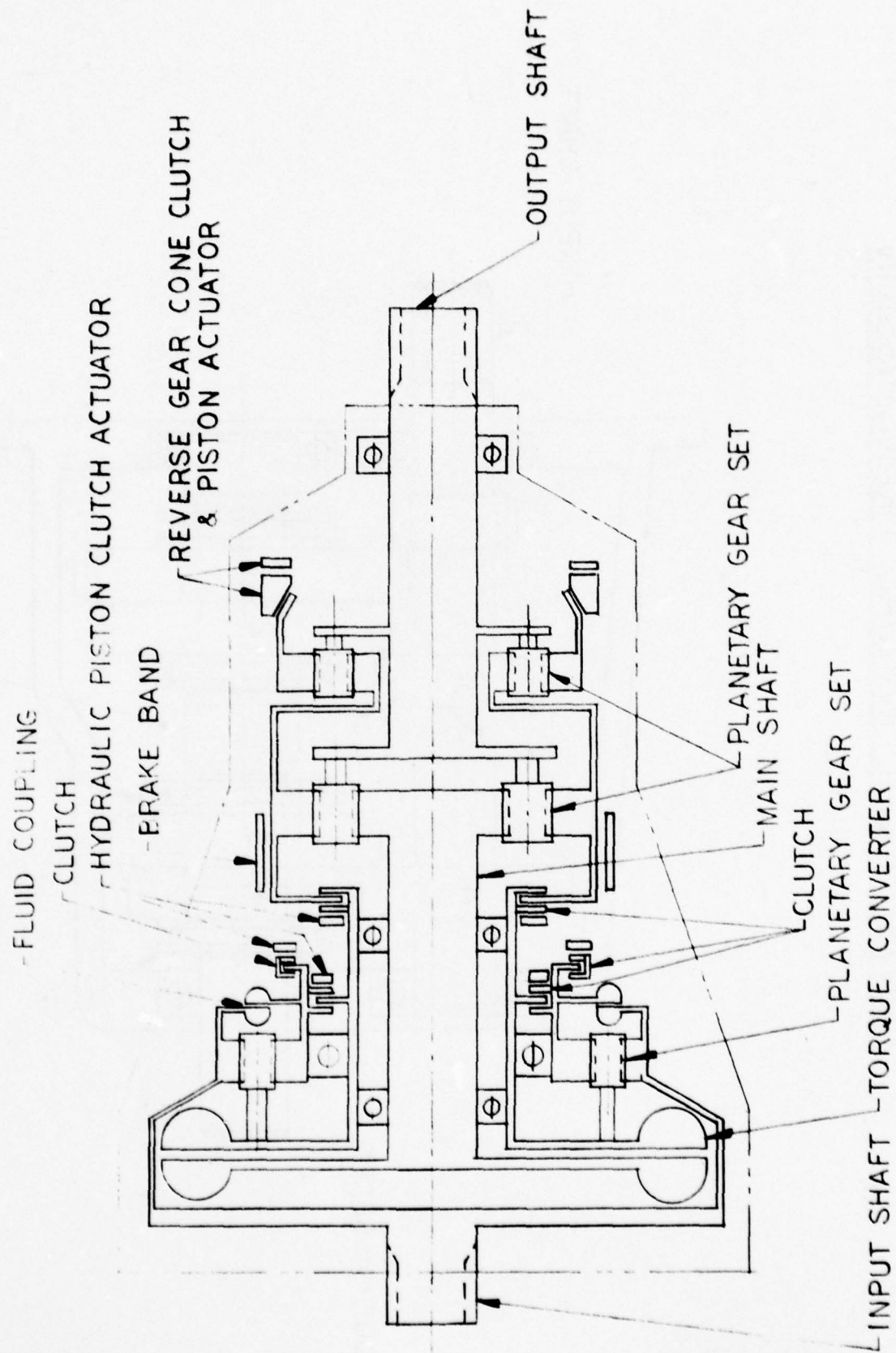


FIG. 4 TRACTION DRIVE

CONICAL ROLLER

CONTACT RADIUS DRIVER

CONICAL ROLLER PITCHES ABOUT THIS AXIS CHANGING CONTACT RADIUS

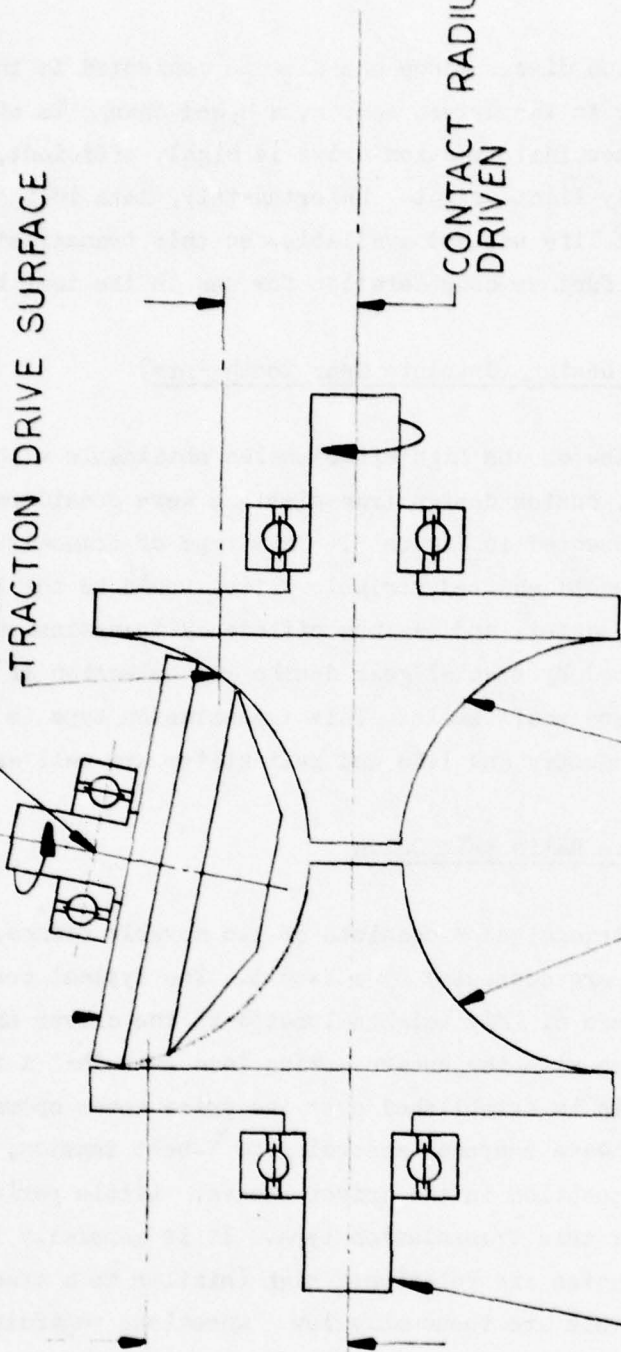
TRACTION DRIVE SURFACE

CONTACT RADIUS DRIVEN

TOROIDAL DRIVEN SURFACE

TOROIDAL DRIVER SURFACE

INPUT SHAFT



roller and each disc. Since one disc is connected to the driver source and the other to the driven source, a speed change is effected. The cone roller toroidal traction drive is highly efficient, compact, quiet, and relatively light-weight. Unfortunately, data indicating reliability and component life was not available, so this transmission type could not be given further consideration for use in the test bed.

5.4 Custom Design (Involute Gear Tooth Form)

In view of the high efficiencies obtainable with involute tooth form gearing, custom design transmissions were considered. A possible design is presented in Figure 5. This type of transmission, whether fixed ratio or solenoid shifted variable ratio, would be the most compact, light-weight, quiet, and maximum efficiency transmission. Maximum efficiency can be obtained by special gear design and selection of optimum bearings, lubricants, and shaft seals. This transmission type is widely used by the automotive industry and life and reliability are well established.

5.5 Variable Ratio Belt Drive

This transmission consists of two movable flange, spring loaded sheaves that are connected by a V-belt. The typical configuration is shown in Figure 6. Fly weights located in the driver sheave are sized in conjunction with the sheave spring load such that a rate of ratio change profile is established over the prime mover operating speed range. The driver sheave responds according to V-belt tension, which is a function of the belt position in the driver sheave. Little performance data is available for this transmission type. It is generally thought, however, that efficiencies are relatively high (similar to a traction drive) and noise levels are reasonably low. Questions regarding life and reliability were not resolved, so this transmission type was not given further consideration.

5.6 Hydrostatic Drive

The hydrostatic drive transmission type consists of two major components usually referred to as the pump and motor. The pump is coupled to the prime mover such that the prime mover drives the pump valve plate.

FIG. 5
CUSTOM DESIGN
(INVOLUTE GEAR TOOTH FORM)

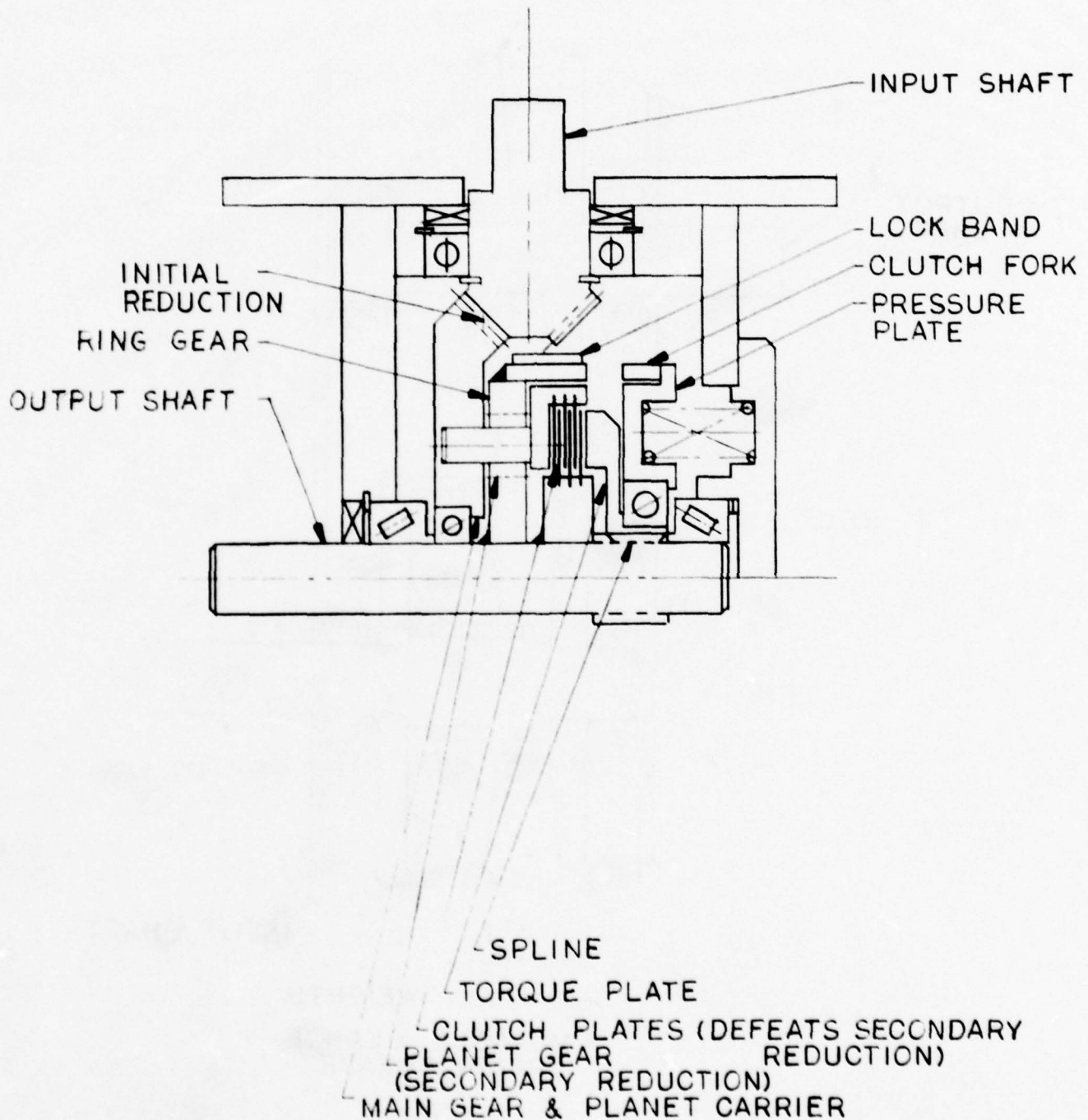
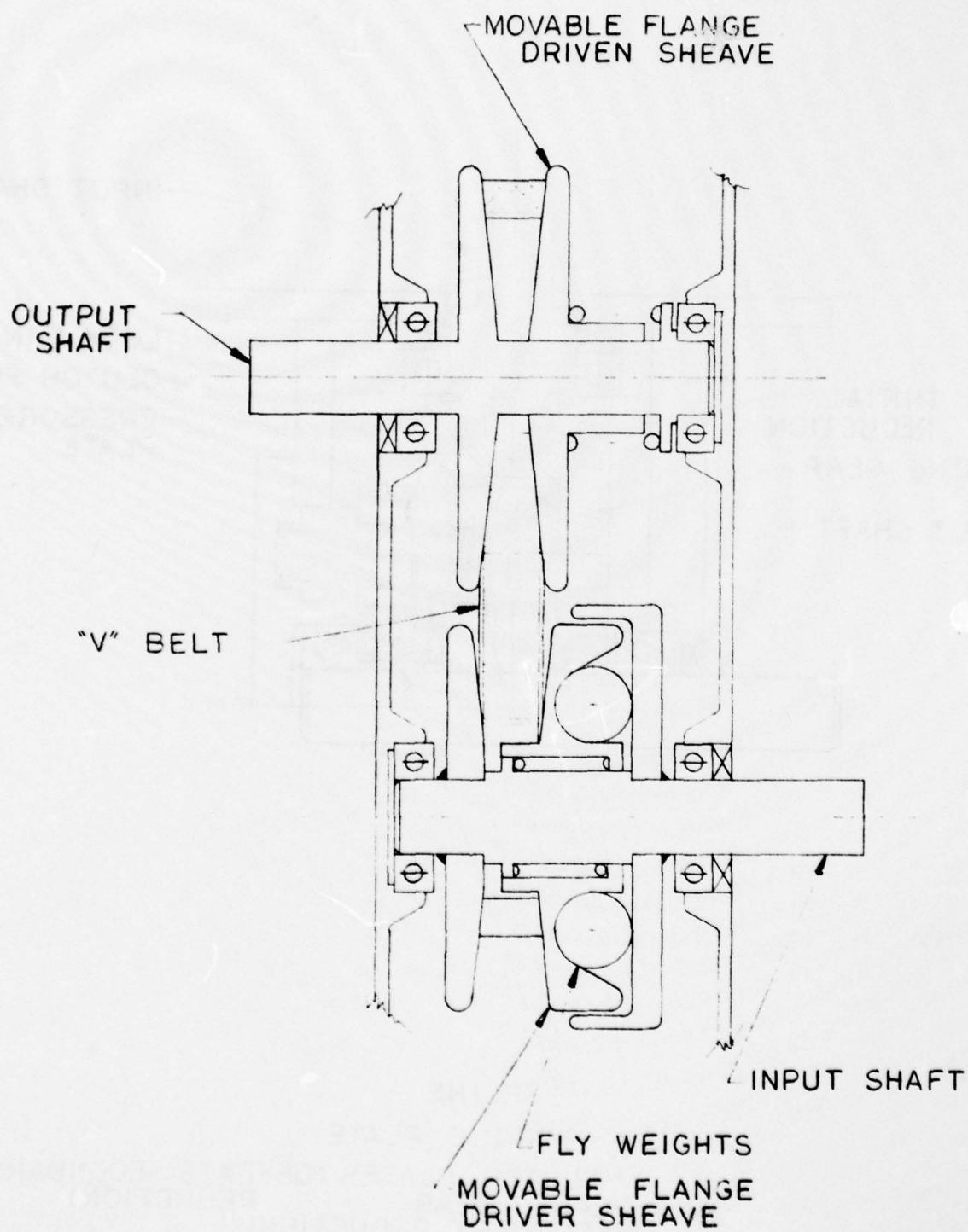


FIG. 6
VARIABLE RATIO BELT DRIVE



This arrangement may be seen in Figure 7. Automatic or manual control of the swash plate angle results in variable quantity displacements of the hydraulic fluid which feeds the motor. This enables the prime mover to maintain constant speed while the hydrostatic drive motor operates within a variable speed range. The pump and motor components may be connected by flexible hoses. This transmission type offers good test bed packaging flexibility, although the low efficiency, high noise level, and large space requirement for support components such as hydraulic fluid reservoirs, heat exchanger, and filter make it unacceptable for use in the test bed.

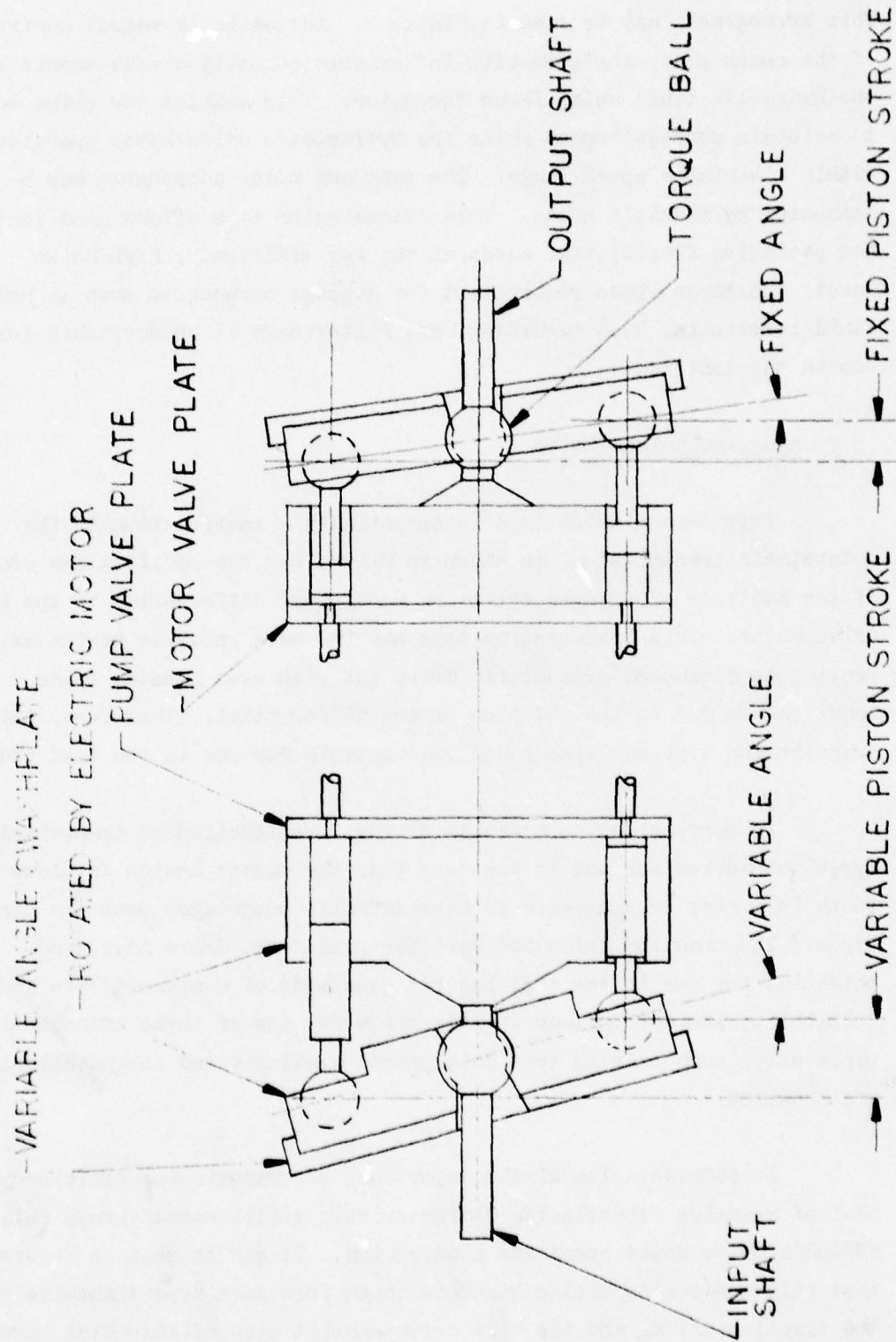
5.7 Hydromechanical Drive

This transmission type is essentially a modification to the hydrostatic transmission, as shown in Figure 8. The modification consists of the addition of a power splitting mechanical differential to the hydrostatic drive motor. This transmission type has the same relative merits as the previously discussed hydrostatic drive but with even greater space requirements due to the addition of the differential. Therefore, this transmission type was also found unacceptable for use in the test bed.

In conclusion, as a result of the investigation of transmission types considered for use in the test bed, the custom design involute tooth form gear type appears to have definite advantages over the other types. The traction drive and variable ratio belt drive have good potential for use in the test bed but questions of component life and reliability prevent further consideration for use of these transmission types until such time as test data become available and the questions are answered.

In consideration of the importance of transmission efficiency, a plot of relative transmission characteristic efficiencies versus relative MERADCOM drive motor speed was constructed. It can be seen in Figure 9a that only the custom design involute tooth form gear type transmission, the traction drive, and the belt drive exhibit high efficiencies throughout the motor operating speed range. The absolute efficiencies shown in

FIG. 7
HYDROSTATIC DRIVE



-DRIVE AXLE

FIG. 8
HYDROMECHANICAL DRIVE

-VARIABLE ANGLE SWASHPLATE

-ROTATED BY ELECTRIC MOTOR

-PUMP VALVE PLATE

-MOTOR VALVE PLATE

-DIFFERENTIAL

-TORQUE BALL

-VARIABLE ANGLE

-VARIABLE PISTON STROKE

-FIXED ANGLE

-FIXED PISTON STROKE

-INPUT SHAFT

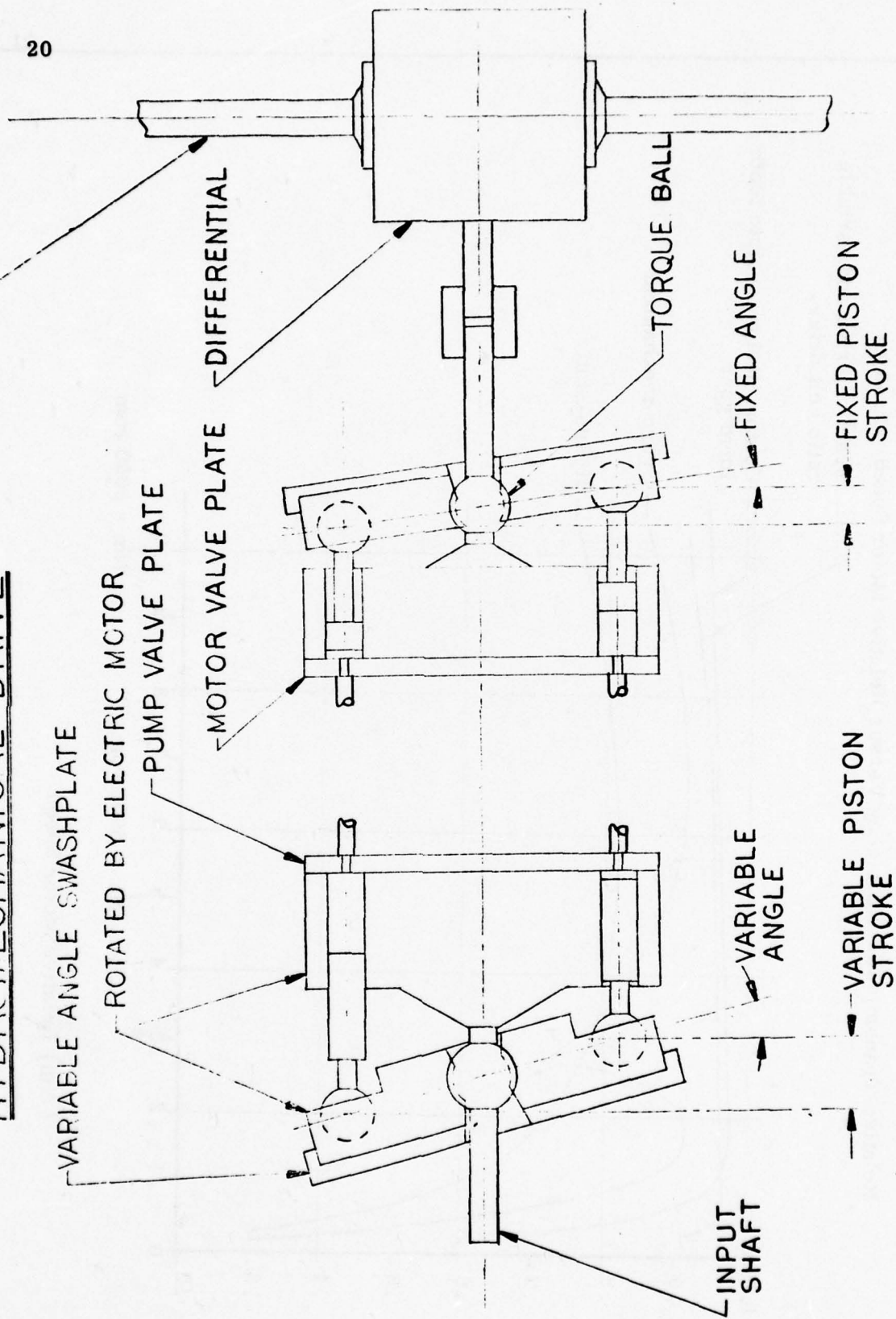
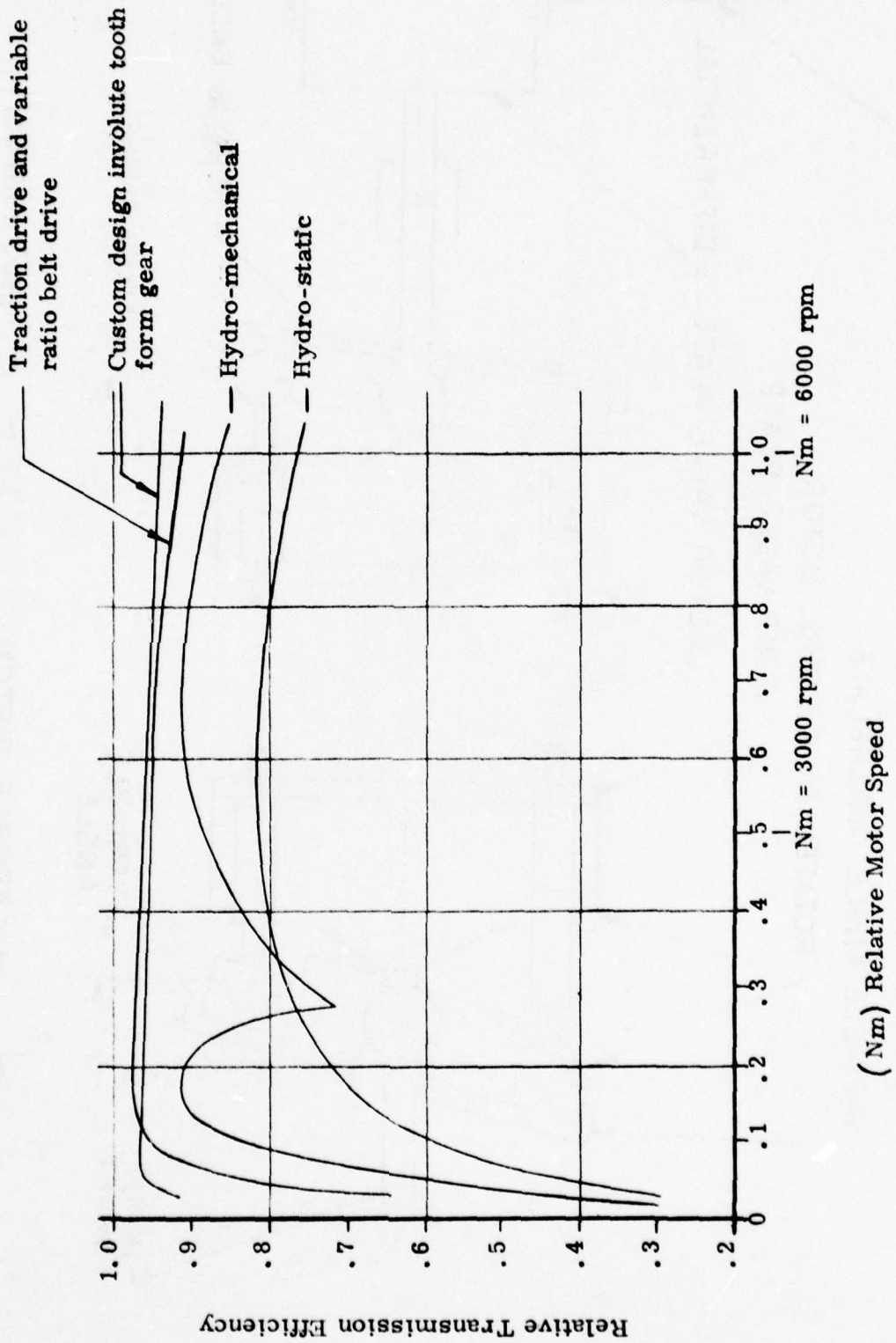


Figure 9a

Relative Transmission Efficiency Versus Relative Motor Speed @ 7.46 kw



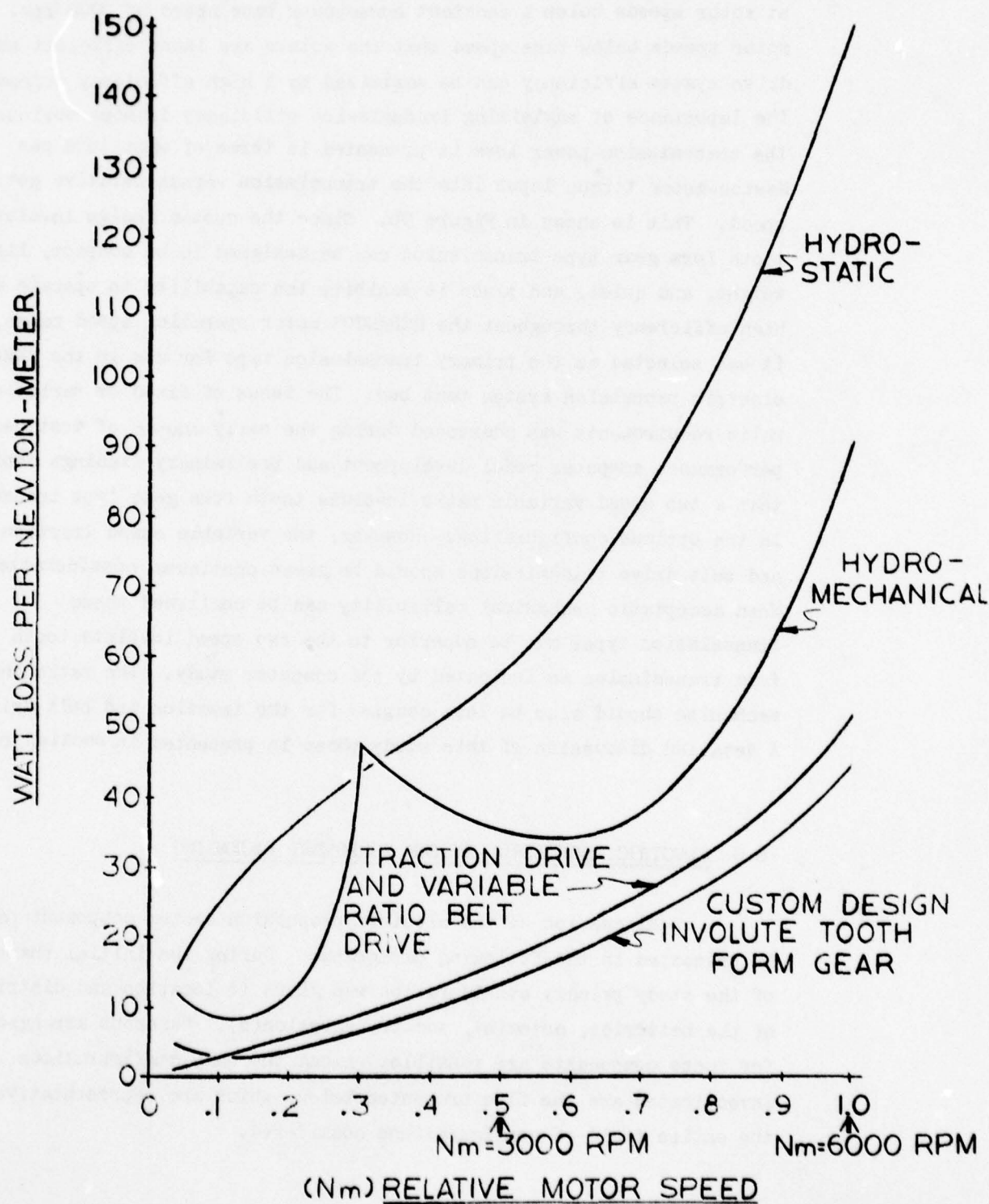
typical characteristic form may vary somewhat according to the source used but this is not important. What is important is the ability of the transmission type to maintain high operating efficiencies not only throughout the entire MERADCOM motor operating speed range, but especially at motor speeds below a constant horsepower base speed of 3000 rpm. It is at motor speeds below base speed that the motors are least efficient and overall drive system efficiency can be maximized by a high efficiency transmission type. The importance of maximizing transmission efficiency is more obvious when the transmission power loss is presented in terms of watt loss per Newton-meter torque input into the transmission versus relative motor speed. This is shown in Figure 9b. Since the custom design involute tooth form gear type transmission can be designed to be compact, lightweight, and quiet, and since it exhibits the capability to operate at high efficiency throughout the MERADCOM motor operating speed range, it was selected as the primary transmission type for use in the MERADCOM electric propulsion system test bed. The issue of fixed or variable ratio requirements was addressed during the early stages of test bed performance computer model development and preliminary findings confirmed that a two speed variable ratio involute tooth form gear type transmission is the optimum configuration. However, the variable speed traction drive and belt drive transmissions should be given continued consideration. When acceptable mechanical reliability can be confirmed these transmission types may be superior to the two speed involute tooth form transmission as indicated by the computer study. The ratio change mechanism should also be less complex for the traction and belt drives. A detailed discussion of this study phase is presented in section 8.2.

6.0 ELECTRIC PROPULSION SYSTEM COMPONENT PACKAGING

A discussion of the electric propulsion system component packaging is presented in the following paragraphs. During the initial phase of the study primary consideration was given to location and distribution of the batteries, motor(s), and transmission(s). Numerous arrangements for these components are possible. Among the many configurations investigated are the five presented below, which are representative of the entire field of configurations considered.

FIGURE 9b

TRANSMISSION WATT LOSS PER NEWTON-METER
TORQUE INPUT VS. RELATIVE MOTOR SPEED



1. Single electric motor and transmission with front wheel drive differential (Figures 10a and 10b).
2. Two electric motors and single transmission with front wheel drive differential (Figures 11a and 11b).
3. Two electric motors and front wheel drive transmissions (transverse mount) (Figures 12a and 12b).
4. Two electric motors and front wheel drive transmissions (longitudinal mount) (Figures 13a and 13b).
5. Two electric motors and single transmission with rear wheel drive differential (Figures 14a and 14b).

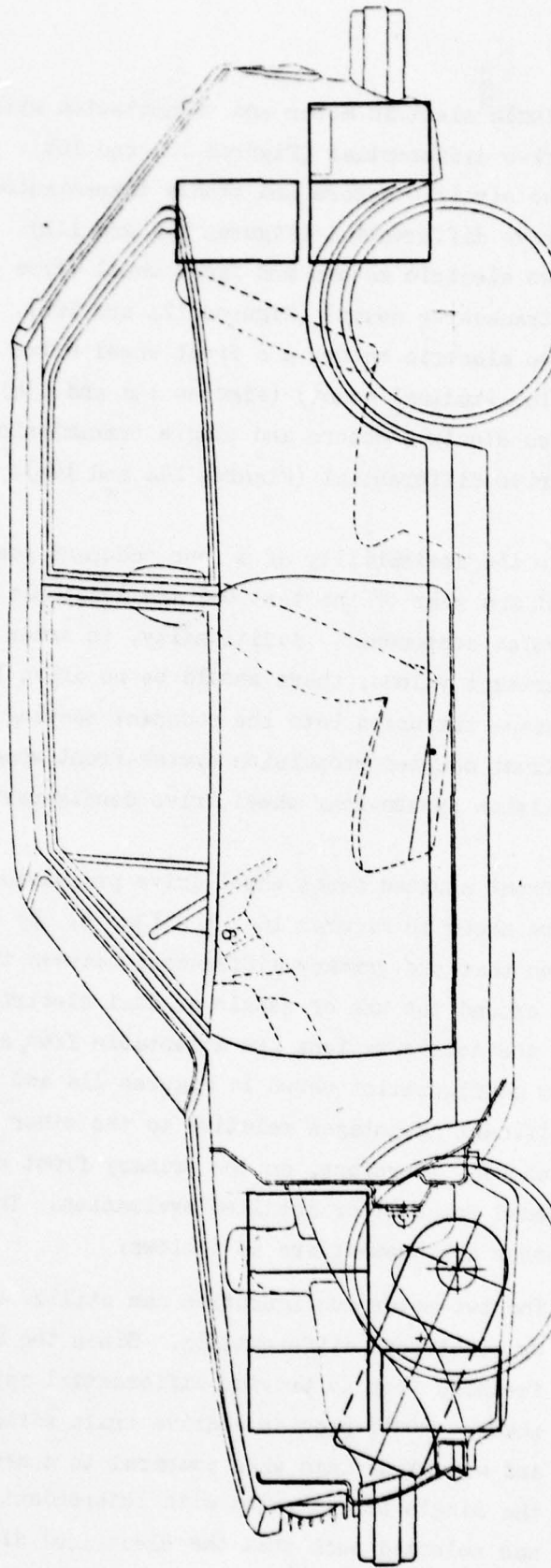
Due to the desirability of a four occupant seating compartment, only the front and rear of the test bed are available to house the propulsion system components. Additionally, in order to maximize occupant seating compartment volume, there should be no drive line hump or other propulsion system intrusion into the occupant seating compartment. This leaves only front mounted propulsion system-front wheel drive or rear mounted propulsion system-rear wheel drive configurations for consideration.

The front mounted front wheel drive propulsion system configurations considered are shown in Figures 10a, b - 13a, b. By studying the figures it can be seen that the primary differences between the configurations are centered around the use of single or dual electric drive motors. While any of the configurations are acceptable from a packaging standpoint, the two-motor configuration shown in Figures 11a and 11b is considered to have significant advantages relative to the other configurations. It has been chosen, therefore, as the primary front wheel drive configuration to be considered for further detailed evaluation. The major advantages of the two-motor arrangement are as follows:

1. The two-motor configuration can utilize either mechanical or electrical differentials. Since the use of an electrical feedback loop to provide differential action for the drive wheels would provide a drive train efficiency improvement and weight savings when compared to a mechanical differential, the single transmission with independent wheel drive arrangement was selected such that the electrical differential could be utilized.
2. Two motors providing power to the independently driven wheels could offer improved test bed reliability. If certain potential electrical

FIG. 10.

SINGLE ELECTRIC MOTOR AND TRANSMISSION
WITH FRONT WHEEL DRIVE DIFFERENTIAL



TOTAL WEIGHT	1195	Kg.
FRONT AXLE WEIGHT	757	Kg.
REAR AXLE WEIGHT	456	Kg.
WEIGHT DISTRIBUTION	F .62 / R .38	
10 BATTERIES FRONT		
8 BATTERIES REAR		

FIG. 10 b SINGLE ELECTRIC MOTOR AND TRANSMISSION
WITH FRONT WHEEL DRIVE DIFFERENTIAL

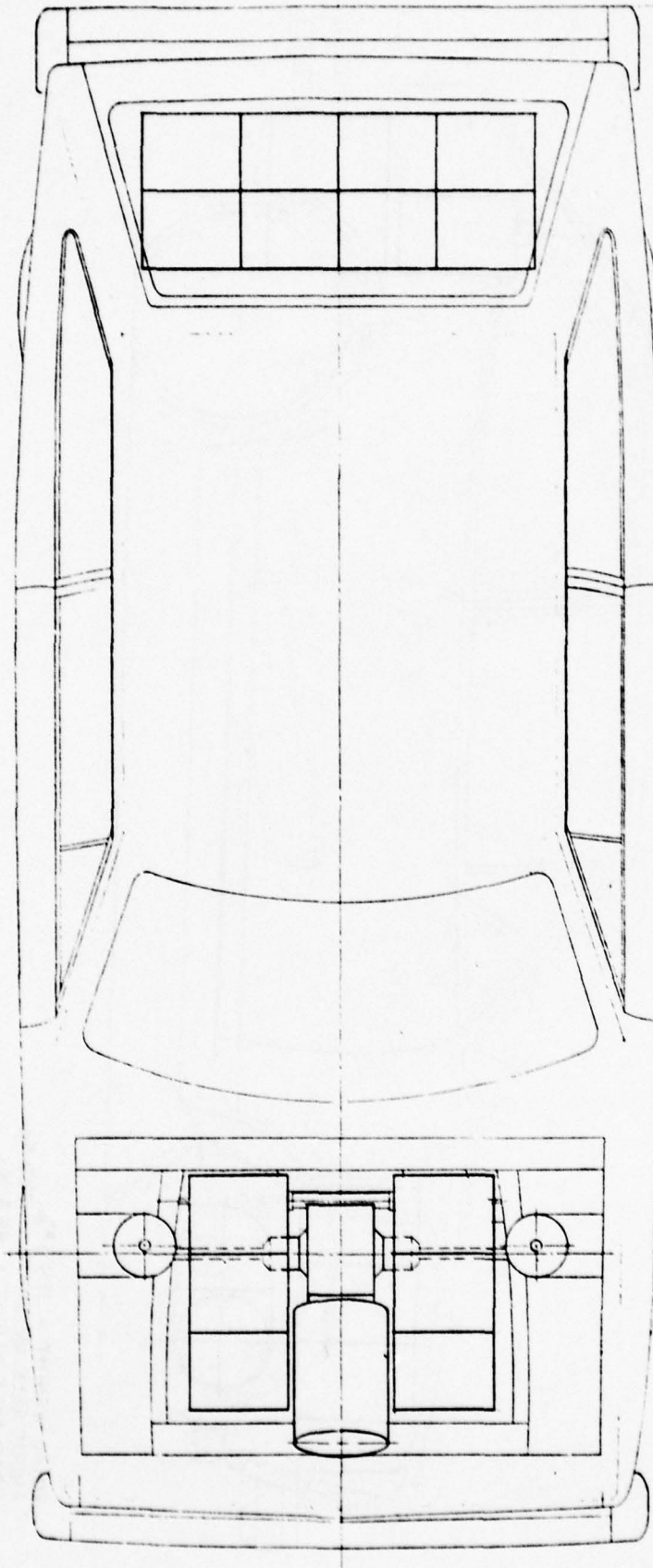
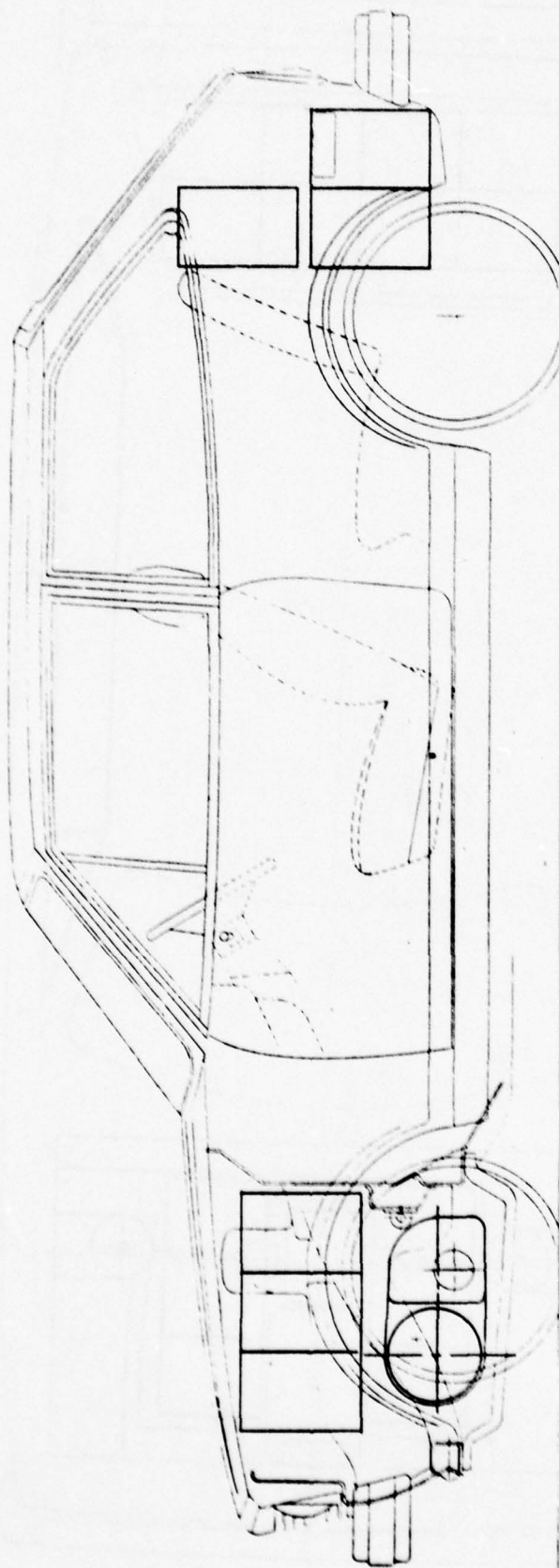


FIG. 11a
TWO ELECTRIC MOTORS AND SINGLE TRANSMISSION WITH FRONT WHEEL
DRIVE DIFFERENTIAL



TOTAL WEIGHT = 1195 Kg
FRONT AXLE WEIGHT = 729 Kg
REAR AXLE WEIGHT = 484 Kg
WEIGHT DISTRIBUTION F 60 / R 40
9 BATTERIES FRONT
9 BATTERIES REAR

FIG. 11b
TWO ELECTRIC MOTORS AND SINGLE TRANSMISSION WITH FRONT WHEEL
DRIVE DIFFERENTIAL

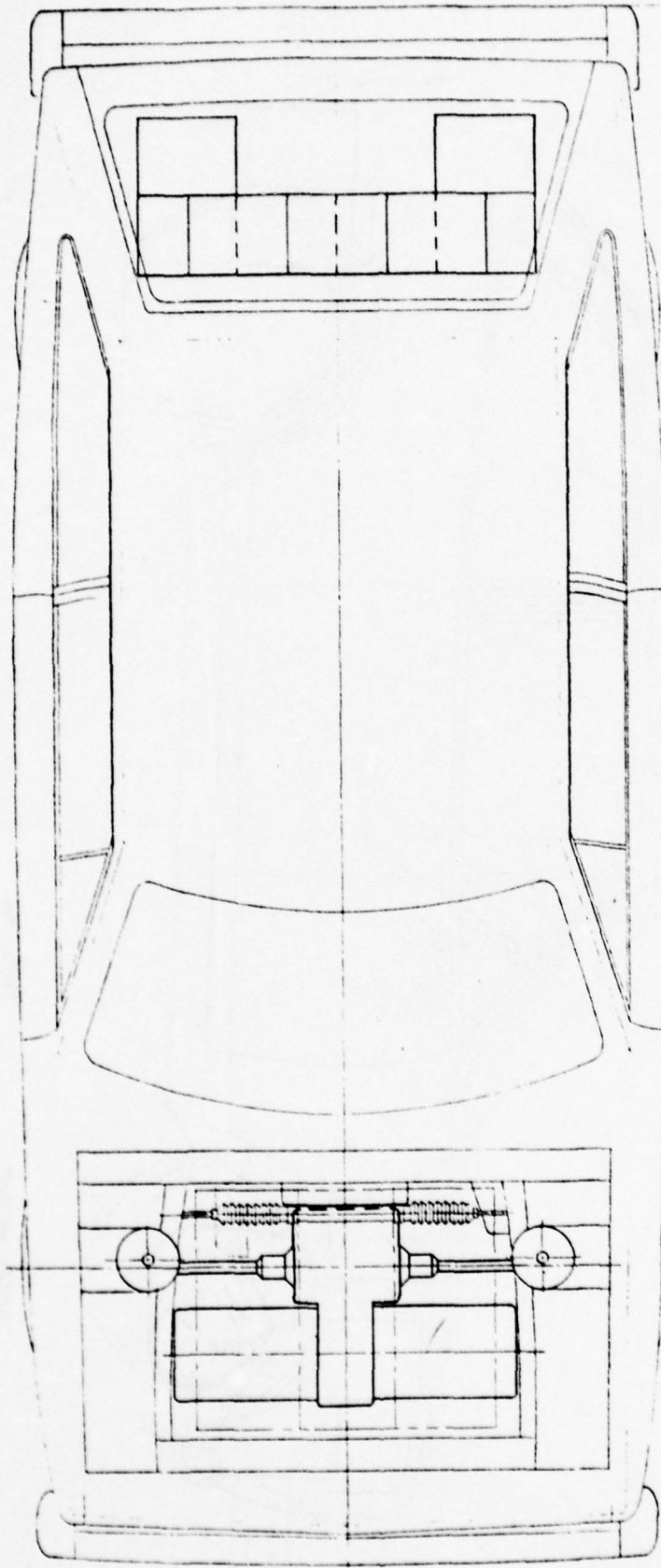
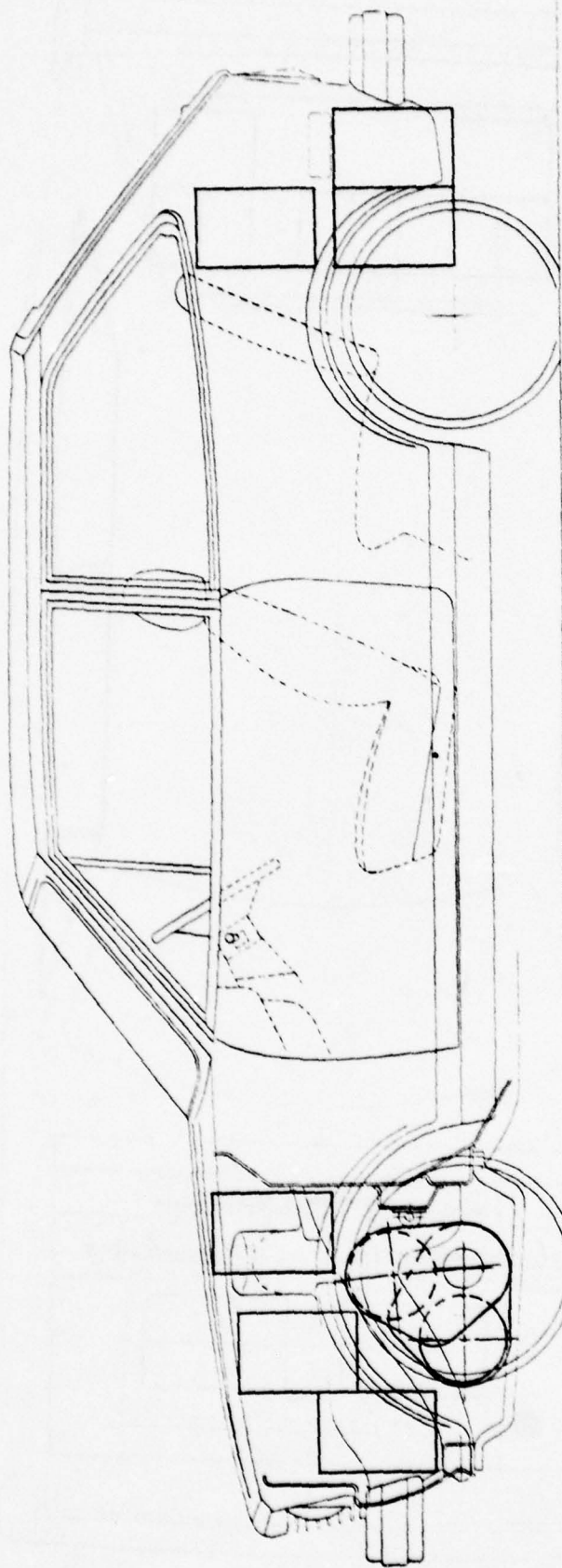


FIG. 12_a TWO ELECTRIC MOTORS WITH TWO TRANSMISSIONS
FRONT WHEEL DRIVE - TRANSVERSE MOUNT



TOTAL WEIGHT	1195	Kg.
FRONT AXLE WEIGHT	702	Kg.
REAR AXLE WEIGHT	484	Kg.
WEIGHT DISTRIBUTION	F. 59 / R. 41	
9 BATTERIES FRONT		
9 BATTERIES REAR		

FIG. 12b TWO ELECTRIC MOTORS AND TWO TRANSMISSIONS
FRONT WHEEL DRIVE - TRANSVERSE MOUNT

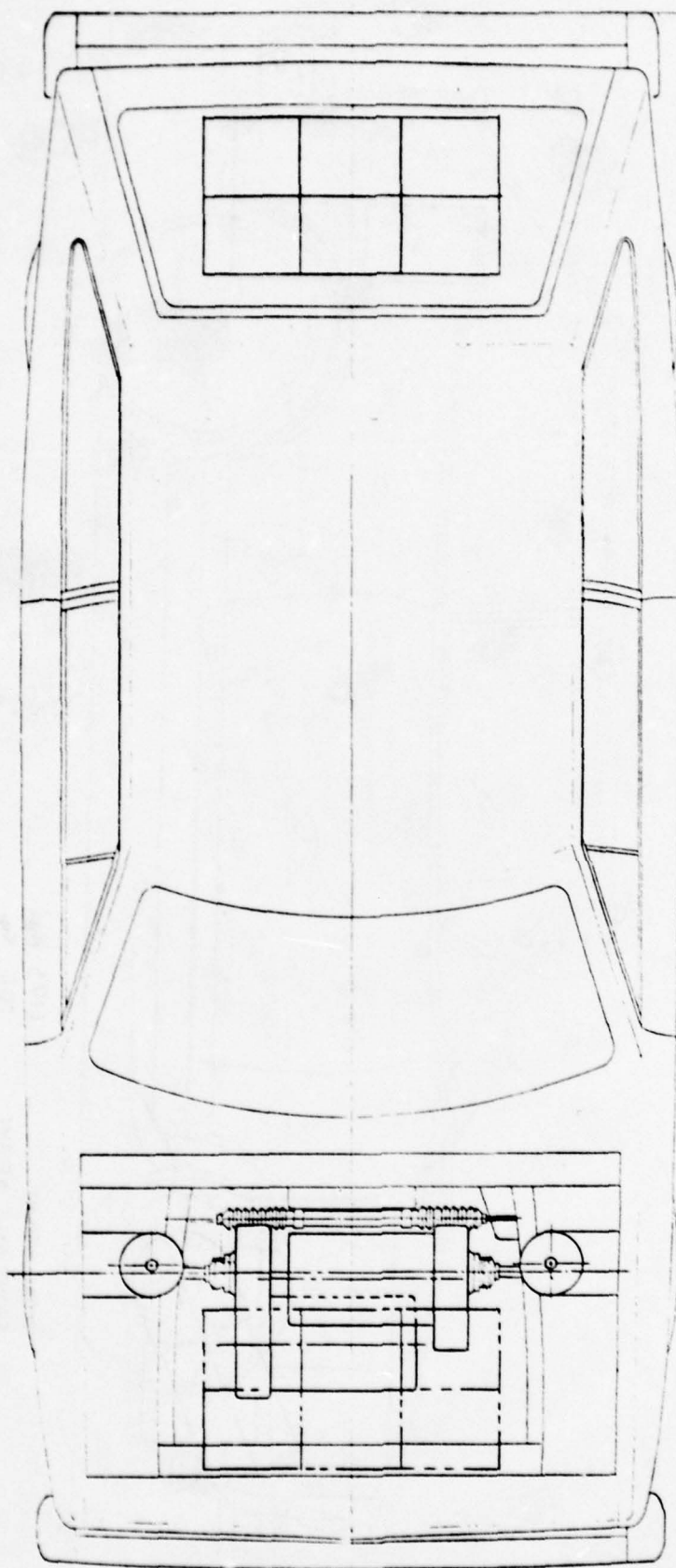
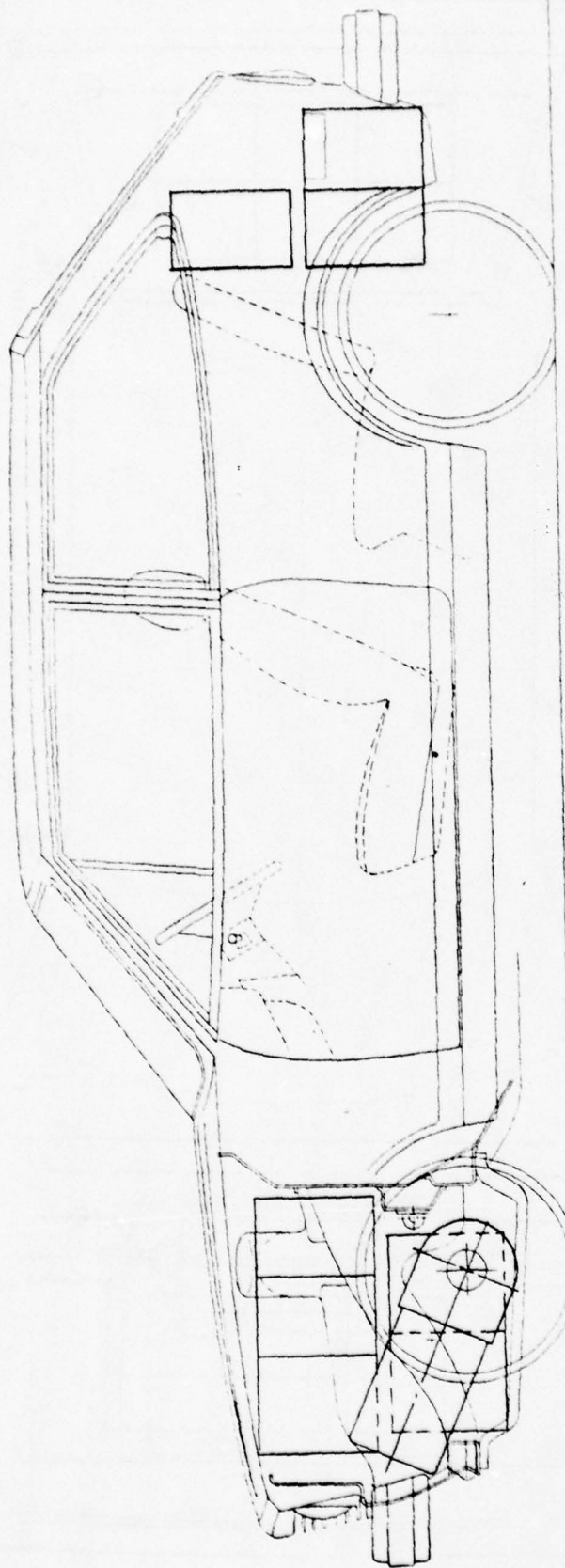


FIG. 13 a TWO ELECTRIC MOTORS WITH TWO TRANSMISSIONS
FRONT WHEEL DRIVE - LONGITUDINAL MOUNT



TOTAL WEIGHT	1195 Kg.
FRONT AXLE WEIGHT	702 Kg.
REAR AXLE WEIGHT	484 Kg.
WEIGHT DISTRIBUTION	F.59 / R.41
9 BATTERIES FRONT	
9 BATTERIES REAR	

FIG. 13 b

TWO ELECTRIC MOTORS WITH TWO TRANSMISSIONS
FRONT WHEEL DRIVE - LONGITUDINAL MOUNT

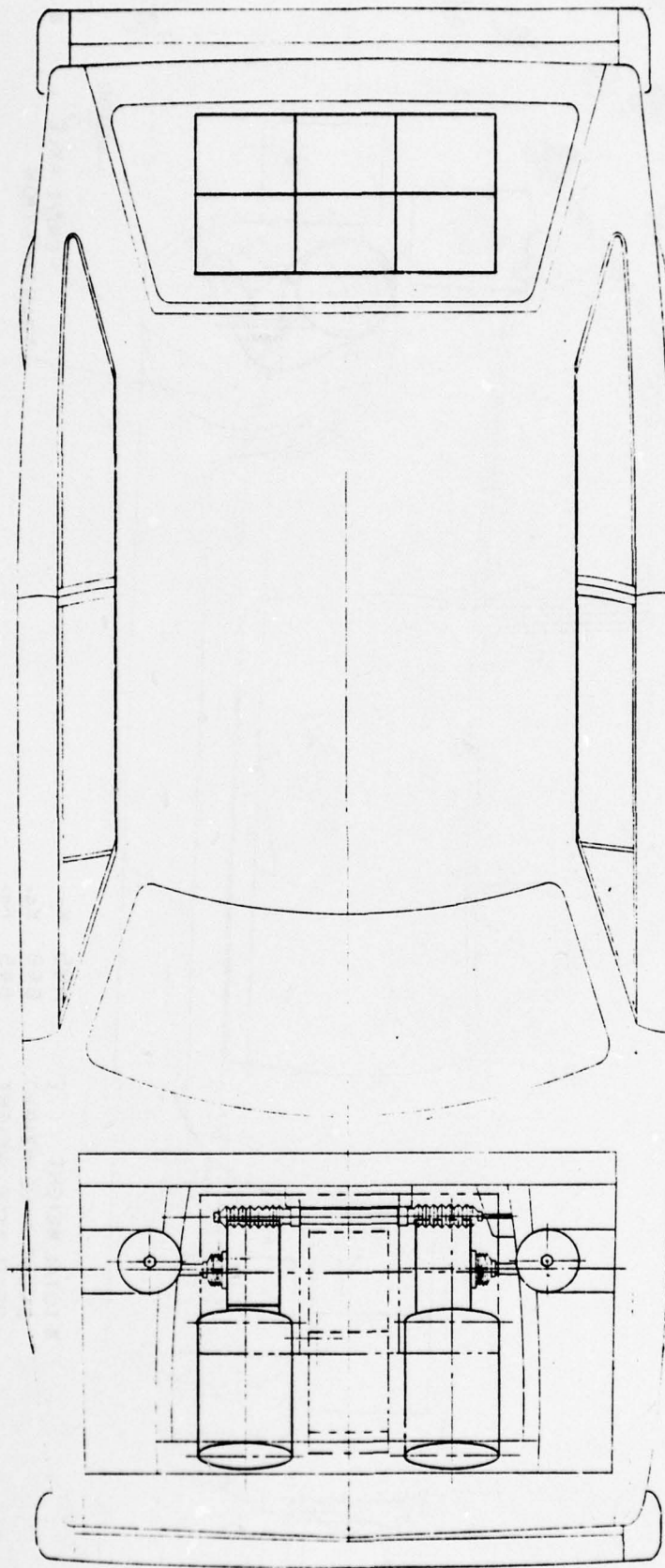
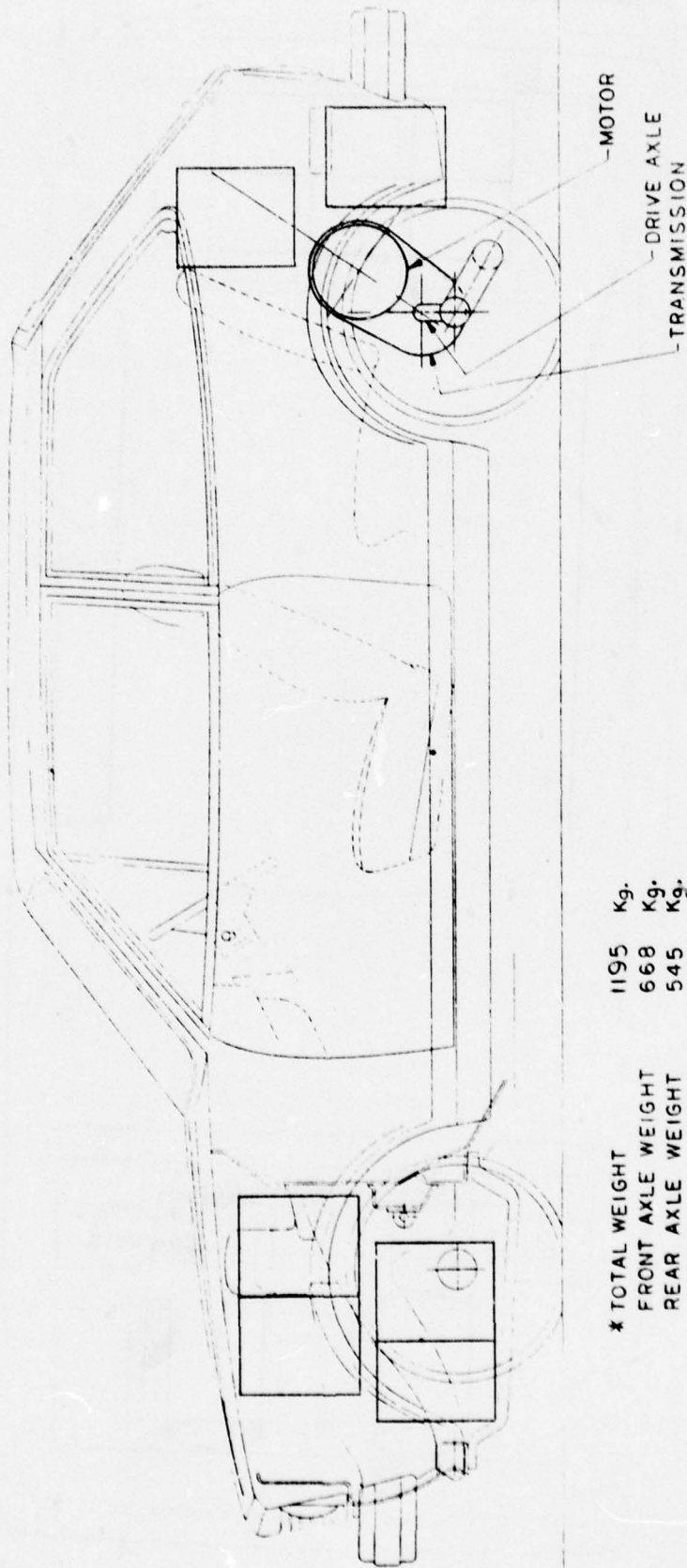


FIG. 14_a TWO ELECTRIC MOTORS AND SINGLE TRANSMISSION
WITH REAR WHEEL DRIVE AND MECHANICAL
OR ELECTRICAL* DIFFERENTIAL

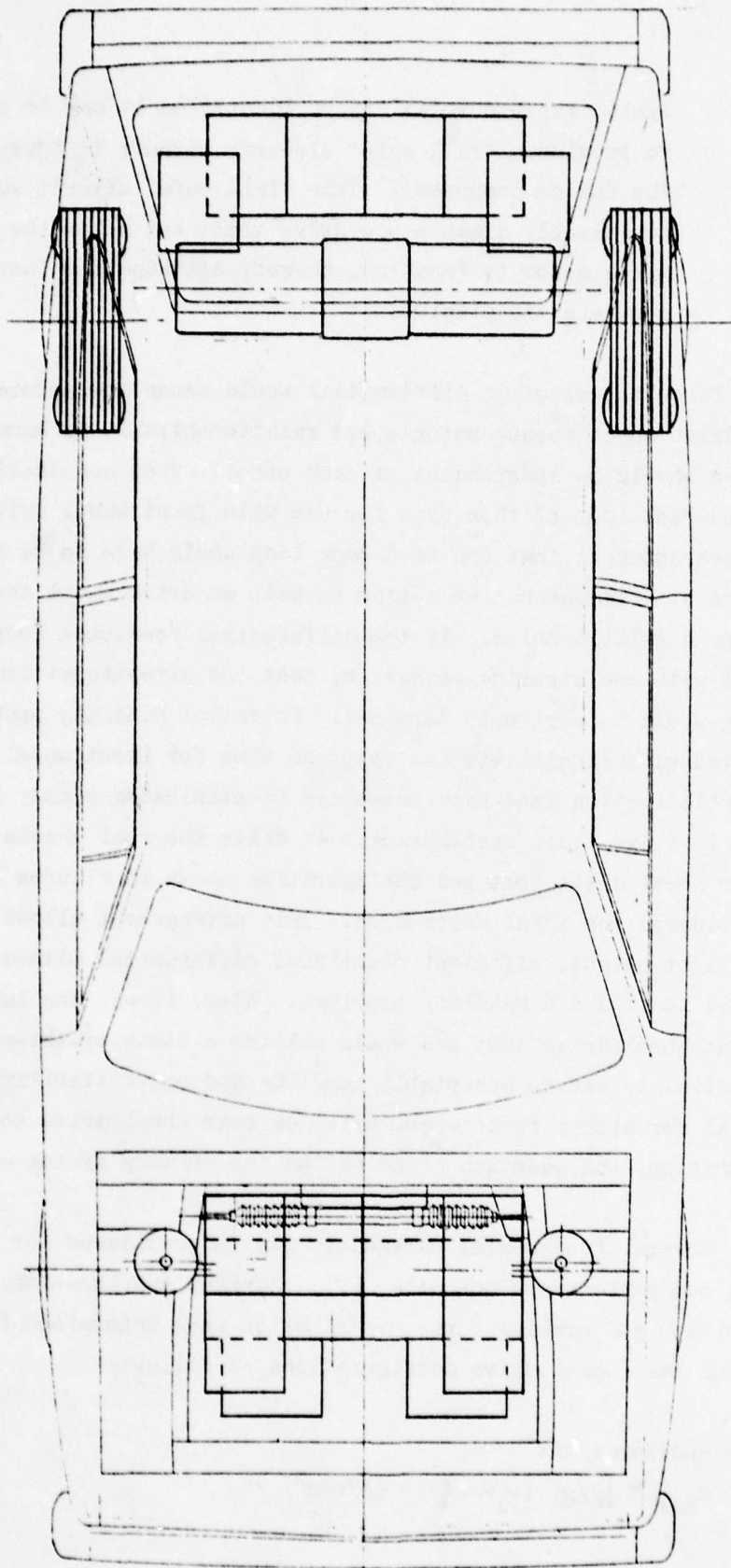


* TOTAL WEIGHT	1195	Kg.
FRONT AXLE WEIGHT	668	Kg.
REAR AXLE WEIGHT	545	Kg.
WEIGHT DISTRIBUTION	F.55 / R.45	
12 BATTERIES FRONT		
6 BATTERIES REAR		

* TOTAL WEIGHT WITH ELECTRICAL DIFFERENTIAL=1165 Kg

FIG. 14 b TWO ELECTRIC MOTORS AND SINGLE TRANSMISSION
WITH REAR WHEEL DRIVE AND MECHANICAL OR
ELECTRICAL DIFFERENTIAL

34



system failure modes can be identified it may be possible to provide a "fail safe" electric circuit to "jumper" the failed component. This "fail safe" circuit would conceivably disable one drive motor but allow the remaining drive motor to function, thereby allowing the test bed to complete its mission.

Since the electric differential would sense and automatically adjust drive wheel torque-motor speed relationships it is mandatory that the drive wheels be independent of each other. When considering the use of a feed-back loop of this type for use with front wheel drive arrangements, it becomes apparent that the feed-back loop would have to be expanded to sense the steering mechanism motion as well as drive wheel torque and motor speed relationships. If the differential feed-back loop did not interact with the steering mechanism, test bed directional control and handling would be seriously impaired. Potential handling problems associated with sensitivity and response time for front wheel drive differential action feed-back loops can be eliminated simply by using the same basic drive train configuration to drive the rear wheels. Therefore, the rear wheel drive test bed configuration shown in Figures 14a and 14b was considered the ideal compromise. This arrangement allows the use of the light-weight, efficient electrical differential without the potential control and handling problems. Also, it was concluded, the front wheel drive test bed would utilize a state-of-the-art mechanical differential to ensure acceptable handling and controllability. With the potential for either front wheel drive or rear wheel drive test bed configuration, the question of selecting the primary system was addressed.

Several fundamental parameters may be considered for an indication of test bed performance potential (2). Maximum acceleration, maximum gradeability and braking force distribution were determined for both front and rear wheel drive configurations as follows:

Maximum Acceleration:

$$a_{\max} = \left[\frac{g}{\mu} \right] (w_1 \mu - f) \quad (\text{m/sec}^2) \quad (6-1)$$

Maximum Gradeability:

$$G_{\max} = 100 (w_1 \mu - \frac{g}{g}) \quad (\%) \quad (6-2)$$

Braking Force Distribution:

$$\frac{B_{4f}}{B_{4r}} = \frac{[L_r + H (\mu + \frac{g}{g})]/L}{[L_f - H (\mu + \frac{g}{g})]/L} \quad (6-3)$$

Weight Distribution Factor: (nondimensional computational factor)

$$w_1 = f, r \quad w_f = \frac{L_r + \frac{g}{g} H}{L + \mu H} \quad w_r = \frac{L_f - \frac{g}{g} H}{L - \mu H} \quad (6-4)$$

where: H = height of test bed center of gravity from ground, cm

L = test bed wheel base, cm

L_f, L_r = distance from center of gravity to front and rear axles, cm

$\frac{g}{g}$ = gravitational constant, m/sec^2

$\frac{g}{g}$ = 1.4 (This factor is provided to represent the effect of rotating parts on the inertia mass of the test bed and is a function of the total reduction ratio between the prime mover and drive axles)

μ = .8 (This factor is a road adhesion coefficient and is valid for test bed operation on dry asphalt)

$\frac{g}{g}$ = .02 (This factor is the coefficient of rolling resistance)

For the front wheel drive configuration:

$$w_f = \frac{137 + .02 (56)}{229 + .8 (56)} = .50 \quad (6-5)$$

$$a_{\max} = \frac{9.8}{1.4} [.50 (.8) -.02] = 2.7 \text{ m sec}^{-2} \quad (6-6)$$

$$G_{\max} = 100 [.50 (.8) -.02] = 38\% \quad (6-7)$$

$$\frac{B_{4f}}{B_{4r}} = \frac{[137 + 56 (.8 + .02)]/229}{[92 - 56 (.8 + .02)]/229} = \frac{.80}{.20} \quad \begin{array}{l} \text{front brakes} \\ \text{rear brakes} \end{array} \quad (6-8)$$

For the rear wheel drive configuration:

$$w_r = \frac{103 - .02 (56)}{229 - .8 (56)} = .55 \quad (6-9)$$

$$a_{\max} = \frac{9.8}{1.4} [.55 (.8) - .02] = 3.2 \text{ m sec}^{-2} \quad (6-10)$$

$$G_{\max} = 100 [.55 (.8) - .02] = 42\% \quad (6-11)$$

$$\frac{B_{4f}}{B_{4r}} = \frac{[126 + 56 (.8 + .02)]/229}{[103 - 56 (.8 + .02)]/229} = \frac{.75}{.25} \quad (6-12)$$

As shown by the results of these calculations, the maximum acceleration potential of the rear wheel drive configuration is 19% greater than the front wheel drive configuration. The rear wheel drive version also has potential for 11% better gradeability and braking loads are more evenly distributed with the front brakes providing 75% of the total braking force. The front wheel drive version front brakes have to furnish 80% of the total braking requirement for that test bed propulsion system arrangement.

In view of the above findings the dual motor, single transmission, electrical differential rear wheel drive configuration (Figures 14a and 14b) was given primary consideration during the final study phase. The dual motor, single transmission with mechanical differential driving test bed front wheels was also given continued consideration as an alternative or backup test bed configuration. The detailed layouts for these configurations appear in Figures 15 and 16.

7.0 ELECTRIC PROPULSION SYSTEM MATHEMATICAL REPRESENTATION

In order to provide a test bed performance simulation computer model the performance characteristics of the electric propulsion system expressed mathematically was a primary requirement. Since it was apparent that the accuracy of the test bed performance calculations was totally dependent on the correctness of the mathematical representation of the

FIGURE 15
Preferred Test Bed Configuration

(Single Transmission with Independent Wheel Drive and Electrical Differential)

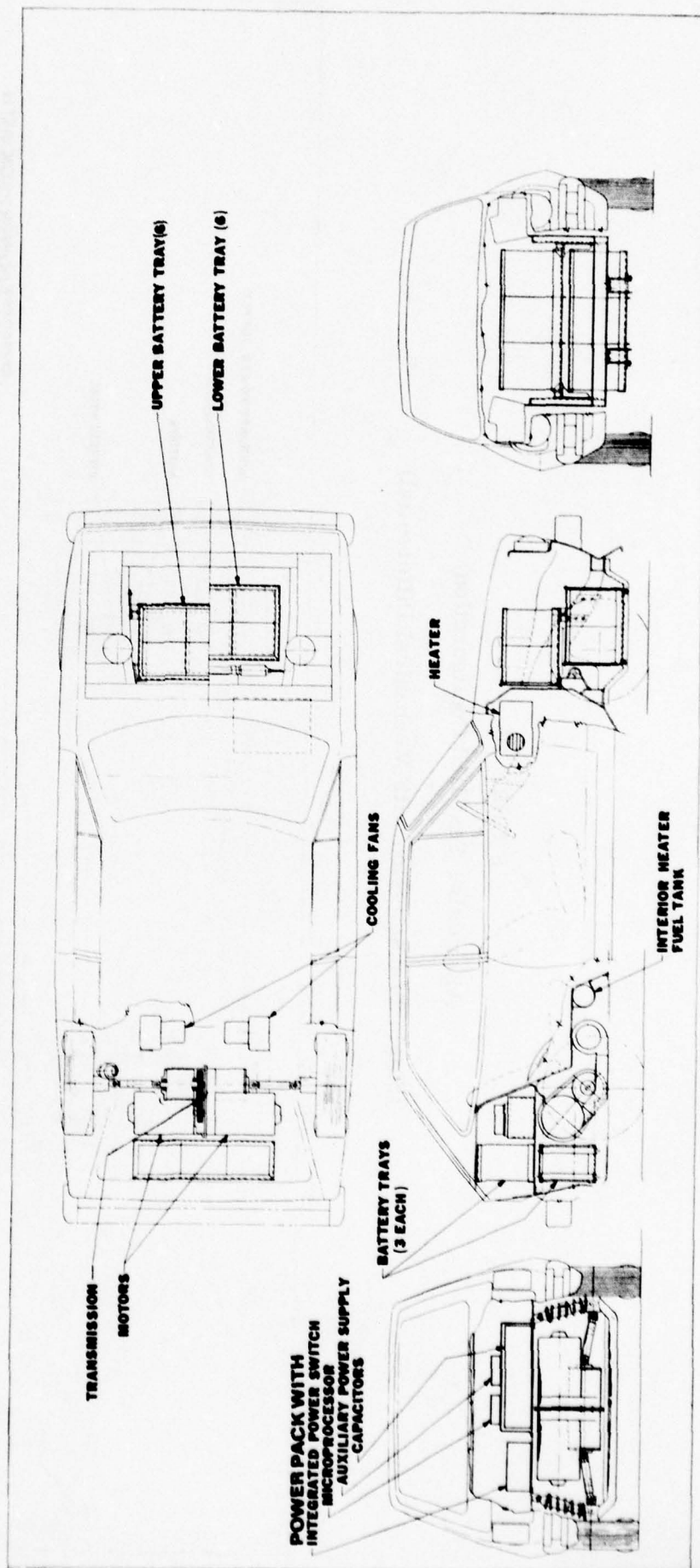
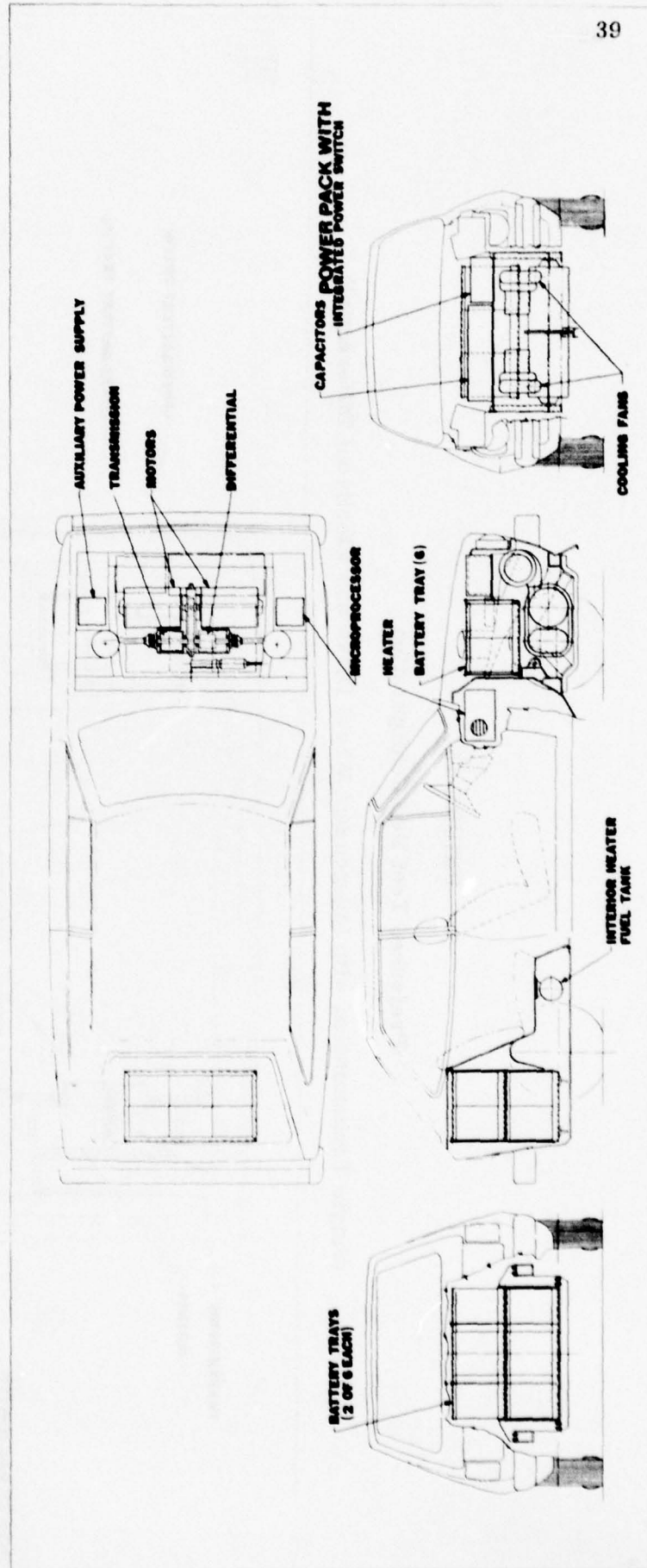


FIGURE 16
Alternative Test Bed Configuration
(Single Transmission with Mechanical Differential)



electric propulsion system, actual test data from a first generation breadboard electric propulsion system developed by MERADCOM to demonstrate the feasibility of such a system was utilized in the derivation of the equations used in the test bed performance computer model program described in section 8.0. It should be noted that the results of this study are conservative since the data used was conservative by present standards. Significantly superior test bed performance is anticipated with the use of the present MERADCOM electric propulsion system design. The test bed performance based on both existing propulsion system test data and the present MERADCOM propulsion system design will be discussed in section 8.0. The following sections describe in detail the basis for the development of the mathematical representation of the proposed electric propulsion system to be used in the test bed.

7.1 BATTERY MODEL

Accurate modeling of vehicle performance and range requires a precise model of the battery, both its capacity characteristics and voltage for all levels of charge. The available data was limited, but a reasonable representation of lead acid cell characteristics was defined. Battery characteristics are quite non-linear and are affected by environmental and previous usage history. The data reviewed indicated that some of the characteristics could be neglected for the study without seriously compromising the accuracy of the model. One of the characteristics that was ignored was the high initial voltage that is present when the cells are first taking off of a full charge cycle. The peak cell voltage in a 100% charge is assumed to be approximately 2.10 volts which is nominally obtained after the cell has had an opportunity to rest after being charged 100%. The other characteristic that was ignored was the rapid change in internal voltage and cell impedance as the charge is depleted below the nominal charge ratings. The effects of cell temperature on battery characteristics were ignored in all of the modeling presented.

The ampere-hour capacity of the battery is used to describe the charge or energy availability. This capacity characterization was chosen because of its general usage in describing batteries and its convenience

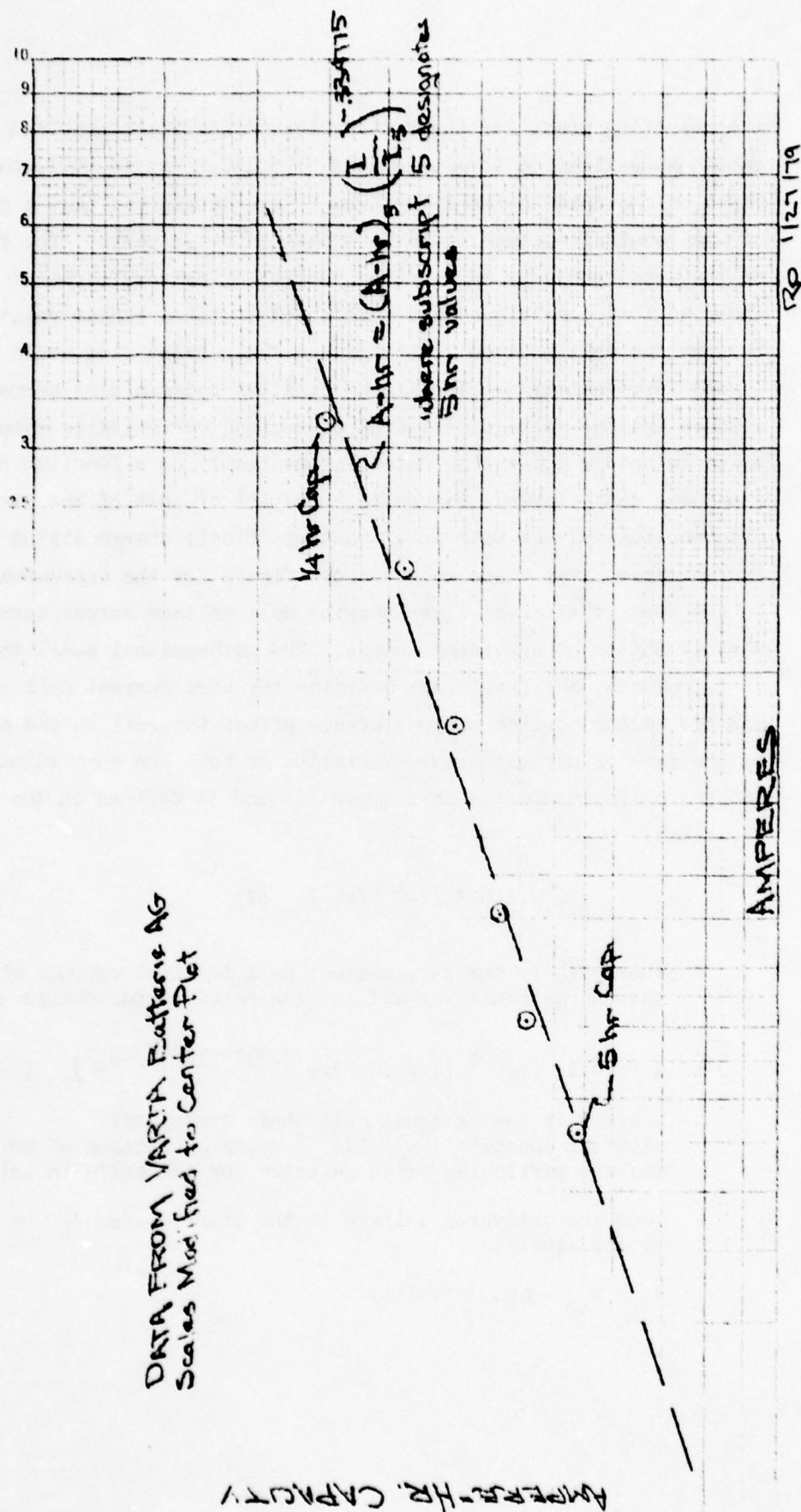
in matching the rest of the propulsion system modeling. For the performance range of interest a good model for the battery was developed based on catalog information published by VARTA Battery AG on one of their standard industrial batteries. The data shows that for continuous discharge rates, the battery capacity could be exponentially related to the published 5 hour rating used to define the cell size. In the vehicle, the battery is not subjected to constant discharge rates but is subjected to a continuously varying current draw. A technical paper from the Japan Storage Battery Company (5) shows that the cell capacity is directly related to the current history. Their test results show that under conditions of pulsed current applications that the used capacity was proportional to the peak current rates rather than to the average current rate. Based on their results, it was decided to model battery capacity for this study on the assumption that the charge used was a function of the instantaneous current being drawn. It was also assumed that this capacity removal rate was proportional to the relationship of the constant current capacities defined for this type of battery. The effect of constant current battery rates on capacity and the approximate mathematical model are shown in Figure 17. Equation 7-1 permits the calculation of the remaining charge in the battery for the actual ampere-hour discharge rate (Ahr), whereby the initial charge (Ahi) of the battery and the current amplitude for a 5 hr battery discharge rate (I_{5hr}) is used as reference.

$$Ahr = Ahi - \int_0^t I \left(\frac{I}{I_{5hr}} \right)^{3.348} dt \quad (A-hr) \quad (7-1)$$

Where Ahr is the charge remaining at time t, Ahi is the charge remaining at time 0, I is the instantaneous current and I_{5hr} the 5 hr rated capacity current. The charge remaining is given in terms of the 5 hr current rate.

Prediction of the battery terminal voltage as a function of capacity remaining and the instantaneous current draw is required to obtain the test bed acceleration performance characteristics. Available data that defined the battery potential as a function of charge state and current draw was not consistent. The data selected for developing the modeling equations was chosen primarily on the basis of the largest number of data points available. Although simplified, it is felt that

FIGURE 17
BATTERY CAPACITY VS. DISCHARGE CURRENT AMPLITUDE



the resulting model for the battery terminal voltage provides an accurate enough approximation to give a good propulsion system performance prediction. Based on the data in the literature it was determined that a description of the terminal voltage could be broken into two parts. The first part of the model would be an equation describing battery terminal voltage under no load conditions, and this coupled with a linear relationship between the delivered cell voltage and the current flow would provide a good representation. The linear relation between zero current cell voltage and the voltage delivered at various current draw rates is ohmic in nature and was adjusted exponentially as a function of the remaining cell charge. Figure 18 is a plot of some of the available data showing voltage both as a function of cell charge status and the current draw rate. Also shown on the figure are the approximations in the form of straight lines showing cell voltage versus current at various states of remaining charge. The mathematical model thus is in two pieces, the first part defining the zero current cell voltage and the second portion the resistance effect internal to the cell caused by the rate of current draw. Variation of both the open circuit cell voltage and the ohmic resistance is exponential and is defined in the following equations:

$$V_{to} = 2.1e^{-.11025 (1 - Ahr/Ah_5)} \quad (V) \quad (7-2)$$

Where V_{to} is the zero current cell terminal voltage with Ahr the charge remaining and Ah_5 the rated 5 hour charge capacity.

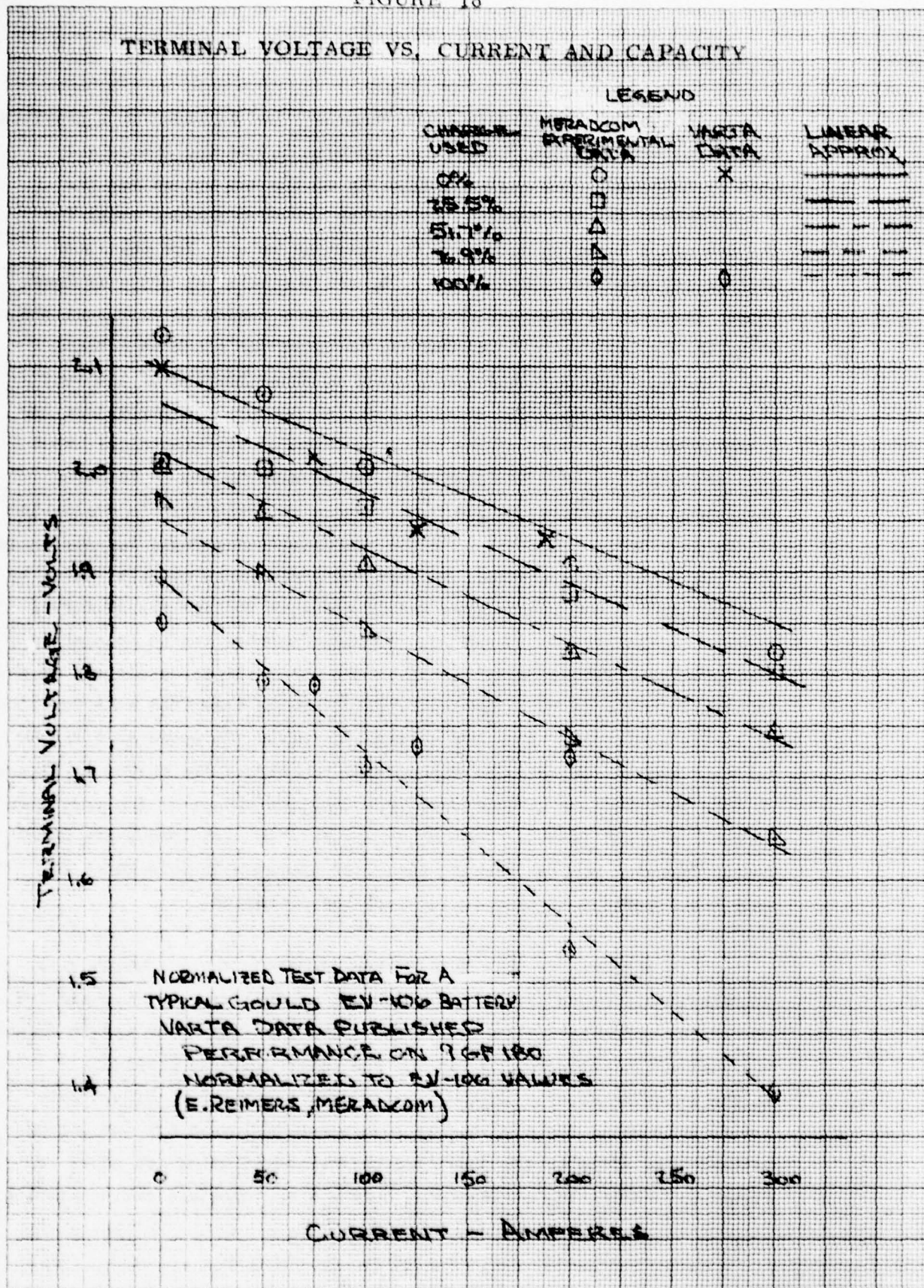
$$R = (4.1) (10)^{-4} [1 + .01772e^{3.839 (1 - Ahr/Ah_5)}] \quad (\text{ohms}) \quad (7-3)$$

Where R is the internal cell ohmic resistance with the constant $(4.1) (10)^{-4}$ being a function of cell size and the particular value selected for the cells in this study.

Thus the delivered voltage to the motor drive, V_t is defined by the equation

$$V_t = V_{to} - IR. \quad (\text{volts}) \quad (7-4)$$

FIGURE 18



46 1512

 10 X 10 TO THE CENTIMETER 10 X 10 CM
 10 X 10 TO THE CENTIMETER 10 X 10 CM

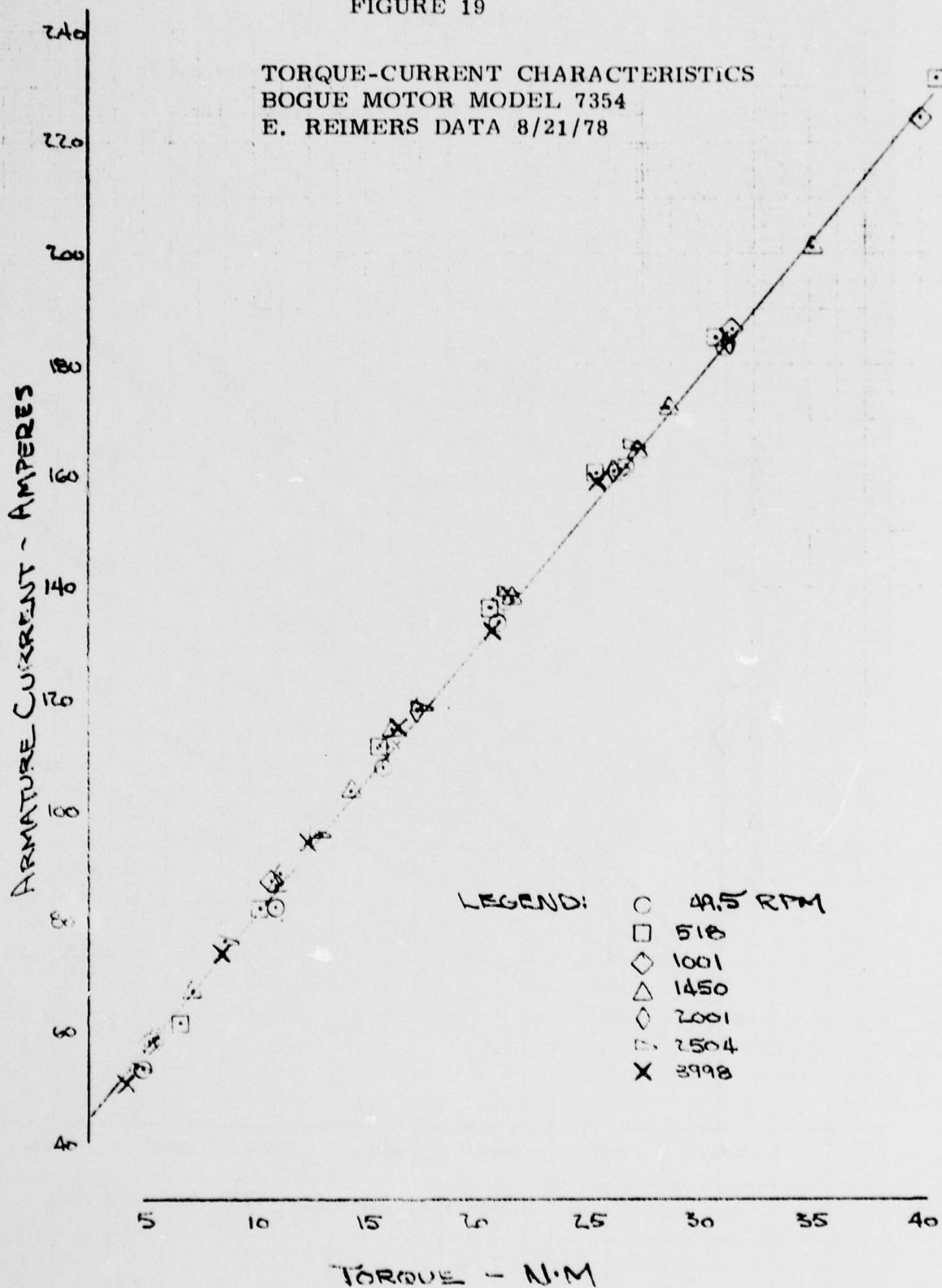
7.2 DC Motor Model

The motor being designed for the test bed is based on a previous model that was designed, built, and has been tested and extensively used by MERADCOM. The design similarity of the two motors was the justification for the decision to develop the mathematical model for the new motor based on data from the existing motor. The new motor will be referred to as Model No. 7896, and the existing motor as Model 7354. To minimize the complexity of equations needed to represent the motor in the test bed, it was decided to treat the motor as a "black box." The best representation was based on an evaluation of the test data available on the 7354 model. A set of performance parameters was established that described the motor in terms of its electrical input and its output power. The data used for developing the performance parameters was provided by Eberhart Reimers of MERADCOM. An evaluation of the data indicated that the motor characteristics could be represented with reasonable accuracy for the test bed performance computer model by a torque armature current curve and an armature voltage set of curves as depicted in Figures 19 and 20. Armature current can be accurately described as a linear relationship to the motor torque developed, as shown in detail in Figure 19. The armature voltage is described as a function of torque and speed. Armature voltage is related to speed as a linear function and to torque as an exponential function. The curves in Figure 20 show that this is a reasonable approximation except at the very high torque-low speed levels. The inaccuracy in this high torque-low speed region is not a problem because the motor operates in this range for very short periods of time during test bed operation.

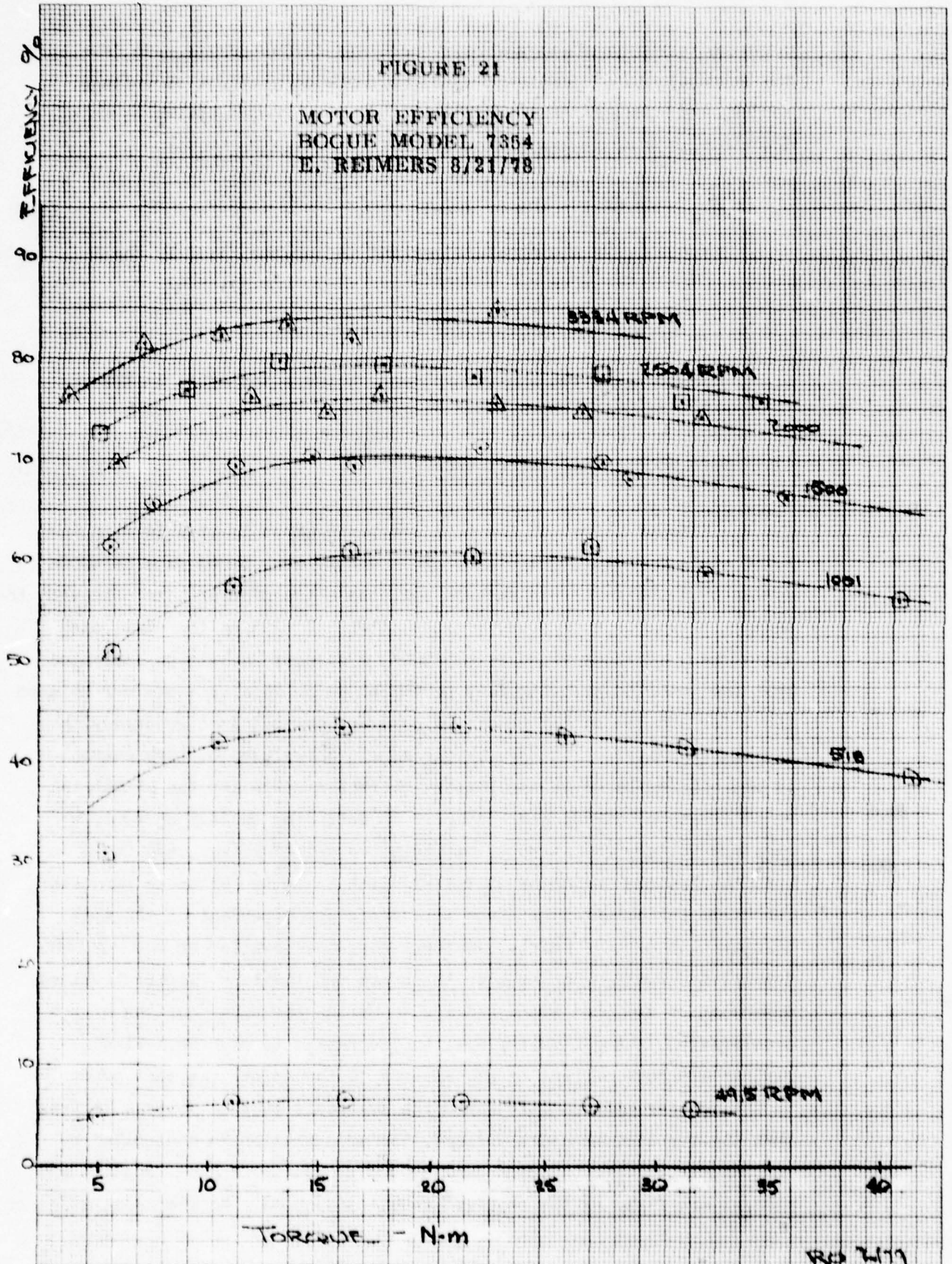
To extrapolate this data to the new motor design, which will operate at different speeds and different power levels, it was decided to use the characteristics established with the test motor and to assume that the efficiency profile for the new motor would be identical to the existing motor. However, later data shows these curves to be low by 2 to 3% at the high torque levels and 9% low at the low torque values. The efficiencies developed by the tested motor are shown in Figure 21. Using these efficiency curves a new armature current-torque

FIGURE 19

TORQUE-CURRENT CHARACTERISTICS
 BOGUE MOTOR MODEL 7354
 E. REIMERS DATA 8/21/78



46 1512

K&E 10 X 10 TO THE CENTIMETER
FLUORIN & EBER CO. WILSON, N.J.

curve and armature voltage versus speed and torque curves were developed. The extrapolated or predicted motor performance in terms of voltage, torque, and speed is that shown in Figure 20. The resulting equations describing the motor are listed below:

$$I_A = .0788 T + 108 \quad (\text{amps}) \quad (7-5)$$

Where I_A is the armature current in amperes and T is the torque in Newton-meters (N-m).

$$V_A = (N + 760) (1.37 \times 10^{-4}) (T)^{.56} + 3.1$$

Where V_A is the armature voltage, N the motor speed in RPM and T the torque.

7.3 Motor-Controller Performance

A major aspect of the test bed performance is tied in with the solid state dc motor controller. This controller, based on a MERADCOM design by E. Reimers,* in essence performs a transformer action between the battery as a source of power and the motor. Utilizing the worst case experimental data provided by MERADCOM, a cursory evaluation indicated that the motor power controller performed as an ideal transformer between the motor and the batteries with a constant current loss accompanying the transformation. In the vehicle model, therefore, battery current is established based on the battery characteristics and the calculated motor armature current and voltage. To determine battery current, armature voltage and current, an iterative procedure was used based on both the battery and motor characteristics to solve for these parameters. The steps for calculating these parameters are dependent on the mode of operation of the vehicle, whether under acceleration or in a cruising condition. During acceleration there are two limiting factors involved, depending on test bed speed and load. During the early portion of the acceleration, the controller will be programmed to provide a fixed maximum armature current of 380 amperes to the motor. At that point in the acceleration profile where the available battery voltage is less than the required armature voltage, the acceleration is controlled by the battery voltage. During cruise conditions the armature voltage and current are fixed by the required torque and speed. In the calculation of

* (Refer to references 6, 7, 8, 9 for detailed information)

battery current, it is assumed that there is a constant 9 amperes added to the ideal transformed current required by the armature. Later evaluations of the data on the transforming action of the controller have indicated that the efficiency of this transformer action was not represented accurately by adding the constant 9 amperes to the ideal transformer current level at the battery. This later evaluation indicated that the power lost in the transforming action is greater at the very high current levels. A cursory evaluation of this modeling error does indicate, however, that it would not have a significant impact on the predicted vehicle and battery performance since there is limited operation at the very high current levels.

REGENERATIVE BRAKING

To describe the motors in the regenerative braking mode, where the motor is acting as a generator instead of a motor, it was decided that the most accurate representation without actual test data was to assume that the generating performance was a mirror image of the motoring performance. Parameterization for this was achieved by changing the signs of the voltage and the current along with the signs for the torque and the speed in the model equations during regenerative braking. Regenerative power, of course, is not available until motor speed and torques are high enough to exceed the thresholds of the region where the motor is neither motoring nor generating. The motor controller was assumed to perform the same transforming function during generation as motoring with a constant current loss in converting the generator power and recharging the batteries. Battery input characteristics were assumed to be a mirror image of their discharge characteristics. For a given charge level, the same internal ohmic resistance and zero current cell potential was assumed to exist and that the input current was a function of this resistance and the cell potential. To account for the out-gassing potential of the battery when being over-charged and the fact that the charging current that is causing the gassing does not result in any energy transfer into the battery, the amount of current credited to recharging was limited by calculation of an acceptable charge rate. The acceptable recharge rate was based on the so-called "ampere-hour rule" which says that the acceptable charge rate for the battery is

directly proportional to its state of charge times its ampere-hour rating. There are discrepant papers indicating both that this "ampere-hour rule" is conservative and nonconservative, but it appears to be the only reasonable relationship that could be used to define the battery's charge status and the rate at which it could be recharged (10). There are indications that the industry is developing techniques to enhance the charge rate acceptability of a battery, but no attempt was made to factor this into the test bed performance modeling program.

8.0 TEST BED PERFORMANCE COMPUTER MODEL AND OPTIMIZATION

In order to project the range and performance of the electric propulsion system test bed, a computer model was developed to simulate the SAE J227a Test Procedure. The following table lists the primary objectives of this computer model.

TABLE II
MODELING PROGRAM OBJECTIVES

- A. Model "Electric Vehicle Test Procedure - SAE J227a"
 - 1. Simulate the various parameters required by J227a.
 - 2. Modeling program should accept any of the four driving cycles defined by J227a.
 - 3. Optimize vehicle performance under the conditions of J227a.
- B. Make model flexible enough to simulate different vehicle configurations
 - 1. Consider different transmission types.
 - a. 1 through 5 speed fixed ratio transmissions
 - b. Infinitely variable transmissions
 - c. Capability for variation of transmission shift point
 - 2. Vehicle weight.
 - 3. Vehicle aerodynamic drag coefficient.
 - 4. Motor characteristics.
 - 5. Vehicle weight distribution.
- C. Determine Optimum Vehicle Transmission
 - 1. Shift point flexibility.
 - 2. Overall test bed performance.

An important aspect of the modeling program was involved with providing the flexibility for making the model a useful tool for choosing an optimum test bed configuration.

Of primary importance was the ability to simulate several drive train configurations. The program is capable of modeling one through five speed fixed ratio transmissions and infinitely variable transmissions. A final drive ratio is included as a separate input, as are the transmission shift points at specified motor speeds. Although the specified driving cycle to be modeled was SAE-J227a schedule D, schedules A, B, and C of J227a can also be simulated.

8.1 Computer Model

To predict the performance of the proposed state-of-the-art test bed, a computer model was developed to simulate the SAE J227a test procedure. The program is entitled "ERAB" and is described in detail in this section of the report.

ERAB Program
Operational Description

I. START-UP

- A. Place ERAB cassette in transport.
- B. Press LOAD, EXECUTE, RUN.

II. ENTERING AND EDITING DATA

- A. Enter file number 1-5 or L (for List all files) or N (for New).
- B. If you entered N, go to Step P.
- C. If you entered a file number, go to Step G.
- D. If you did not enter L, go to Step A.
- E. The program will display and print each file's date and title.
- F. Go to Step A.
- G. The program will print the file date and title and ask if it is the proper file.
- H. Enter Y or N to indicate that it is or is not the desired file.
- I. If you entered N, go to Step A.
- J. If you did not enter Y, go to Step H.
- K. Enter R (for Run), E (for Edit), or L (for List).
- L. If you entered E, go to Step P.
- M. If you entered L, go to Step OO.
- N. If you did not enter R, go to Step K.
- O. Go to Part III.

- P. Enter date and title, cruising speed, acceleration time, cruising time, coasting time, braking time, idling time, speed at which linear acceleration is to begin, change in velocity during linear acceleration, and analysis time resolution.
- Q. Enter F (for front-wheel) or R (for rear-wheel) drive.
- R. If you entered neither F nor R, go to Step Q.
- S. Enter Y if regenerative braking is to be used, N if it is not.
- T. If you entered neither Y nor N, go to Step S.
- U. Enter vehicle weight, fraction of weight over front wheels, center of gravity height, wheelbase, rolling radius of tires, wheel moment, motor moments, battery capacity, frontal area, drag coefficient, air pressure, air temperature, wind speed, and angle of wind to direction of travel.
- V. If you did not enter E at Step K, go to Step AA.
- W. Enter Y if transmission is okay, otherwise enter N.
- X. If you entered N, go to Step AA.
- Y. If you did not enter Y, go to Step W.
- Z. Go to Step GG.
- AA. Enter the number of ratios in transmission (0 for an infinitely variable transmission).
- BB. If you did not enter 0, go to Step EE.
- CC. Enter maximum and minimum reduction ratios, maximum motor speed and final drive ratio.
- DD. Go to Step GG.
- EE. Enter final drive ratio and motor shift speed.
- FF. Enter all reduction ratios.
- GG. Enter Y if you wish to record data, otherwise enter N.
- HH. If you entered N, go to Step K.
- II. If you did not enter Y, go to Step GG.

- JJ. Enter a file number.
- KK. If the file number was not in the range 1-5, go to Step JJ.
- LL. If the calculator displays, "Put tape in RECORD POSITION", remove the tape from the transport, slide the record tab into the record position, and replace the tape in the transport.
- MM. When the calculator is finished recording the data, remove the tape, slide the record tab into the write protect position, and replace the tape.
- NN. Go to Step K.
- OO. The calculator will print a list of the data in the requested file.
- PP. Go to Step GG.

III. RUNNING THE ANALYSIS PROGRAM

- A. The calculator will run through all of the ERAB performance model, and print out the results.
- B. Go to Part II, Step K.

8.1.2 Explanation of Data Input

The data entry section of the modeling program allows the user to model a wide range of test conditions and test bed configurations. Figure 22, a sample input data listing, will be the reference throughout the description of the data inputs.

FIGURE 22

Sample Listing of Input Data
Schedule "D" ,2-speed Trans.

Accel. to what speed? (KPH)	72.000	
Accel. in How Much Time (sec)	28.000	
Cruise in How Much Time (sec)	50.000	
Coast in How Much Time (sec)	10.000	
Brake in How Much Time (sec)	9.000	
Idle in How Much Time (sec)	25.000	
Speed to Begin Linear Accel(KPH)	70.000	
Linear Accel. Delta Velocity (KPH)	2.000	
Time Increment for calcs (sec)	0.200	
Rear Wheel Drive :		
Regenerative Braking Used		
Vehicle Weight (KG)	1245.000	*
Fraction of Weight on Front Wheels	0.560	
Center of Gravity Height (cm)	56.000	
Wheelbase (cm)	228.600	
Rolling Radius of tires (cm)	28.000	
Mom. of Inertia of Wheels (N-m-m)	4.160	
Moment of Inertia of Motors (N-m-m)	0.502	
Battery Amp-hr capacity (5hr discharge)	180.000	
Frontal Area in direc. of travel (sq.m)	1.670	
Wind Drag Coefficient	0.420	
Barometric Pressure (mm Hg)	760.000	
Ambient Temperature (C)	20.000	
Wind Velocity (KPH)	0.000	
Ang. of wind to Dir. of Trav.(deg)	0.000	
2 SPEED TRANSMISSION		
Final Drive Ratio	5.000	
Motor Shift Speed (rpm)	4500.000	
Ratio # 1	2.00	
Ratio # 2	1.00	

* Weight includes 80 kg driver

Note: Moment of inertia is expressed in weight units throughout this section

$$\begin{aligned} \text{i.e. mass inertia} &= \int dm y^2 \\ \text{weight inertia} &= \int dw y^2 \end{aligned}$$

$$\text{Since } dw = dm \cdot g = \text{kg} \frac{\text{m}}{\text{sec}^2} = \text{N}$$

$$\text{Weight inertia} = \text{N m}^2$$

Explanation of Data Input

A) Driving Cycle Definition

The first six inputs allow the user to define any of the four driving schedules presented by J227a. The inputs are as follows:

1. Speed at end of acceleration, i.e. cruise speed (kph)
2. Time allowed to reach cruise speed (sec.)
3. Time spent at cruise speed (sec)
4. Time spent coasting (sec)
5. Braking time to zero speed (sec)
6. Idle time at zero speed (sec)

B) Acceleration Path

Provided that the test bed has the capability of accelerating to cruise speed in less than the allotted time, the speed-time curve can be varied. This is done by specifying a linear acceleration section in combination with maximum available acceleration. The inputs are as follows:

1. Speed to begin linear acceleration (kph)
2. Linear acceleration delta velocity (kph)

C) The time increment used in calculations is a variable input that allows the program user to change the accuracy of calculations and the time of program execution. Reasonable values for the time increment are: .05, .1, .2, .25, .5, sec.

D) Test bed configuration/specifications

This group of inputs allows the user to describe the test bed:

1. Front or rear wheel drive.
2. The option of using regenerative braking.
3. Total test bed weight (kg)
4. Fraction of weight on front wheels.
5. Height from ground to test bed center of gravity (cm)
6. Test bed wheelbase (cm)
7. Moment of inertia of each wheel, including tire (N-m-m)
8. Moment of inertia of motor(s) total (N-m-m)
9. Battery ampere-hr capacity for 5 hour discharge
10. Test bed frontal area (m²)
11. Test bed aerodynamic drag coefficient.

E) Ambient conditions of test

These variables are used in aerodynamic drag force calculations.

1. Barometric pressure (mm hg)
2. Air temperature ($^{\circ}\text{C}$)
3. Wind velocity (kph)
4. Wind angle, e.g. 0° = head wind, 180° = tail wind.

F) Transmission information

This section allows two types of transmissions to be modeled; multiple fixed ratio and infinitely variable ratio.

Multiple fixed ratio trans.

1. Number of ratios in transmission
2. Final drive ratio
3. Motor speed where shifting
4. Transmission ratios

Infinitely variable ratio trans.

1. Maximum reduction ratio
2. Minimum reduction ratio
3. Motor constant shift speed
4. Final drive ratio

8.1.3 Explanation of Computer Printout

The following is a print out from the ERAB electric test bed performance simulation program. It will be referred to throughout this section.

The computer printout consists of three parts:

- A) Test bed performance at three initial battery charge levels: 90%, 30%, and 10%.
- B) Range at constant speed, at incremented speeds and incremented grades.
- C) Test bed performance results under J227a at point of complete battery discharge.

The following parameters are printed at each charge level:

Maximum acceleration: The amount of time taken to accelerate from rest to the indicated speed, at full motor power.

Maximum gradeability: The largest grade that the test bed can maintain at the corresponding velocity is determined. If the printout reads:

SAE J227a TEST PROCEDURE

90.0 Percent Charge Remaining

60

MAXIMUM ACCELERATION
Speed (KPH) Time (sec)

0 to 10	1.33
0 to 20	2.63
0 to 30	3.95
0 to 40	5.74
0 to 50	8.32
0 to 60	11.27
0 to 70	15.09
0 to 80	20.30
0 to 90	27.94
0 to 100	40.37

MAXIMUM GRADABILITY
Speed (KPH) Percent Grade

0	24.2
10	24.2
20	24.1
30	21.0
40	13.9
50	10.5
60	8.9
70	6.5
80	4.6
90	3.0

SCHEDULE "D" DRIVING CYCLE

ACCELERATION

Time (sec)	Speed (KPH)	Motor (RPM)	Torque (N-M)	Motor (HP)	Drive L (HP)	Wind L (HP)	Poll L (HP)	Battery Voltage	Armature Voltage	Battery Current	Armature Current	Motor Efficiency
0.0	0.00	0.0	88.12	0.00	0.00	0.00	0.00	105.9	26.1	101.9	380.0	0.0
1.0	7.43	703.8	88.12	9.71	0.51	0.00	0.40	103.6	44.5	172.5	380.0	38.3
2.0	15.17	1437.1	88.12	17.78	1.04	0.04	0.82	100.0	63.8	251.5	380.0	54.7
3.0	22.89	2169.2	88.12	26.83	1.78	0.15	1.24	96.0	83.0	337.3	380.0	63.5
4.0	30.37	2877.4	77.95	31.46	2.20	0.34	1.67	95.1	95.2	357.6	348.3	70.8
5.0	36.35	3443.2	62.72	30.33	2.12	0.58	2.01	97.2	97.3	310.7	301.6	77.1
6.0	41.18	3901.2	53.51	29.32	2.05	0.85	2.29	98.6	98.6	282.3	273.2	81.1
7.0	45.27	4298.3	47.20	28.43	1.93	1.12	2.53	99.5	99.5	262.8	253.7	84.0
8.0	48.87	4615.0	42.12	28.65	2.01	1.42	2.75	95.2	86.8	355.6	380.0	64.9
9.0	52.43	4813.7	39.12	30.74	2.15	1.75	2.96	94.2	91.2	377.1	380.0	56.1
10.0	55.94	4949.6	35.47	31.80	2.23	2.12	3.17	94.0	94.1	381.1	321.8	67.9
11.0	59.18	5003.3	30.13	31.55	2.21	2.51	3.37	94.8	94.8	364.4	355.3	69.8
12.0	62.16	5044.2	25.79	31.33	2.19	2.91	3.56	95.4	95.4	351.2	341.0	71.6
13.0	64.90	5074.1	22.03	31.10	2.18	3.31	3.73	95.9	96.0	339.6	330.3	73.1
14.0	67.44	5194.5	18.73	30.83	2.16	3.72	3.89	96.4	96.4	328.1	320.1	74.5
15.0	69.80	5304.3	15.97	30.53	2.14	4.12	4.04	96.9	96.9	320.9	311.6	75.7
16.0	72.39	5374.1	12.48	30.24	0.74	4.23	4.08	106.9	56.1	102.2	177.4	78.8
17.0	70.56	3342.0	22.53	10.57	0.74	4.26	4.09	106.3	56.3	102.5	177.5	78.9
18.0	70.72	3350.0	22.59	10.62	0.74	4.29	4.10	106.6	56.5	102.9	177.7	79.0
19.0	70.89	3357.9	22.63	10.67	0.75	4.32	4.12	106.8	56.6	103.3	177.8	79.1
20.0	71.06	3365.9	22.68	10.72	0.75	4.35	4.13	106.8	56.8	103.6	178.0	79.1
21.0	71.23	3373.0	22.72	10.77	0.75	4.39	4.14	106.9	56.9	104.0	178.1	79.2
22.0	71.39	3381.8	22.77	10.82	0.75	4.41	4.15	106.8	57.1	104.3	178.3	79.2
23.0	71.56	3389.7	22.82	10.86	0.76	4.44	4.16	106.8	57.3	104.7	178.4	79.3
24.0	71.73	3397.6	22.87	10.91	0.76	4.47	4.17	106.7	57.4	105.1	178.5	79.4
25.0	71.90	3405.6	22.92	10.96	0.77	4.51	4.18	106.7	57.5	105.4	178.8	79.4
26.0	72.06	3413.5	22.97	11.01	0.77	4.54	4.19	106.7	57.7	105.8	178.9	79.5
27.0	72.23	3421.5	23.02	11.06	0.77	4.57	4.20	106.7	57.9	106.2	179.1	79.6
28.0	72.40	3429.4	23.07	11.11	0.78	4.60	4.21	106.7	58.1	106.5	179.2	79.6

CRUISE

29.0	72.40	3429.4	19.58	9.43	0.66	4.56	4.21	107.3	53.5	93.0	158.4	79.0
79.0	72.40	3429.4	19.58	9.43	0.66	4.56	4.21	107.3	53.5	93.0	158.4	79.0

90.0 Percent Charge Remaining

COAST

Time (sec)	Speed (KPH)	Water (SPM)	Torque (N-M)	Drive L (HP)	Wind L (MP)	Poll L (HP)	Battery Voltage	Armature Voltage	Battery Current	Armature Current	Recharge Current	Gen. Eff.
77.0	72.40	3459.4	0.00	0.62	4.60	4.21	110.9	0.0	0.0	0.0	0.0	0.0
79.0	71.40	3391.4	0.00	0.60	4.44	4.15	110.9	0.0	0.0	0.0	0.0	0.0
80.0	70.41	3344.5	0.00	0.58	4.26	4.09	110.9	0.0	0.0	0.0	0.0	0.0
81.0	69.44	3299.4	0.00	0.57	4.03	4.02	110.9	0.0	0.0	0.0	0.0	0.0
82.0	68.42	3253.0	0.00	0.55	3.92	3.95	110.9	0.0	0.0	0.0	0.0	0.0
83.0	67.54	3209.1	0.00	0.54	3.76	3.90	110.9	0.0	0.0	0.0	0.0	0.0
84.0	66.61	3164.0	0.00	0.52	3.60	3.84	110.9	0.0	0.0	0.0	0.0	0.0
85.0	65.69	3120.4	0.00	0.51	3.46	3.78	110.9	0.0	0.0	0.0	0.0	0.0
86.0	64.79	3077.5	0.00	0.49	3.32	3.73	110.9	0.0	0.0	0.0	0.0	0.0
87.0	63.90	3035.1	0.00	0.48	3.13	3.67	110.9	0.0	0.0	0.0	0.0	0.0
88.0	63.02	2993.3	0.00	0.47	2.95	3.61	110.9	0.0	0.0	0.0	0.0	0.0

BRAKE

Time (sec)	Speed (KPH)	Water (SPM)	Torque (N-M)	Drive L (HP)	Wind L (MP)	Poll L (HP)	Battery Voltage	Armature Voltage	Battery Current	Armature Current	Recharge Current	Gen. Eff.
89.0	55.95	2646.0	88.12	0.37	2.11	3.17	124.6	95.5	282.2	380.0	23.2	67.3
90.0	49.98	2315.3	98.12	0.29	1.42	2.75	123.5	96.8	259.1	380.0	23.2	64.8
91.0	41.90	3959.0	60.23	0.23	0.89	2.33	122.9	106.4	245.4	293.9	23.2	80.1
92.0	34.91	3307.5	60.72	0.17	0.52	1.93	121.6	92.8	216.4	295.4	23.2	76.7
93.0	27.93	2646.0	61.12	0.13	0.26	1.53	120.2	79.0	185.9	296.7	23.2	72.3
94.0	20.95	1994.5	61.44	0.09	0.11	1.14	118.7	65.0	154.0	297.6	23.2	66.0
95.0	13.97	1323.0	61.67	0.05	0.03	0.75	117.2	50.9	120.7	298.4	23.2	56.2
96.0	6.98	661.5	61.92	0.03	0.00	0.37	115.6	36.8	86.0	298.8	23.2	39.0
97.0	-0.00	-0.0	61.89	-0.00	-0.00	-0.00	113.9	22.5	50.2	299.0	23.2	-0.0

30.0 Percent Charge Remaining

MAXIMUM ACCELERATION		MAXIMUM CRADABILITY	
Speed (KPH)	Time (sec)	Speed (KPH)	Percent Grade
0 to 10	1.33	0	24.2
0 to 20	2.53	10	24.2
0 to 30	4.09	20	24.1
0 to 40	6.27	30	17.1
0 to 50	9.35	40	11.4
0 to 60	12.97	50	9.2
0 to 70	17.96	60	6.9
0 to 80	24.77	70	5.0
0 to 90	35.56	80	3.4
0 to 100	57.72	90	2.0

SCHEDULE "D" DRIVING CYCLE

ACCELERATION

Time (sec)	Speed (KPH)	Motor (RPM)	Torque (N-m)	Motor (HP)	Drive L (HP)	Wind (HP)	Roll L (HP)	Battery Voltage	Armature Voltage	Battery Current	Armature Current	Motor Efficiency
0.0	0.00	703.8	88.12	0.00	0.00	0.00	0.00	98.2	26.1	110.1	380.0	0.0
1.0	7.43	1437.1	88.12	8.71	0.61	0.00	0.40	93.7	44.6	189.8	380.0	38.3
2.0	15.17	2168.2	87.26	17.78	1.24	0.04	0.82	88.4	63.8	283.3	380.0	54.7
3.0	22.89	2795.3	66.94	26.57	1.85	0.15	1.24	82.5	92.5	386.4	377.3	63.5
4.0	29.51	3284.7	55.60	26.28	1.84	0.31	1.62	85.1	86.1	323.7	314.6	72.3
5.0	34.67	3690.0	48.21	25.65	1.80	0.51	1.91	88.1	88.1	288.8	279.6	77.6
6.0	38.95	4037.5	42.96	24.36	1.75	0.72	2.16	89.4	89.4	265.9	256.8	81.1
7.0	42.52	4342.4	39.06	23.82	1.71	0.94	2.37	90.3	90.3	249.7	240.6	83.6
8.0	45.84	4615.3	36.56	23.82	1.67	1.17	2.56	91.0	91.0	229.5	229.5	85.4
9.0	48.88	4864.5	34.36	23.82	1.65	1.42	2.75	92.5	92.5	210.1	210.1	85.9
10.0	52.03	5095.0	32.39	23.82	1.65	1.71	2.94	94.4	94.4	194.3	194.3	86.0
11.0	54.92	5301.6	30.63	23.82	1.65	2.01	3.11	95.1	95.1	180.5	180.5	86.9
12.0	57.50	5483.2	29.06	23.82	1.65	2.32	3.28	95.7	95.7	168.8	168.8	87.5
13.0	60.07	5645.6	27.66	23.82	1.64	2.63	3.43	96.3	96.3	158.9	158.9	87.9
14.0	62.38	5795.0	26.41	23.82	1.63	2.94	3.57	96.8	96.8	150.1	150.1	88.2
15.0	64.54	5927.1	25.30	23.82	1.62	3.25	3.71	97.2	97.2	142.3	142.3	88.3
16.0	66.56	6042.8	24.36	23.82	1.61	3.57	3.84	97.6	97.6	135.4	135.4	88.3
17.0	68.46	6142.6	23.55	23.82	1.60	3.89	3.96	97.9	97.9	129.4	129.4	88.0
18.0	70.24	6227.2	22.85	23.82	1.59	4.20	4.07	98.2	98.2	124.2	124.2	87.8
19.0	71.96	6297.3	22.24	23.82	1.58	4.48	4.17	98.4	98.4	119.8	119.8	87.2
20.0	73.57	6352.7	21.70	23.82	1.57	4.74	4.24	98.5	98.5	116.4	116.4	86.9
21.0	75.09	6397.7	21.20	23.82	1.56	4.98	4.28	98.5	98.5	113.8	113.8	86.4
22.0	76.54	6437.8	20.73	23.82	1.55	5.20	4.32	98.4	98.4	111.8	111.8	85.9
23.0	77.92	6472.6	20.30	23.82	1.54	5.40	4.36	98.3	98.3	110.1	110.1	85.4
24.0	79.24	6501.6	19.90	23.82	1.53	5.58	4.40	98.2	98.2	108.5	108.5	84.9
25.0	80.51	6525.0	19.53	23.82	1.52	5.74	4.44	98.1	98.1	107.0	107.0	84.4
26.0	81.74	6545.6	19.19	23.82	1.51	5.88	4.48	98.0	98.0	105.6	105.6	83.9
27.0	82.92	6563.2	18.88	23.82	1.50	6.00	4.52	97.9	97.9	104.2	104.2	83.4
28.0	84.07	6578.7	18.59	23.82	1.49	6.11	4.55	97.7	97.7	102.9	102.9	82.9
29.0	85.20	6592.1	18.33	23.82	1.48	6.21	4.58	97.6	97.6	101.6	101.6	82.4
30.0	86.30	6603.5	18.09	23.82	1.47	6.30	4.60	97.5	97.5	100.2	100.2	81.9

CRUISE

23.0	72.39	3428.8	19.58	24.43	0.55	4.50	4.21	98.8	53.5	100.2	168.4	78.0
78.0	72.39	3428.8	19.58	24.43	0.55	4.50	4.21	98.8	53.5	100.2	168.4	78.0

10.0 Percent Charge Remaining

COAST

Time (SEC)	Speed (KPH)	Motor (RPM)	Torque (N-W)	Drive L (HP)	Wind L (HP)	Poll L (HP)	Battery Voltage	Armature Voltage	Battery Current	Armature Current	Recharge Current	Gen. Pff.
78.0	72.39	3429.8	0.00	0.62	4.60	4.21	103.6	0.0	0.0	0.0	0.0	0.0
79.0	71.39	3390.8	0.00	0.60	4.44	4.15	103.6	0.0	0.0	0.0	0.0	0.0
80.0	70.40	3344.0	0.00	0.58	4.25	4.08	103.6	0.0	0.0	0.0	0.0	0.0
81.0	69.43	3297.9	0.00	0.57	4.08	4.02	103.6	0.0	0.0	0.0	0.0	0.0
82.0	68.47	3252.4	0.00	0.55	3.91	3.96	103.6	0.0	0.0	0.0	0.0	0.0
83.0	67.53	3207.6	0.00	0.54	3.75	3.90	103.6	0.0	0.0	0.0	0.0	0.0
84.0	66.60	3163.4	0.00	0.52	3.60	3.84	103.6	0.0	0.0	0.0	0.0	0.0
85.0	65.68	3119.9	0.00	0.51	3.45	3.78	103.6	0.0	0.0	0.0	0.0	0.0
86.0	64.78	3077.0	0.00	0.49	3.31	3.73	103.6	0.0	0.0	0.0	0.0	0.0
87.0	63.99	3034.6	0.00	0.48	3.18	3.67	103.6	0.0	0.0	0.0	0.0	0.0
88.0	63.01	2992.8	0.00	0.47	3.05	3.61	103.6	0.0	0.0	0.0	0.0	0.0

BRAKE

Time (SEC)	Speed (KPH)	Motor (RPM)	Torque (N-W)	Drive L (HP)	Wind L (HP)	Poll L (HP)	Battery Voltage	Armature Voltage	Battery Current	Armature Current	Recharge Current	Gen. Pff.
89.0	55.85	2645.6	98.12	0.37	2.11	3.17	121.0	95.5	291.0	380.0	131.6	67.3
90.0	48.87	2314.9	98.12	0.29	1.42	2.75	119.6	86.8	266.9	380.0	131.5	64.8
91.0	41.89	3969.4	60.22	0.23	0.89	2.33	118.9	106.4	254.0	293.9	131.5	80.1
92.0	34.91	3307.0	60.71	0.17	0.52	1.93	117.2	92.7	224.7	295.4	131.4	76.7
93.0	27.93	2645.6	61.11	0.13	0.26	1.53	115.4	78.9	193.6	296.6	131.4	72.3
94.0	20.94	1984.2	61.43	0.09	0.11	1.14	113.6	65.0	161.2	297.6	131.3	65.0
95.0	13.96	1322.8	61.66	0.05	0.03	0.75	111.7	50.9	127.0	298.3	127.0	56.2
96.0	6.98	661.4	61.81	0.03	0.00	0.37	109.6	36.8	91.2	298.8	91.2	39.0
97.0	-0.00	-0.0	51.88	-0.00	-0.00	-0.00	107.5	22.5	53.7	299.0	53.7	-0.0

SAE J272a TEST PROCEDURE

10.0 Percent Charge Remaining

MAXIMUM ACCELERATION		MAXIMUM GRADABILITY	
Speed (KPH)	Time (sec)	Speed (KPH)	Percent Grade

0 to 10	1.33	0	24.2
0 to 20	2.63	10	24.2
0 to 30	4.27	20	23.5
0 to 40	5.74	30	15.0
0 to 50	10.24	40	10.0
0 to 60	14.46	50	7.9
0 to 70	20.23	60	5.9
0 to 80	28.58	70	4.2
0 to 90	42.48	80	2.7
0 to 100	80.41	90	1.4

SCHEDULE "D" DRIVING CYCLE

ACCELERATION

Time (sec)	Speed (KPH)	Motor (RPM)	Torque (N-M)	Motor (HP)	Drive L (HP)	Wind L (HP)	Poll L (HP)	Battery Voltage	Armature Voltage	Battery Current	Armature Current	Motor Efficiency
0.0	0.00	0.0	88.12	0.00	0.00	0.00	0.00	94.1	26.1	114.5	390.0	0.0
1.0	7.43	703.9	88.12	8.71	0.61	0.00	0.40	88.0	44.6	201.4	380.0	38.3
2.0	15.17	1437.1	88.12	17.78	1.24	0.04	0.82	80.3	63.8	380.0	380.0	54.7
3.0	22.69	2150.0	77.51	23.40	1.54	0.14	1.23	77.2	77.2	356.5	347.3	55.1
4.0	28.64	2713.0	61.55	23.45	1.64	0.28	1.57	80.5	80.7	307.3	298.0	72.7
5.0	33.40	3163.9	51.95	23.08	1.62	0.45	1.84	82.7	82.7	277.5	269.4	77.5
6.0	37.40	3542.5	45.52	22.65	1.59	0.63	2.07	84.1	84.1	257.6	248.5	80.8
7.0	40.85	3870.4	40.86	22.21	1.55	0.83	2.27	85.1	85.1	243.2	234.1	83.1
8.0	43.91	4159.8	37.30	21.79	1.53	1.03	2.45	85.9	85.9	232.1	223.1	84.8
9.0	46.65	4418.9	34.48	21.40	1.50	1.23	2.61	86.5	86.5	223.5	214.4	85.0
10.0	49.34	4637.3	31.60	21.00	1.46	1.46	2.77	87.4	87.4	214.4	205.3	85.0
11.0	52.03	4815.6	28.73	20.51	1.45	1.71	2.94	88.0	88.0	205.3	196.2	85.0
12.0	54.53	4953.0	26.73	20.00	1.41	1.97	3.09	89.2	89.2	196.2	187.1	85.0
13.0	56.86	5063.3	25.02	19.46	1.34	2.23	3.23	90.5	90.5	187.1	178.0	85.0
14.0	59.04	5149.5	23.54	18.88	1.24	2.49	3.37	91.0	91.0	178.0	168.9	85.0
15.0	61.08	5213.3	22.43	18.26	1.13	2.76	3.49	91.5	91.5	168.9	160.0	85.0
16.0	63.00	5254.3	21.46	17.61	1.03	3.03	3.61	91.9	91.9	160.0	151.1	85.0
17.0	64.81	5277.0	20.73	16.93	0.92	3.30	3.73	92.3	92.3	151.1	142.2	85.0
18.0	66.52	5283.0	20.21	16.30	0.82	3.57	3.83	92.6	92.6	142.2	133.3	85.0
19.0	68.13	5273.3	20.78	15.71	0.71	3.83	3.94	92.9	92.9	133.3	124.4	85.0
20.0	69.66	5249.7	20.41	15.18	0.61	4.10	4.04	93.2	93.2	124.4	115.5	85.0
21.0	70.42	5205.5	20.00	14.62	0.51	4.23	4.08	93.4	93.4	115.5	106.6	85.0
22.0	70.70	5144.7	19.58	14.10	0.42	4.28	4.10	93.3	93.3	106.6	97.7	85.0
23.0	70.97	5071.9	19.15	13.61	0.32	4.33	4.12	93.2	93.2	97.7	88.8	85.0
24.0	71.25	5000.1	18.71	13.16	0.23	4.39	4.14	93.2	93.2	88.8	79.9	85.0
25.0	71.53	4938.3	18.26	12.71	0.14	4.44	4.16	93.1	93.1	79.9	71.0	85.0
26.0	71.81	4881.5	17.81	12.26	0.04	4.49	4.17	93.1	93.1	71.0	62.1	85.0
27.0	72.09	4829.7	17.36	11.81	0.00	4.54	4.19	93.0	93.0	62.1	53.2	85.0
28.0	72.37	4782.9	16.91	11.36	0.00	4.59	4.21	93.0	93.0	53.2	44.3	85.0

CRUISE

23.0	72.37	3427.9	19.57	9.42	0.56	4.59	4.21	94.2	53.5	103.9	168.4	78.0
24.0	72.37	3427.9	19.57	9.42	0.56	4.59	4.21	94.2	53.5	103.9	168.4	78.0

10.0 Percent Charge Remaining

COAST

Time (sec)	Speed (RPM)	Motor (RPM)	Torque (N-m)	Drive L (HP)	Wind L (HP)	Poll L (HP)	Battery Voltage	Armature Voltage	Battery Current	Armature Current	Recharge Current	Gen. Pff.
78.0	72.37	3427.9	0.00	0.52	4.59	4.21	101.1	0.0	0.0	0.0	0.0	0.0
79.0	71.37	3389.9	0.00	0.60	4.43	4.15	101.1	0.0	0.0	0.0	0.0	0.0
80.0	70.38	3343.1	0.00	0.58	4.28	4.08	101.1	0.0	0.0	0.0	0.0	0.0
81.0	69.41	3297.0	0.00	0.57	4.08	4.02	101.1	0.0	0.0	0.0	0.0	0.0
82.0	68.45	3251.5	0.00	0.55	3.91	3.96	101.1	0.0	0.0	0.0	0.0	0.0
83.0	67.51	3206.7	0.00	0.54	3.75	3.90	101.1	0.0	0.0	0.0	0.0	0.0
84.0	66.58	3162.6	0.00	0.52	3.60	3.84	101.1	0.0	0.0	0.0	0.0	0.0
85.0	65.67	3119.0	0.00	0.51	3.45	3.78	101.1	0.0	0.0	0.0	0.0	0.0
86.0	64.76	3076.1	0.00	0.49	3.31	3.72	101.1	0.0	0.0	0.0	0.0	0.0
87.0	63.87	3033.8	0.00	0.48	3.18	3.67	101.1	0.0	0.0	0.0	0.0	0.0
88.0	62.99	2992.0	0.00	0.47	3.05	3.61	101.1	0.0	0.0	0.0	0.0	0.0

BRAKE

Time (sec)	Speed (RPM)	Motor (RPM)	Torque (N-m)	Drive L (HP)	Wind L (HP)	Poll L (HP)	Battery Voltage	Armature Voltage	Battery Current	Armature Current	Recharge Current	Gen. Pff.
89.0	55.84	2644.8	88.12	0.37	2.11	3.17	122.4	95.5	287.5	380.0	167.8	67.3
90.0	48.95	2314.2	88.12	0.29	1.41	2.74	120.7	88.8	284.2	380.0	167.7	64.7
91.0	41.88	3967.3	60.20	0.23	0.89	2.33	119.9	106.3	251.6	293.8	167.6	90.1
92.0	34.90	3306.1	60.69	0.17	0.52	1.92	117.9	92.7	223.3	295.3	167.6	76.7
93.0	27.92	2544.8	61.09	0.13	0.26	1.53	115.7	78.9	193.2	296.6	167.5	72.3
94.0	20.94	1983.6	61.41	0.09	0.11	1.14	113.5	65.0	161.3	297.6	161.3	65.0
95.0	13.96	1322.4	61.54	0.05	0.03	0.75	111.1	50.9	127.6	298.3	127.6	56.2
96.0	6.98	561.2	61.79	0.03	0.00	0.37	108.8	36.7	92.0	298.7	92.0	39.0
97.0	-0.00	-0.0	61.86	-0.00	-0.00	-0.00	106.0	22.5	54.6	298.9	54.6	-0.0

RANGE AT STEADY SPEED

Range at constant speed, 0 percent grade:

Speed (KPH)	Range (KM)	Motor RPM	Torque (N-M)	Motor HP	Wind L HP	Roll L HP	Time (hrs)	Trans. Gear	Amp-HR used	Motor Efficiency
10.00	77.95	947.4	4.41	0.59	0.01	0.54	7.90	1	201.19	24.7
20.00	115.69	1894.7	4.75	1.26	0.10	1.09	5.93	1	197.08	33.9
30.00	132.22	2842.1	5.29	2.11	0.33	1.64	4.41	1	174.37	49.2
40.00	133.27	3789.4	6.02	3.21	0.78	2.22	3.33	1	162.55	57.7
50.00	124.76	2368.4	13.93	4.63	1.52	2.81	2.50	2	151.18	64.5
60.00	113.11	2342.1	16.20	6.47	2.62	3.42	1.89	2	140.91	71.3
70.00	98.95	3315.7	18.88	8.79	4.16	4.06	1.41	2	131.09	76.9
80.00	84.36	3789.4	21.96	11.69	6.21	4.71	1.05	2	121.79	81.8
90.00	70.53	4263.1	25.44	15.23	8.84	5.39	0.78	2	113.04	84.7
100.00	59.05	4736.8	29.32	19.50	12.12	6.10	0.58	2	104.84	87.2

Range at constant speed, 5 percent grade:

Speed (KPH)	Range (KM)	Motor RPM	Torque (N-M)	Motor HP	Wind L HP	Roll L HP	Time (hrs)	Trans. Gear	Amp-HR used	Motor Efficiency
10.00	28.50	947.4	22.21	2.95	0.01	0.54	2.86	1	156.44	46.4
20.00	37.02	1894.7	22.55	6.00	0.10	1.09	1.85	1	140.26	65.2
30.00	39.03	2842.1	23.08	9.21	0.33	1.64	1.30	1	128.38	75.4
40.00	38.31	3789.4	23.82	12.58	0.78	2.22	0.96	1	118.88	82.0
50.00	29.00	2368.4	49.52	16.47	1.52	2.81	0.56	2	103.89	71.8
60.00	26.03	2842.1	51.80	20.67	2.62	3.42	0.43	2	97.44	75.4
70.00	19.47	3315.7	54.47	25.36	4.16	4.06	0.26	2	69.34	78.0

Range at constant speed, 10 percent grade:

Speed (KPH)	Range (KM)	Motor RPM	Torque (N-M)	Motor HP	Wind L HP	Roll L HP	Time (hrs)	Trans. Gear	Amp-HR used	Motor Efficiency
10.00	15.16	947.4	39.88	5.30	0.01	0.54	1.52	1	133.40	49.0
20.00	18.48	1894.7	40.21	10.70	0.10	1.09	0.92	1	117.82	67.3
30.00	18.80	2842.1	40.75	16.25	0.33	1.64	0.63	1	106.87	76.8
40.00	17.22	3789.4	41.49	22.08	0.78	2.22	0.43	1	93.37	82.5
50.00	6.94	2368.4	84.85	28.22	1.52	2.81	0.14	2	49.18	65.8

RANGE AT STEADY SPEED

Range at constant speed, 15 percent grade:

Speed (KPH)	Range (KM)	Motor RPM	Torque (N-M)	Motor HP	Wind L HP	Roll L HP	Time (hrs)	Trans. Gear	Amp-HR used	Motor Efficiency
10.00	9.31	947.4	57.28	7.52	0.01	0.54	0.93	1	118.05	48.2
20.00	10.89	1894.7	57.62	15.33	0.10	1.09	0.54	1	103.16	65.5
30.00	10.00	2842.1	58.15	23.21	0.33	1.64	0.33	1	85.43	74.3

Range at constant speed, 20 percent grade:

Speed (KPH)	Range (KM)	Motor RPM	Torque (N-M)	Motor HP	Wind L HP	Roll L HP	Time (hrs)	Trans. Gear	Amp-HR used	Motor Efficiency
10.00	6.25	947.4	74.31	9.89	0.01	0.54	0.52	1	106.79	46.5
20.00	7.03	1894.7	74.64	19.36	0.10	1.08	0.35	1	92.42	62.9
30.00	2.50	2842.1	75.18	30.01	0.33	1.64	0.08	1	28.26	71.1

Range at constant speed, 25 percent grade:

Speed (KPH)	Range (KM)	Motor RPM	Torque (N-M)	Motor HP	Wind L HP	Roll L HP	Time (hrs)	Trans. Gear	Amp-HR used	Motor Efficiency
----------------	---------------	--------------	-----------------	-------------	--------------	--------------	---------------	----------------	----------------	---------------------

Range Driving Schedule "D" (KM): 57.58

Total Driving Time (hrs): 1.15

Number of Cycles Completed : 34.00

A-hr Gained by Regenerative Braking : 7.12

Percent Energy Gained by Regen. Braking : 3.81

MAXIMUM GRADEABILITY

Speed (kph)	Percent Grade
0-16.5	38

This means that the maximum gradeability is 38% from 0 kph to 16.5 km/hr. This condition occurs when the test bed is traction limited and has the capability to spin the tires at low speeds. Since the tires would slip at steeper grades (even though the motor has sufficient power to climb steeper grades), the traction limiting grade is printed out.

A) Acceleration portion of J227a driving cycle: The following 13 parameters are printed at one second intervals:

1. Time (sec): Time from beginning of cycle
2. Speed (kph): Test bed speed in kph
3. Motor (rpm): Test bed motor speed
4. Motor (hp): Test bed motor horsepower
5. Torque (N-M): Motor torque required, N-M
6. Drive L (hp): Horsepower consumed by transmission, axle bearings, and wheel bearings.
7. Wind L (hp): Aerodynamic horsepower loss
8. Roll L (hp): Horsepower to overcome rolling resistance of tires.
9. Battery voltage: Voltage across battery terminals.
10. Armature voltage: Voltage at armature.
11. Battery current: Amperes drawn from battery.
12. Armature current: Amperes flowing through armature.
13. Motor efficiency: Power out of motor/power in of motor x 100.

During the "coast" and "brake" sections of the driving cycle the following column headings are added to cover regenerative braking:

1. Recharge current: amperes accepted by the battery during regenerative braking.
2. Generating efficiency: generating efficiency of motor.

B) Range at steady speed

The tables are incremented by percent grade; 0% to 30%. The following column headings designate generated data corresponding to test bed velocity:

1. Range (km): Distance traveled before battery energy is depleted or test bed can no longer maintain speed.

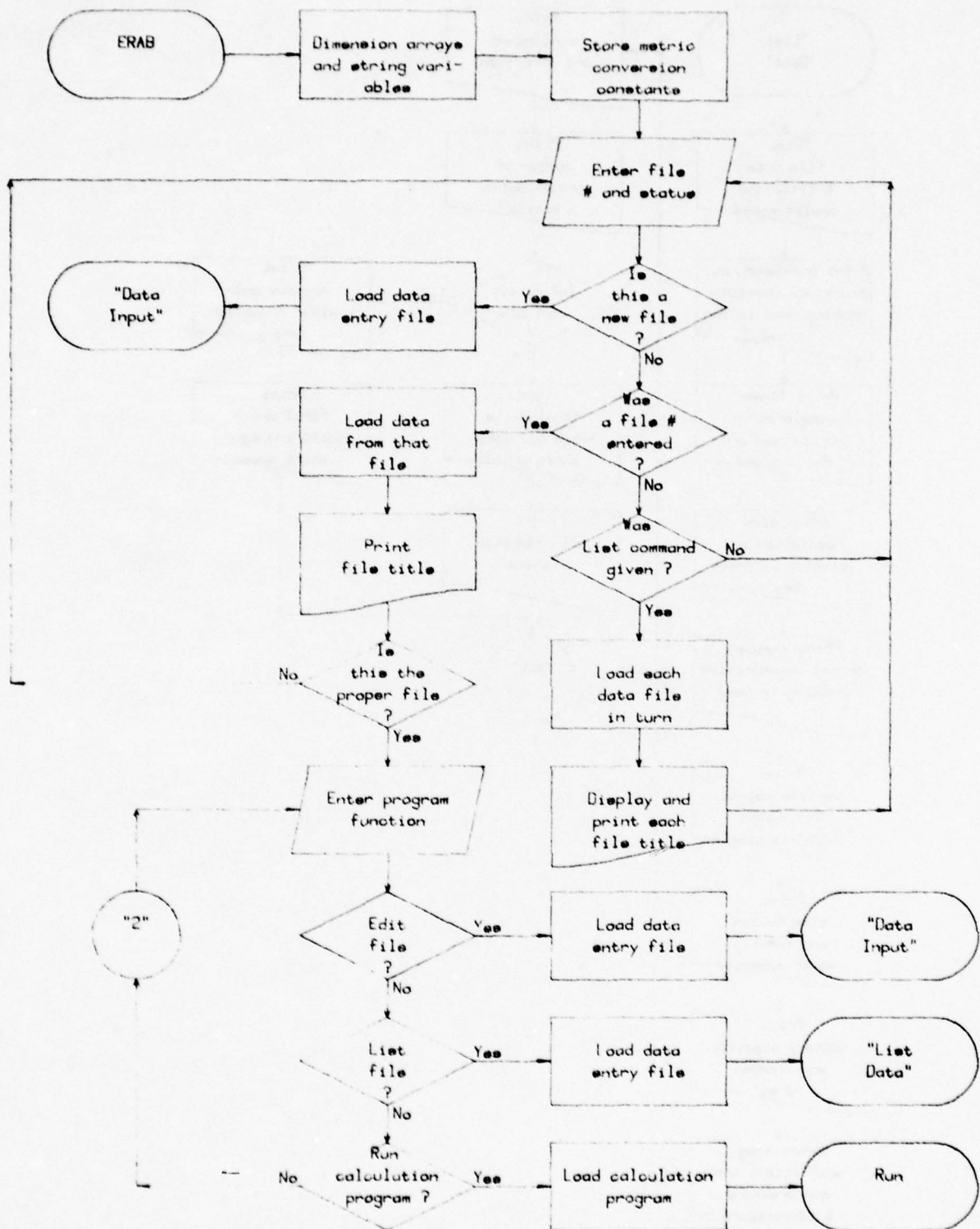
2. Motor (rpm): See part A
3. Torque (N-M): See part A
4. Motor (hp): See part A
5. Wind L (hp): See part A
6. Roll L (hp): See part A
7. Time (hrs): Time taken to deplete battery at cruise speed.
8. Trans. gear: Gear used to cruise speed, 1 = greatest reduction ratio.
9. Ampere hours used: Energy extracted from battery during run.
10. Motor efficiency: See part A

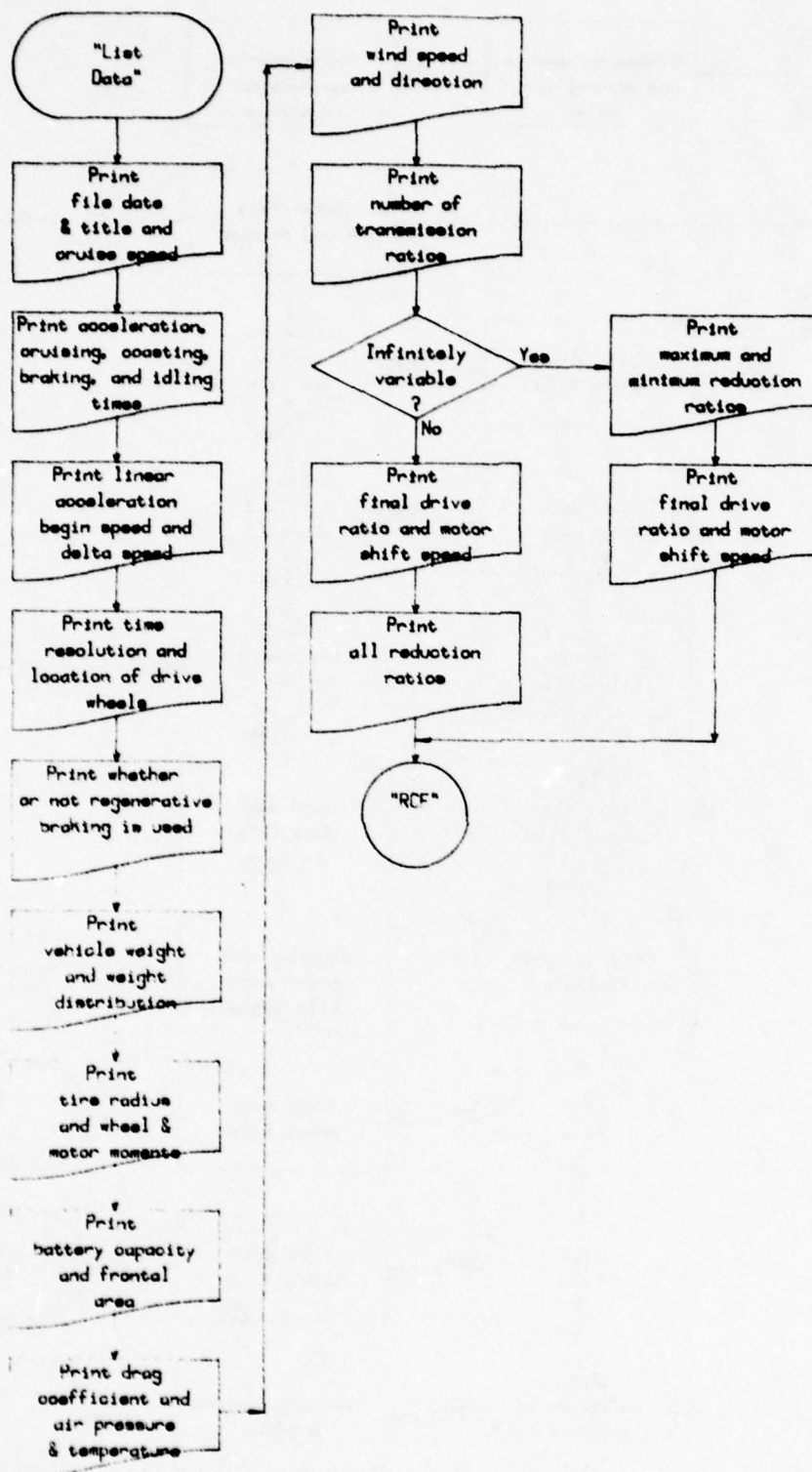
C) The last part of the printout defines the overall result of the driving cycle. The end of the run is realized when battery level drops below 5% of initial charge, or test bed can no longer meet the acceleration requirements.

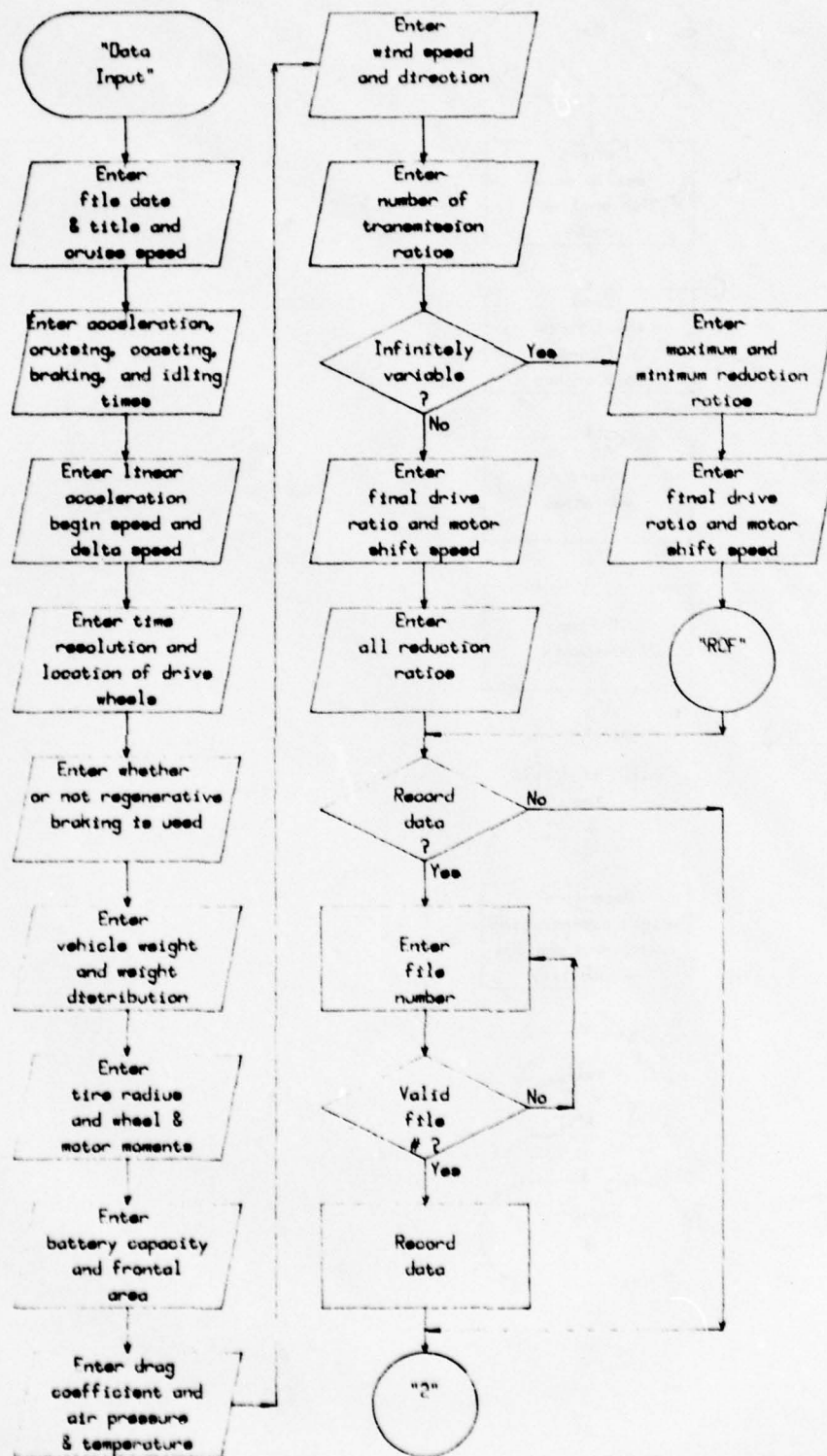
8.1.4 Computer Model Flow Chart

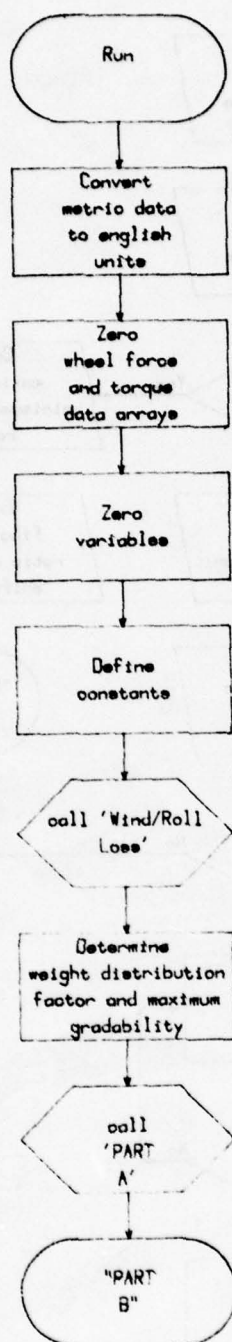
The following pages are a series of flow charts that illustrate the logic used in the development of the electric test bed performance computer simulation. A complete program listing is provided in section 8.1.5 and a discussion of the program subroutines is presented in section 8.1.6.

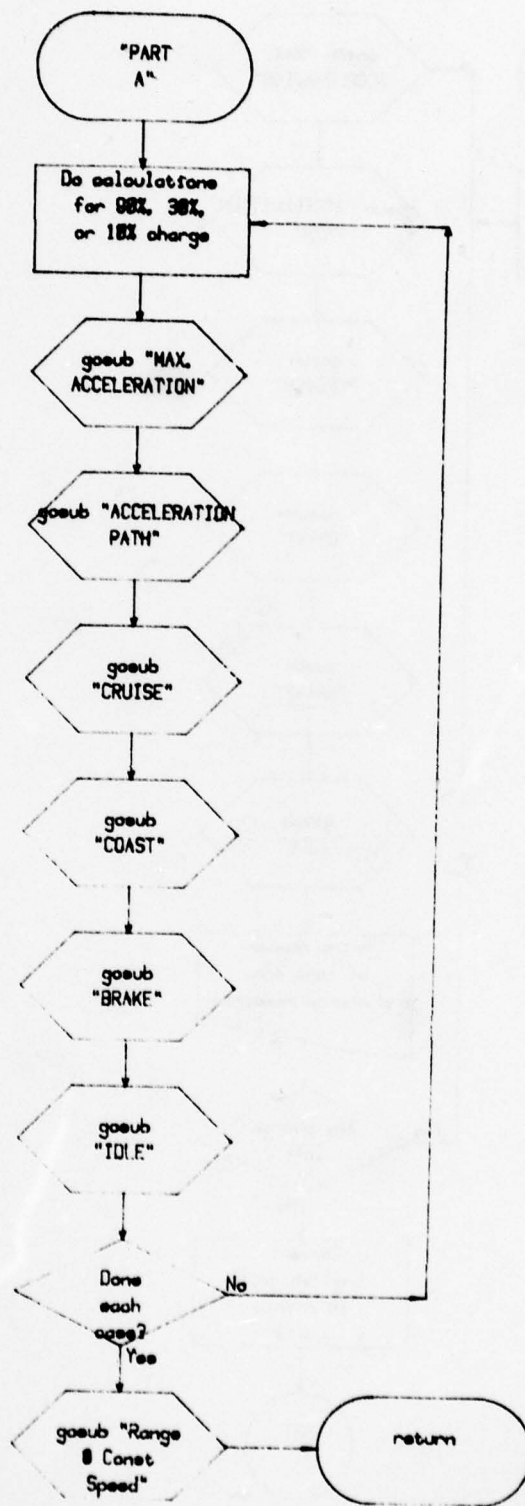
The first three flow charts are the control section of the program, i.e. program beginning, data entering/editing, and data listing. The remaining flow charts comprise the operational section of the modeling program.

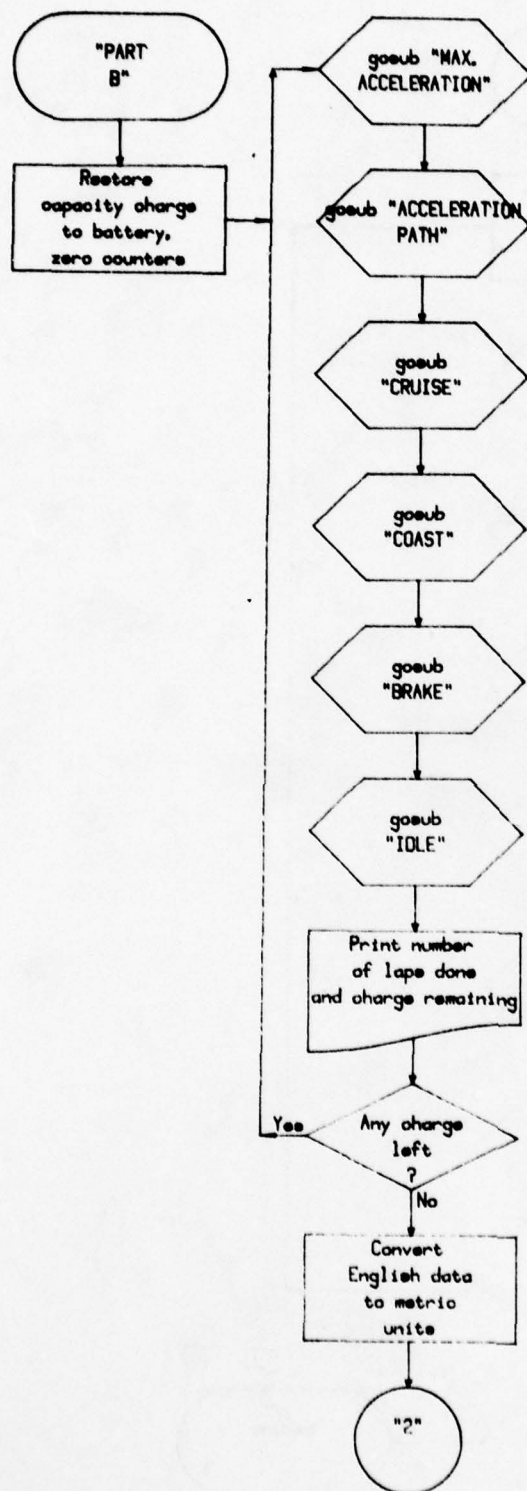


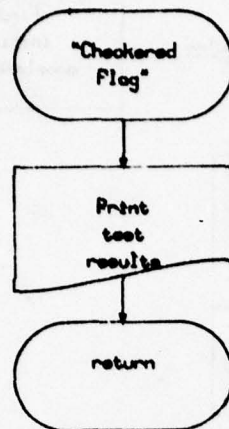


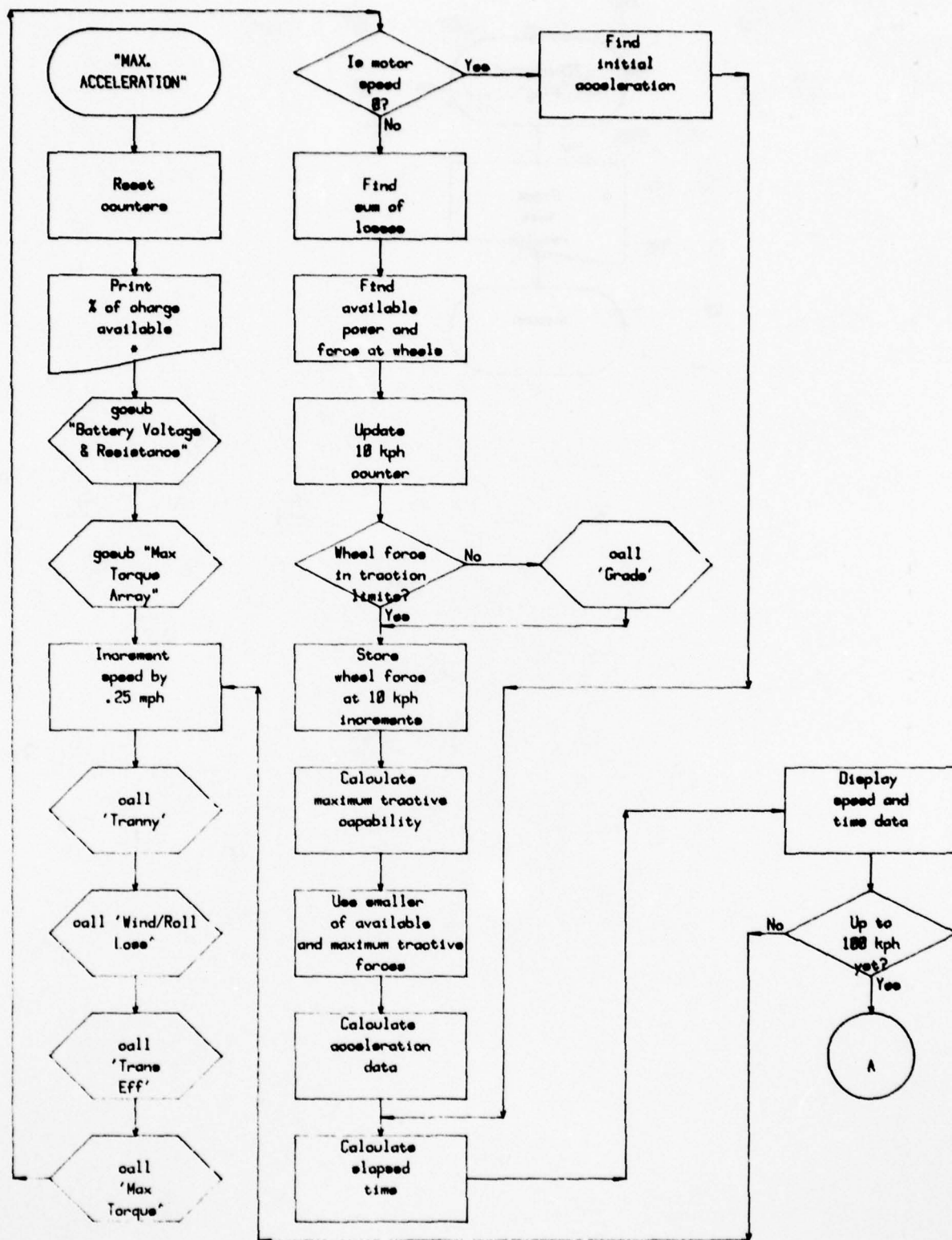




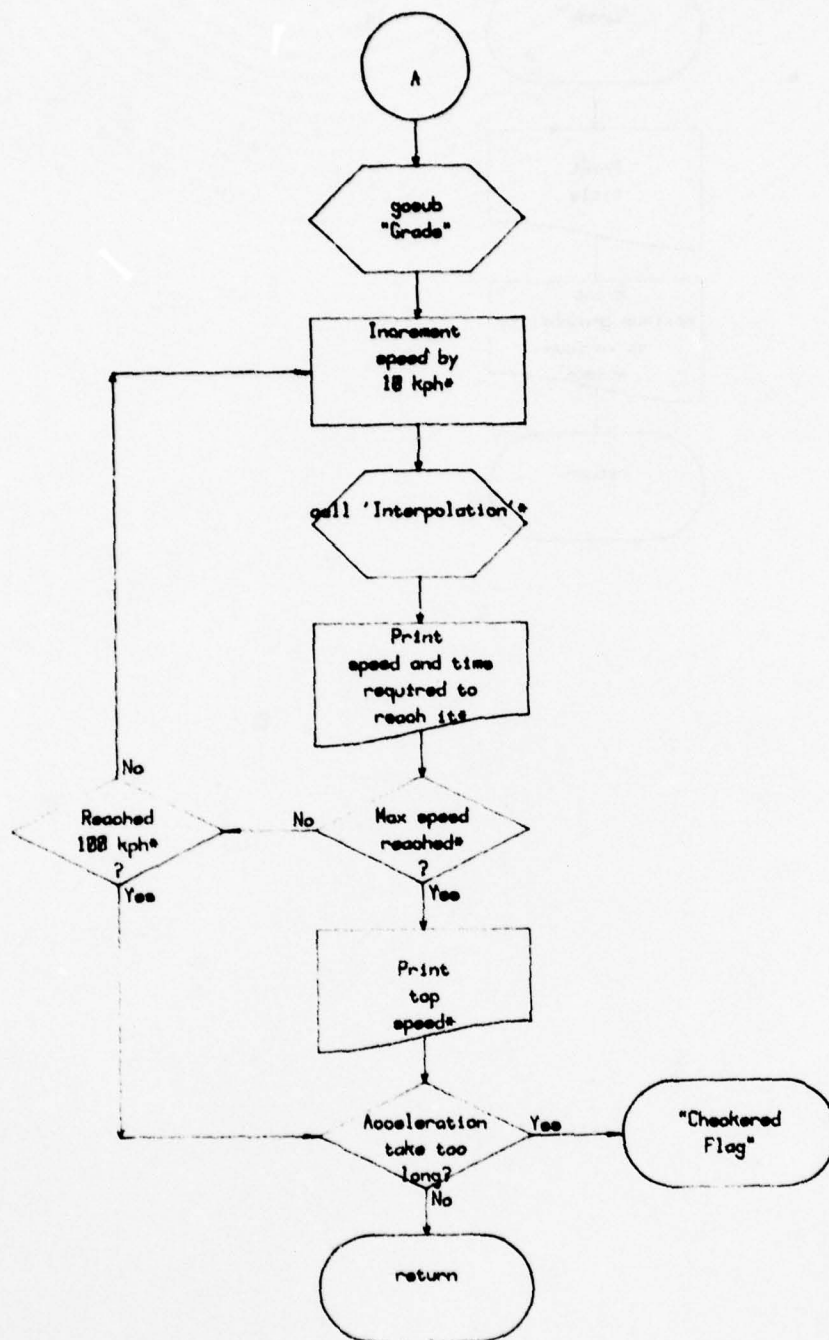




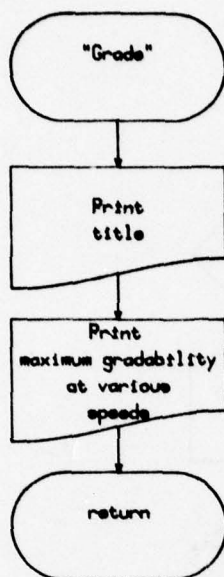


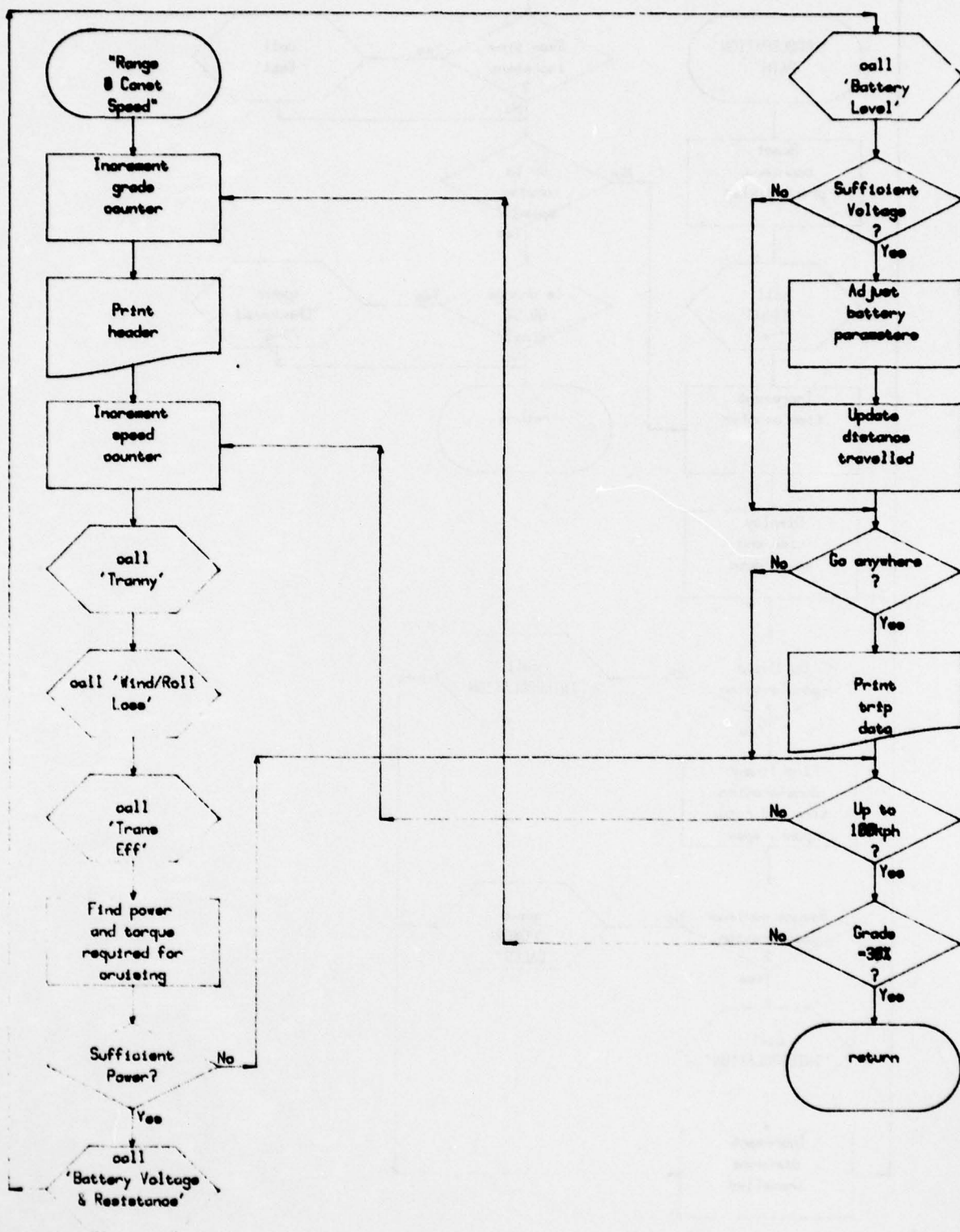


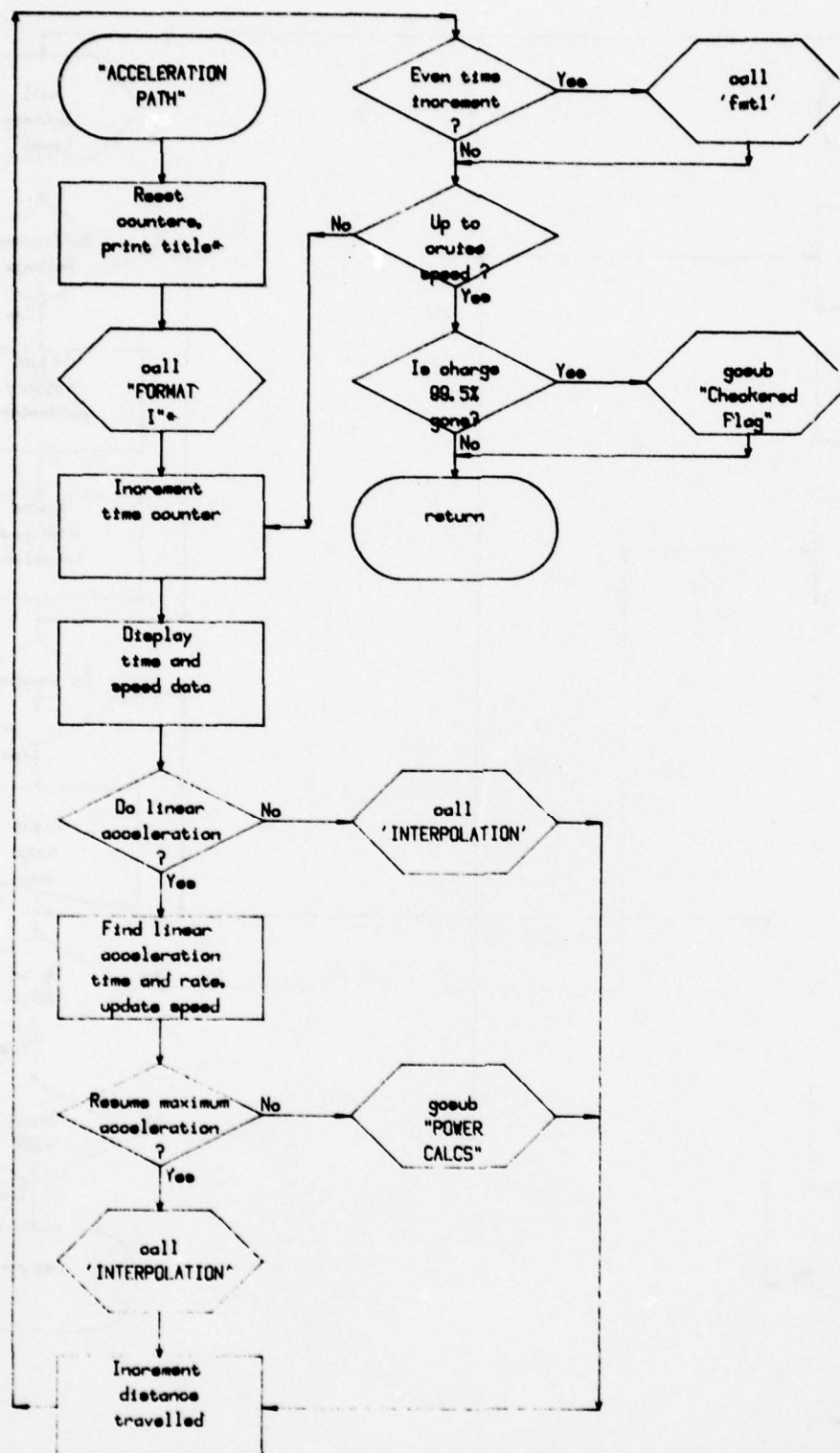
* These modules are not executed after completion of "PART A".



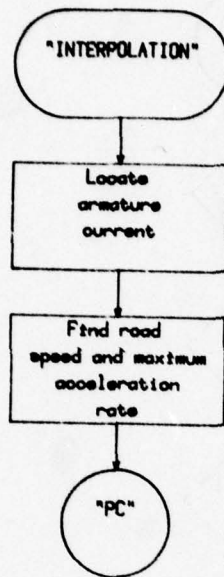
* These modules are not executed after completion of "PART A".

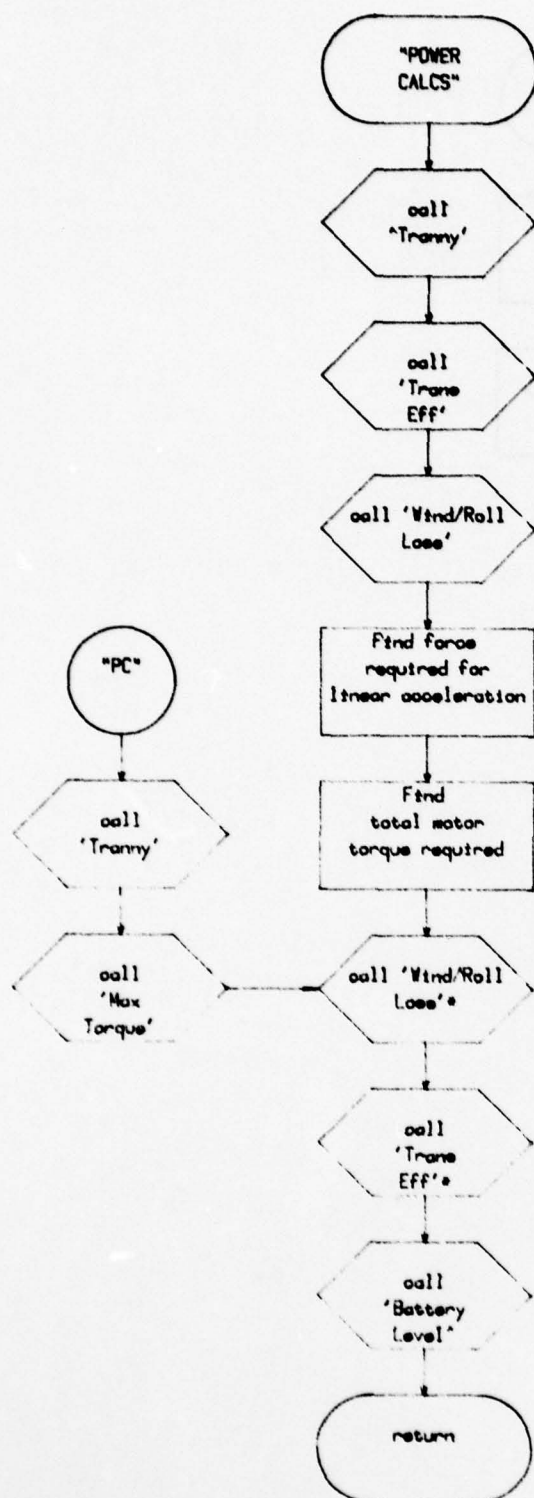




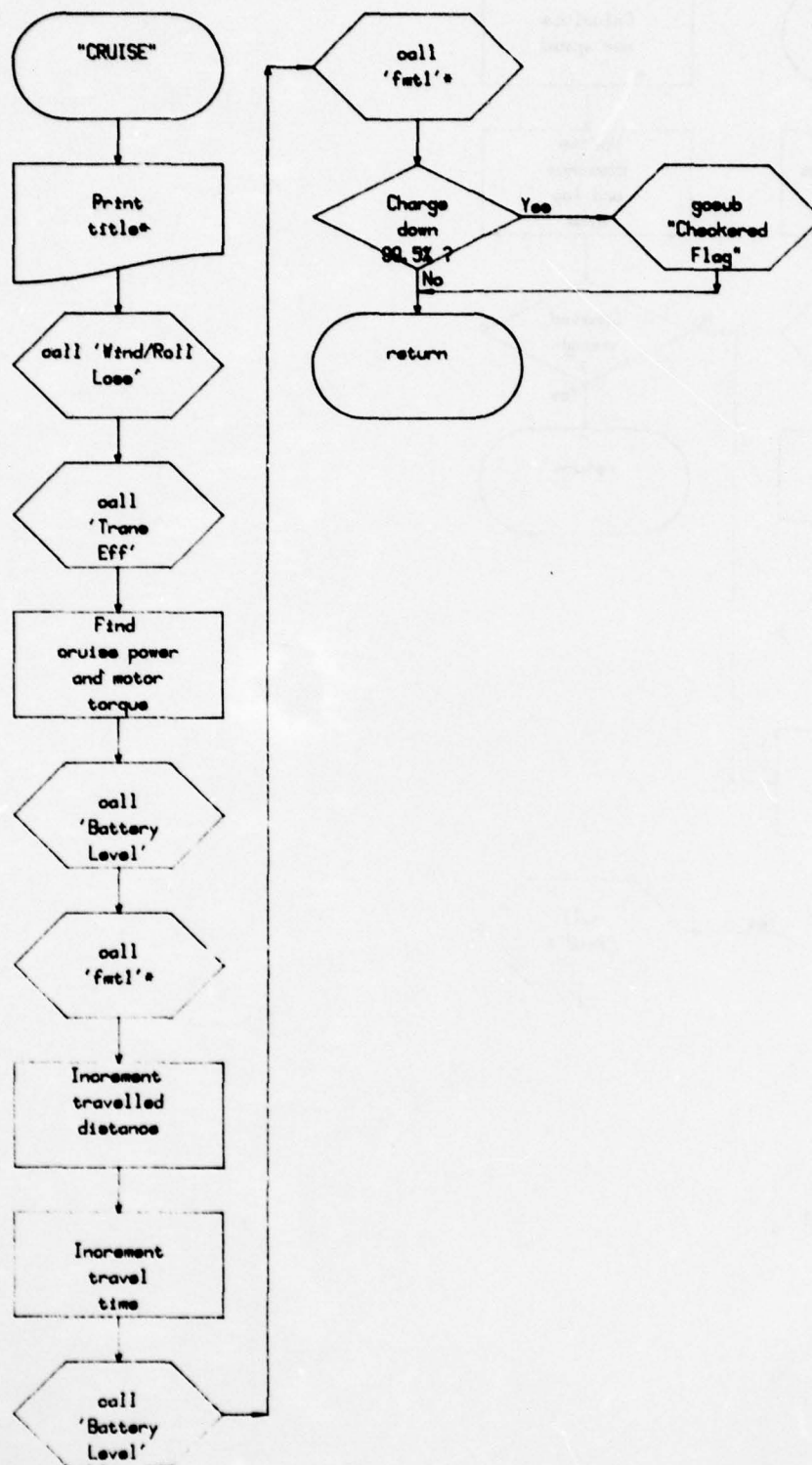


* These modules are not executed after completion of "PART A".

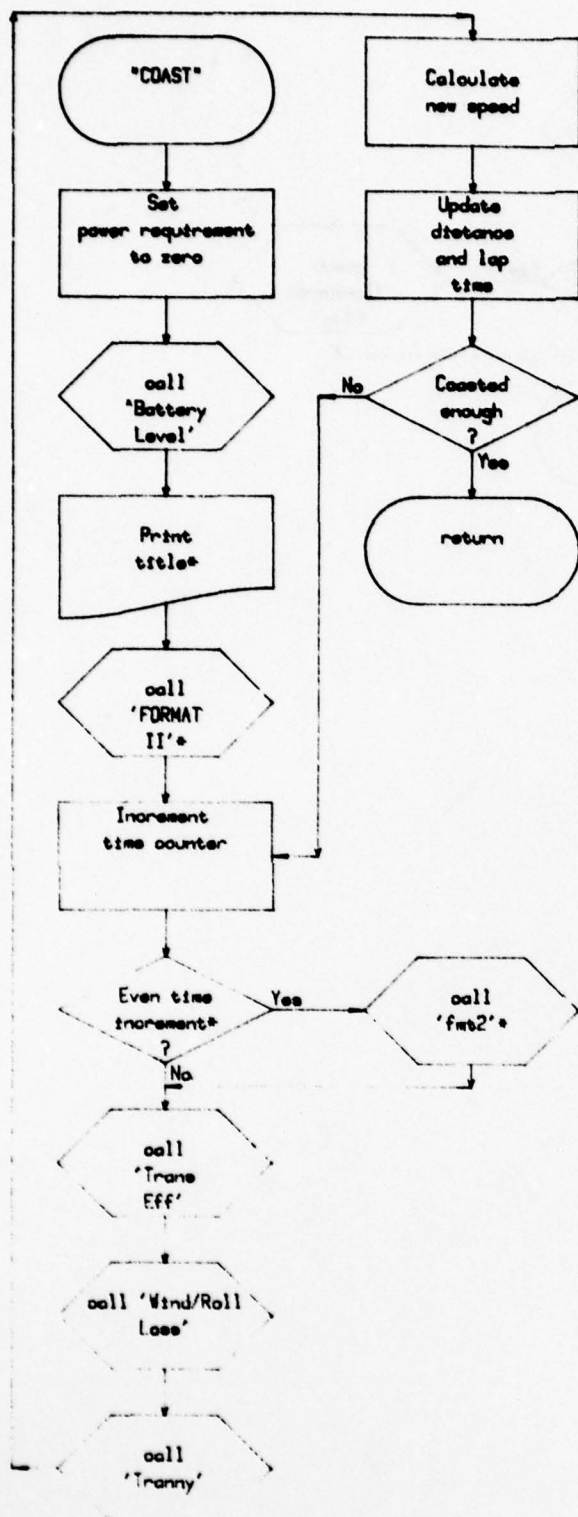




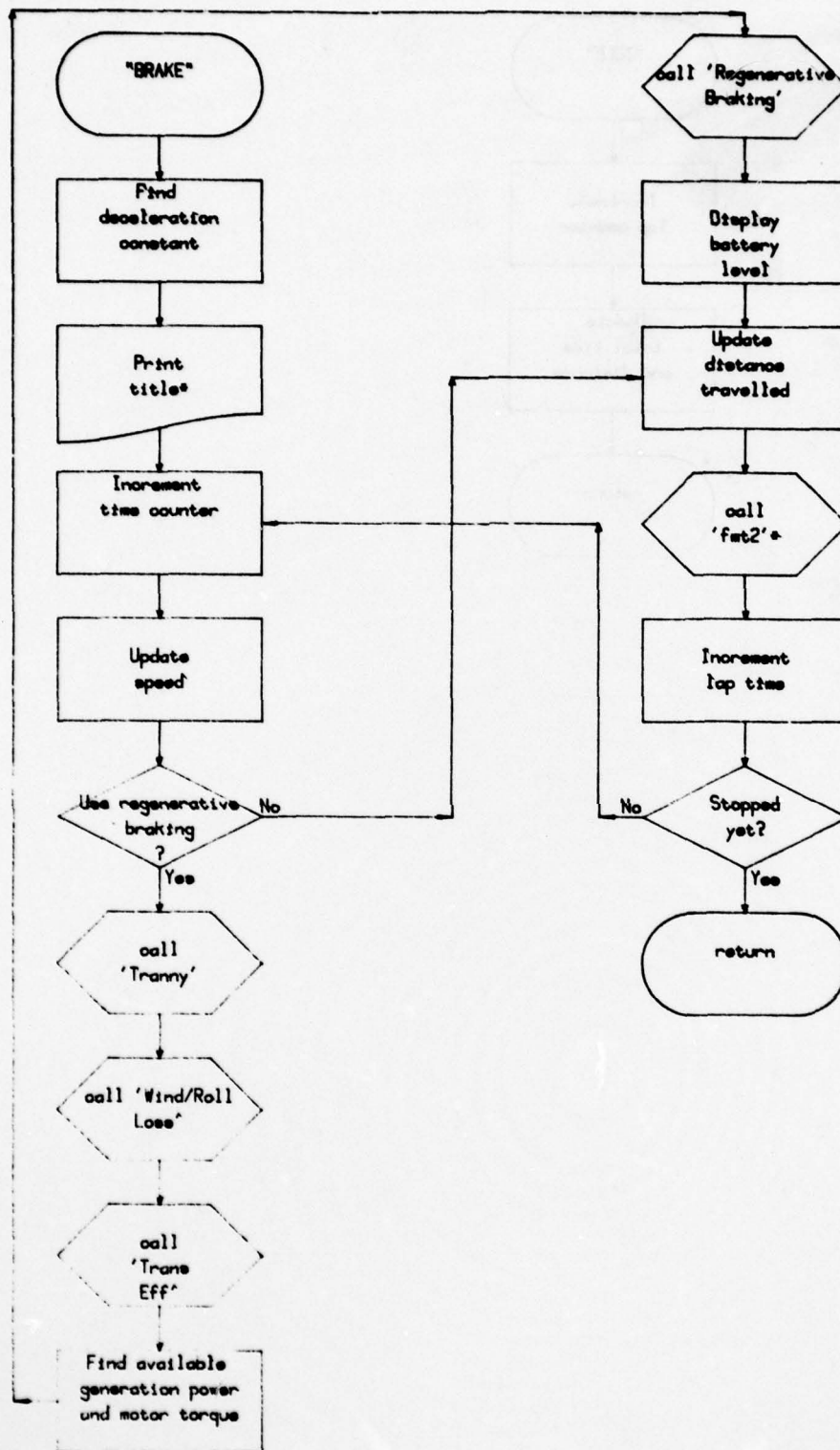
* These modules are not executed after completion of "PART A".



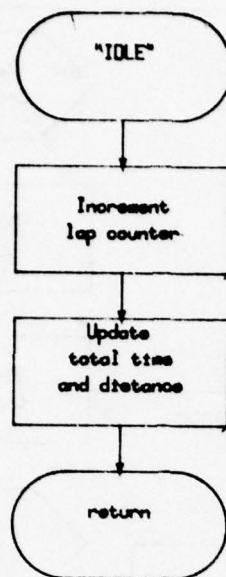
* These modules are not executed after completion of "PART A".



* These modules are not executed after completion of "PART A".



* These modules are not executed after completion of "PART A".



AD-A069 070

BARBER-NICHOLS ENGINEERING CO ARVADA COLO

F/G 21/3

MECHANICAL INTERFACE FOR AN ELECTRIC PROPULSION TEST BED.(U)

DAAK70-78-C-0055

UNCLASSIFIED

NL

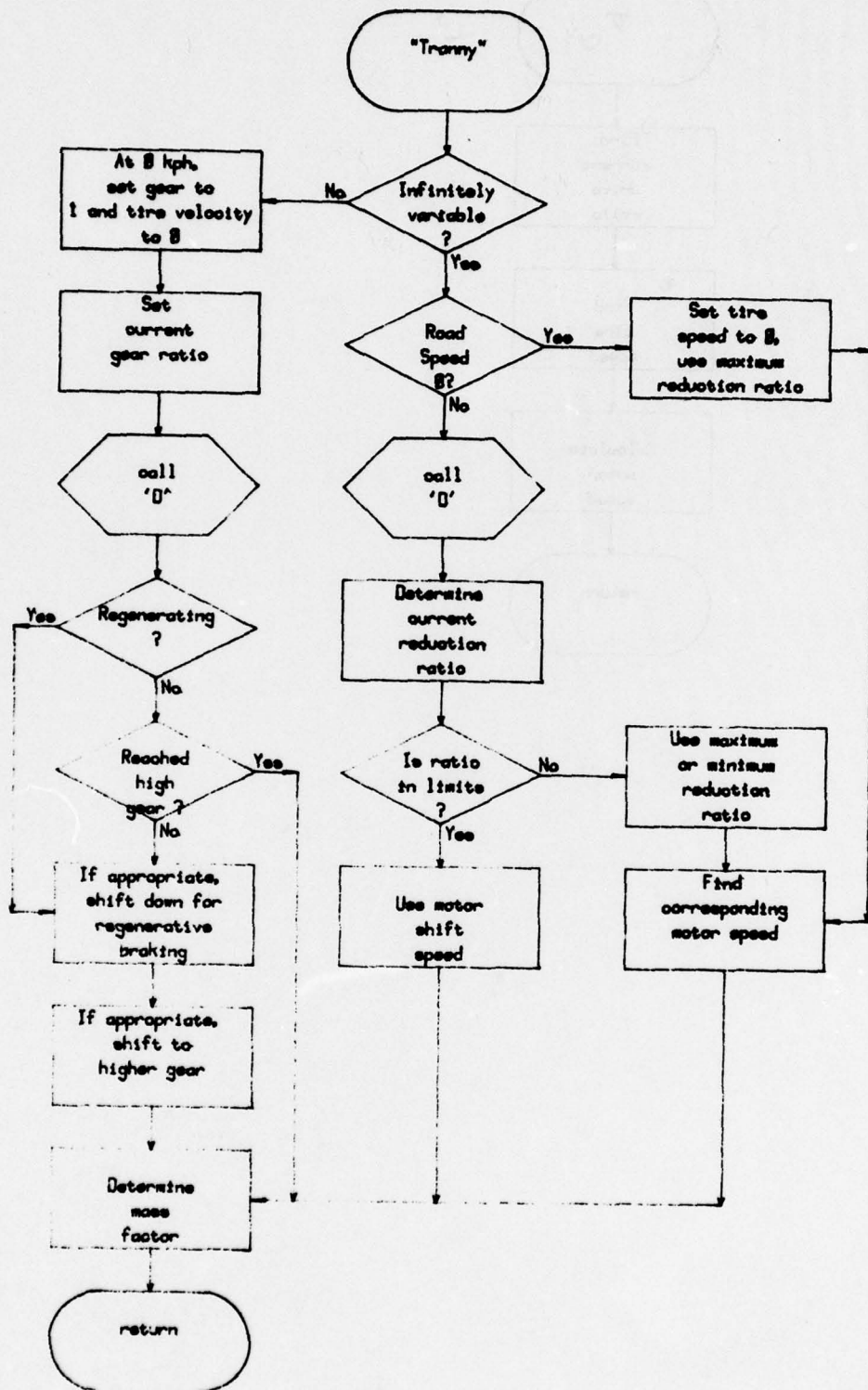
2 OF 2

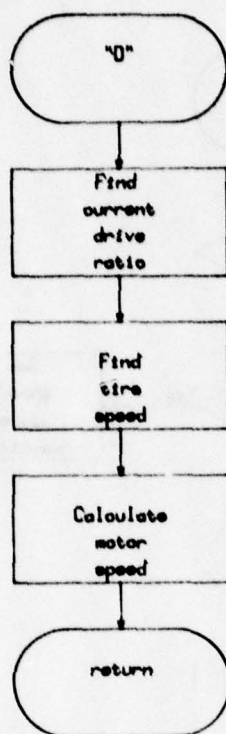
AD
A069070

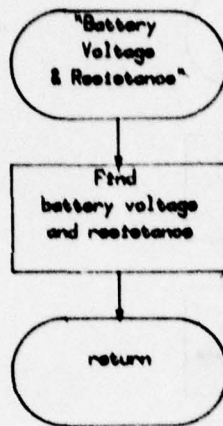


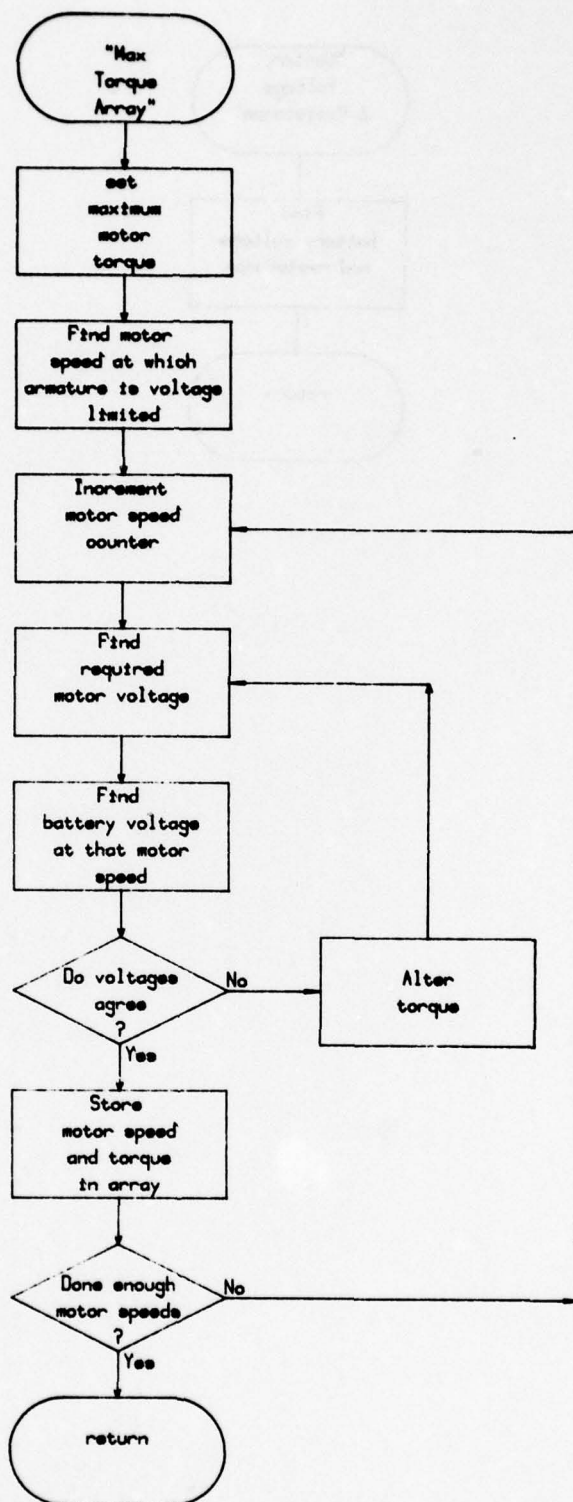
END
DATE
FILMED
6-79

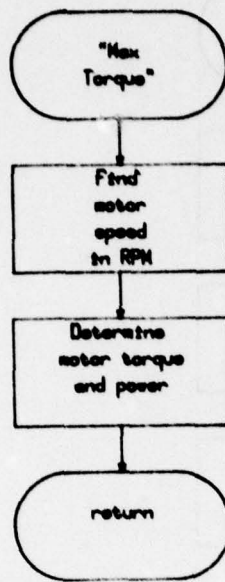
DDC

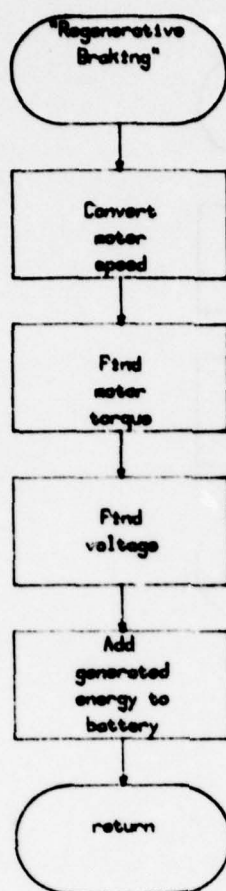


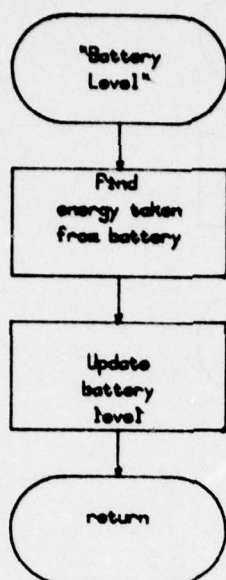


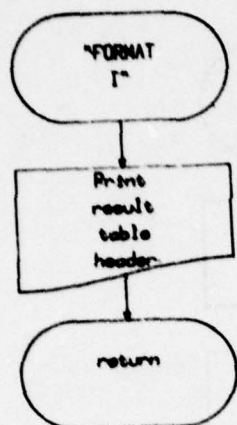


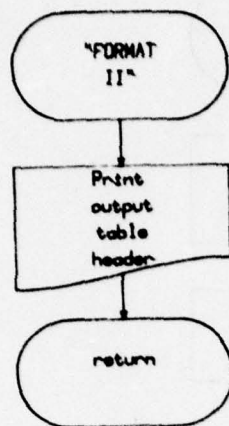


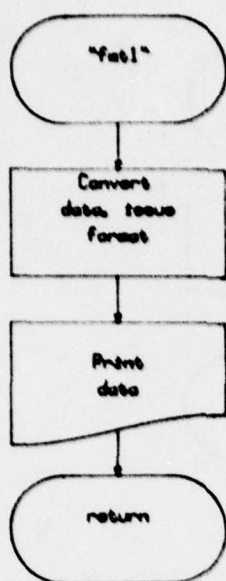


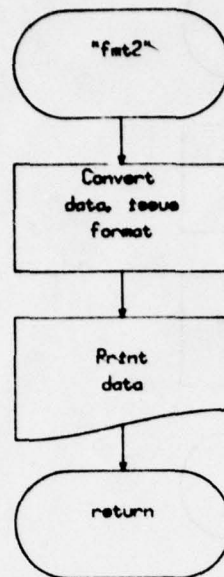


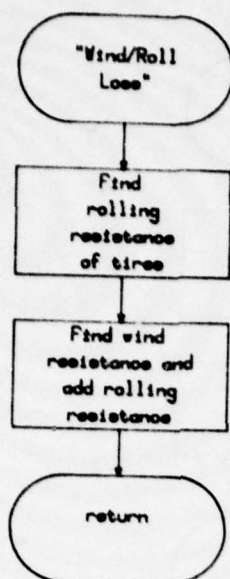


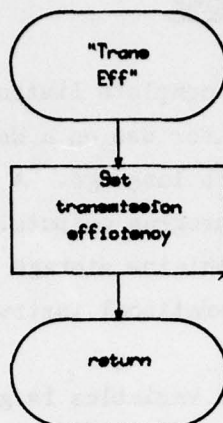












8.1.5 Listing of Computer Program

This section contains a complete listing of the ERAB computer model. The program was written for use on a Hewlett-Packard 9825 calculator which utilizes the HPL language. A Hewlett-Packard 9871 impact printer is used for all program outputs. The program is stored on a data cartridge that also contains storage for 5 sets of test bed data. See section 8.1.4 for operational instructions.

A listing of all program variables is given in Table III at the end of the program listing.

PROGRAM CONTROL SECTION

```

0: dim DS[60],A[10],B[20],C[5],D[8],T[15],T,E[10]
1: dim AS[1],ES[13],FS[5],GS[50],HS[50],Y[3,0:250],Z[3,20]
2: dim V[2],I[0:2],F[2,7],S[2,30]
3: fxd 0;"0123456789.e-">ES
4: .621371>F[1,1];2.20462>F[1,2];.393701>F[1,3];349.4546>F[1,4]
5: 10.76391>F[1,5];F[1,3]/10>F[1,6];1.8>F[1,7]
6: for I=1 to 7;1/F[1,I]>F[2,I];next I
7: "START":ent " File # (1-5) / L=List / N=New",FS
8: if cap(FS)="N";cll 'ldfl';gto "Data Input"
9: pos(ES[2,1],FS)>r22
10: if r22;gto "LDF"
11: if cap(FS)="#L";beep;dsp "Invalid Entry";wait 3000;gto "START"
12: dsp " Getting File Descriptions"
13: for C=1 to 5
14: ldf C+3,DS,A[*],B[*],C[*],D[*],T[*],T
15: dsp "File #",C,":",DS;wait 1500
16: HS[1,35-len(DS)]>DS[len(DS)+1,35]
17: fmt 5x,fl.,2x,c35;wrt 6,C,DS[1,35]
18: next C
19: wtb 6,l0,l0,l0;gto "START"
20: "ldfl":if flq4;ret
21: sfq 4;ldf l,34
22: "LDF":dsp "Loading File #",r22
23: ldf r22+3,DS,A[*],B[*],C[*],D[*],T[*],T
24: HS[1,35-len(DS)]>DS[len(DS)+1,35]
25: fmt 5x,"Data File # ",fl.,": ",c35,2/;wrt 6,r22,DS[1,35]
26: ent "Is this the proper file ? (y/n)",AS
27: if cap(AS)="N";gto "START"
28: if cap(AS)="#Y";gto -2
29: "2":ent " R=Run / E=Edit / L=List",AS
30: if cap(AS)="E";cll 'ldfl';gto "Data Input"
31: if cap(AS)="L";cll 'ldfl';gto "List Data"
32: if cap(AS)="#R";gto -3
33: cfa 4;ldf 2,34
34:

```

THIS PAGE IS BEST QUALITY PRACTICABLE
FROM COPY FURNISHED TO DDC

DATA ENTRY, EDITING, AND LISTING

```

0: ret
1: "List Data":sfg 2;qto +4
2:
3: wait 3000
4: "Data Input":sfg 1
5: if flq1;ent "Enter Date / Title (35 char max)",DS
6: if (len(DS)+r22)>35;dsp "Title is",r22-35,"char. too long";jmp -3
7: if flq2;fmt 10x,c35,2/;wrt 6,DS
8: "Accel. to what speed? (KPH)">GS;if flq1;dsp GS;ent "",A[1]
9: if flq2;c11 'FMT';wrt 6,GS,A[1]
10: "Accel. in How Much Time (sec)">GS;if flq1;dsp GS;ent "",A[2]
11: if flq2;c11 'FMT';wrt 6,GS,A[2]
12: "Cruise in How Much Time (sec)">GS;if flq1;dsp GS;ent "",A[3]
13: if flq2;c11 'FMT';wrt 6,GS,A[3]
14: "Coast in How Much Time (sec)">GS;if flq1;dsp GS;ent "",A[4]
15: if flq2;c11 'FMT';wrt 6,GS,A[4]
16: "Brake in How Much Time (sec)">GS;if flq1;dsp GS;ent "",A[5]
17: if flq2;c11 'FMT';wrt 6,GS,A[5]
18: "Idle in How Much Time (sec)">GS;if flq1;dsp GS;ent "",A[6]
19: if flq2;c11 'FMT';wrt 6,GS,A[6]
20: "Speed to Begin Linear Accel(KPH)">GS;if flq1;dsp GS;ent "",A[8]
21: if flq2;c11 'FMT';wrt 6,GS,A[8]
22: "Linear Accel. Delta Velocity (KPH)">GS;if flq1;dsp GS;ent "",A[9]
23: if flq2;c11 'FMT';wrt 6,GS,A[9]
24: "Time Increment for calcs (sec)">GS;if flq1;dsp GS;ent "",T
25: if flq2;c11 'FMT';wrt 6,GS,T
26: if flq1;ent "Front or Rear Wheel Drive? (F/R)",GS;jmp 2
27: qto +4
28: if cap(GS)="F";l+B[13];jmp 3
29: if cap(GS)="R";0+B[13];jmp 2
30: qto -4
31: if flq2 and B[13]=0;" Rear Wheel Drive :">GS;c11 'FMT';wrt 6,GS
32: if flq2 and B[13]=1;" Front Wheel Drive :">GS;c11 'FMT';wrt 6,GS
33: if flq1;ent "Is Regen. Braking Used? (Y/N)",GS;jmp 2
34: qto +4
35: if cap(GS)="Y";l+B[3];jmp 3
36: if cap(GS)="N";0+B[3];jmp 2
37: qto -4
38: if flq2 and B[8]=1;" Regenerative Braking Used">GS;c11 'FMT';wrt 6,GS
39: "Vehicle Weight (KG)">GS;if flq1;dsp GS;ent "",B[1]
40: if flq2;c11 'FMT';wrt 6,GS,B[1]
41: "Fraction of Weight on Front Wheels">GS;if flq1;dsp GS;ent "",B[11]
42: if flq2;c11 'FMT';wrt 6,GS,B[11]
43: "Center of Gravity Height (cm)">GS;if flq1;dsp GS;ent "",B[12]
44: if flq2;c11 'FMT';wrt 6,GS,B[12]
45: "Wheelbase (cm)">GS;if flq1;dsp GS;ent "",B[10]
46: if flq2;c11 'FMT';wrt 6,GS,B[10]
47: "Rolling Radius of tires (cm)">GS;if flq1;dsp GS;ent "",B[5]
48: if flq2;c11 'FMT';wrt 6,GS,B[5]
49: "Mom. of Inertia of Wheels (N-m-m)">GS;if flq1;dsp GS;ent "",B[6]
50: if flq2;c11 'FMT';wrt 6,GS,B[6]
51: "Moment of Inertia of Motors (N-m-m)">GS;if flq1;dsp GS;ent "",B[7]
52: if flq2;c11 'FMT';wrt 6,GS,B[7]
53: "Battery Amp-hr capacity (5hr discharge)">GS;if flq1;dsp GS;ent "",C[1]
54: if flq2;c11 'FMT';wrt 6,GS,C[1]
55: "Frontal Area in direc. of travel (sq.m)">GS;if flq1;dsp GS;ent "",B[2]
56: if flq2;c11 'FMT';wrt 6,GS,B[2]

```



```

56: if flq2;c11 'FMT';wrt 6,GS,B[2]
57: "Wind Drag Coefficient"+GS;if flq1;dsp GS;ent "",B[3]
58: if flq2;c11 'FMT';wrt 6,GS,B[3]
59: "Barometric Pressure (mm Hg)"+GS;if flq1;dsp GS;ent "",D[2]
60: if flq2;c11 'FMT';wrt 6,GS,D[2]
61: "Ambient Temperature (C)"+GS;if flq1;dsp GS;ent "",D[1]
62: if flq2;c11 'FMT';wrt 6,GS,D[1]
63: "Wind Velocity (KPH)"+GS;if flq1;dsp GS;ent "",D[3]
64: if flq2;c11 'FMT';wrt 6,GS,D[3]
65: "Ang. of wind to Dir. of Trav.(deg)"+GS;if flq1;dsp GS;ent "",D[4]
66: if flq2;c11 'FMT';wrt 6,GS,D[4]
67: if cap(AS)="E";ent "Is Present Transmission OK?(y/n)",AS;jmp 2
68: jmp 4
69: if cap(AS)="N";jmp 3
70: if cap(AS)#"Y";jmp -3
71: gto "Q"
72: if flq1;ent "Transmission Efficiency ? (%)",T[6];T[6]/100+T[6]
73: if flq1;ent "# of RATIOS in Trans (1-5),0=inf",r6;gto +2
74: gto +3
75: if r6>5 or int(r6)#r6;jmp -2
76: r6+T[10]
77: if T[10]>0;gto "OO"
78: if flq2;fmt 1/,10x,"INFINITELY VARIABLE TRANSMISSION";wrt 6
79: "Max Trans. Reduction Ratio"+GS;if flq1;dsp GS;ent "",T[4]
80: if flq2;c11 'FMT';wrt 6,GS,T[4]
81: "Min Trans. Reduction Ratio"+GS;if flq1;dsp GS;ent "",T[3]
82: if flq2;c11 'FMT';wrt 6,GS,T[3]
83: "Motor Shift Speed (rpm)"+GS;if flq1;dsp GS;ent "",T[5];2πT[5]/60+T[2]
84: if flq2;c11 'FMT';wrt 6,GS,T[5]
85: "Final Drive Ratio"+GS;if flq1;dsp GS;ent "",T[1]
86: if flq2;c11 'FMT';wrt 6,GS,T[1]
87: gto "Q"
88: "OO":if flq2;fmt 1/,10x,fl., " SPEED TRANSMISSION";wrt 6,T[10]
89: "Final Drive Ratio"+GS;if flq1;dsp GS;ent "",T[1]
90: if flq2;c11 'FMT';wrt 6,GS,T[1]
91: "Motor Shift Speed (rpm)"+GS;if flq1;dsp GS;ent "",T[9]
92: if flq2;c11 'FMT';wrt 6,GS,T[9]
93: for C=1 to T[10]
94: if flq1;fxd 0;dsp "Ratio #",C;ent "",T[C+10]
95: if flq2;fmt ,10x,"Ratio # ",fl.,4lx,f7.2;wrt 6,C,T[C+10]
96: next C
97: "Q": " "+AS;cfq 1;cfq 2;gto "RCF"
98:
99: "FMT":FS[1,50-len(GS)]+GS[len(GS)+1,50]
100: fmt 10x,c50,f8.3;ret
101:
102: "RCF":ent "Do you want to record data (y/n)",AS
103: if cap(AS)="N";gto "2"
104: if cap(AS)#"Y";gto -2
105: ent "Which Data File ? (1-5)",FS
106: pos(FS[2,6],FS)+r22
107: if not r22 or len(FS)>1;dsp "Invalid File #";wait 3000;jmp -2
108: dsp "Put tape in RECORD POSITION";imp rds(1)<128
109: dsp "Recording Data"
110: rcf r22+3,DS,A[*],B[*],C[*],D[*],T[*],T
111: dsp "Please WRITE PROTECT TAPE";imp rds(1)>128
112: gto "2"

```

PERFORMANCE MODELING SECTION

```

0: "From Metric":A[1]F[1,1]+A[1];A[8]F[1,1]+A[8];A[9]F[1,1]+A[9]
1: D[3]F[1,1]+D[3];B[1]F[1,2]+B[1];B[12]F[1,3]+B[12];B[10]F[1,3]+B[10]
2: B[6]F[1,4]+B[6];B[7]F[1,4]+B[7];B[2]F[1,5]+B[2];D[2]F[1,6]+D[2]
3: D[1]F[1,7]+32+D[1];B[5]F[1,3]+B[5];qto +5
4: "To Metric":A[1]F[2,1]+A[1];A[8]F[2,1]+A[8];A[9]F[2,1]+A[9]
5: D[3]F[2,1]+D[3];B[1]F[2,2]+B[1];B[12]F[2,3]+B[12];B[10]F[2,3]+B[10]
6: B[6]F[2,4]+B[6];B[7]F[2,4]+B[7];B[2]F[2,5]+B[2];D[2]F[2,5]+D[2]
7: (D[1]-32)F[2,7]+D[1];B[5]F[2,3]+B[5];qto "2"
8: for C=1 to 10;0+E[C];next C
9: for A=1 to 3;for C=0 to 250;0+Y[A,C];next C;next A
10: 0+Z+S+N+D+J+X+R+Y+r33+r49;cfq 7
11: 32.2+D[5];l2*33000/2π+r10;(C[1]+U)/5+r27
12: (44/30+r41)D[3]+r29;.75+r21;54+V
13:
14: "Traction":c11 'Wind/Roll Loss'
15: if B[13]=0;((1-R[11])B[10]+r5B[12])/(B[10]+r21B[12])+r25
16: if B[13]=1;(B[11]B[10]+r5B[12])/(B[10]+r21B[12])+r25
17: r25r21-r5+B;B[1]sin(atan(B))+r26
18: c11 'PART A'
19: lde 3,209
20:
21: "ACCELERATION PATH":0+R+S+D;1+C+0;2+r44
22: if flall;fmt ,54x,"SCHEDULE "D" DRIVING CYCLE",1;/wrt 6
23: if flall;fmt ,50x,"ACCELERATION",1;/wrt 5;c11 'FORMAT I'
24: T+r35;cfq 3;cfq 5;if A[3]=0;0+C
25: 1+0;for Z=0 to A[2] by T
26: dsp "Time :",Z," Speed :",R/r41
27: if R/r41<A[3];Z+r4;c11 'INTERPOLATION';qto +9
28: if flq3;imp 3
29: A[2]-Y[2,A[1]/E]+Y[2,C+A[9]/E]-Y[2,C]+c11
30: (Y[3,C+A[9]/E]r41-R)/r11+A;sfg 3
31: if Z>0;AT+R+R
32: if flq5;imp 2
33: if R>r41Y[3,C+A[9]/E] and A[8]+A[9]<A[1];Y[2,C+A[9]/E]+r4;l0+C;sfg 5
34: if flq5;c11 'INTERPOLATION';imp 2
35: asb "POWER CALCS"
36: RT+S+S
37: if int(Z)=Z and flall;c11 'fmt1'
38: next Z
39: A[2]+Z;if flall;wth 6,10,10
40: if U<.0052[1] and not flall;cfq 7;asb "Checkered Flag"
41: ret
42:
43: "INTERPOLATION":
44: if r4<Y[r44,C-1];C-1+C;imp 0
45: if r4>Y[r44,C];C+1+C;imp 0
46: (r4-Y[r44,C-1])/(Y[r44,C]-Y[r44,C-1])+r3
47: if r44=3;Y[2,C-1]+r3(Y[2,C]-Y[2,C-1])+r45;ret
48: (Y[3,C-1]+r3(Y[3,C]-Y[3,C-1]))r41+R
49: Y[1,C-1]+r3(Y[1,C]-Y[1,C-1])+A
50: r4+T+r1;qto "PC"
51:

```

THIS PAGE IS BEST QUALITY PRACTICABLE
FROM COPY FURNISHED TO DDC

```

52: "POWER CALCS":
53: cll 'Tranny'; cll 'Trans Eff'; cll 'Wind/Roll Loss'
54: GB[1]A/D[5]→L
55: (H+L)R/550→r13; if D=0; (H+L)/r15B[5]2→r2; jmp 3
56: (1-r18)r13+r13+r16; r15r10/(30D/π)2→r2; jmp 2
57: "PC": cll 'Tranny'; cll 'Max Torque'
58: if flg11; cll 'Wind/Roll Loss'; cll 'Trans Eff'
59: cll 'Battery Level'; 2*30Dr2/πr10→r16; ret
60:
61: "CRUISE":
62: if flq11; fmt 1/,63x, "CRUISE", 1/; wrt 5
63: cll 'Wind/Roll Loss'; HR/550→r13
64: cll 'Trans Eff'; (1-r18)r13+r13+r16; r16r10/(30D/π)2→r2
65: 0→r35; cll 'Battery Level'
66: if flq11; cll 'fmt1'
67: RA[3]→S→S; Z+A[3]→Z
68: A[3]→r35; cll 'Battery Level'
69: if flq11; cll 'fmt1'; wtb 6,10,10
70: if U<.005C[1] and not flq11; cfa 7; gsb "Checkered Flag"
71: ret
72:
73: "COAST": 0→r16→r2; cll 'Battery Level'; 0→V[2]→I[2]→I[1]→I[0]
74: if flq11; fmt 1/,64x, "COAST", 1/; wrt 5; cll 'FORMAT II'
75: for C=0 to A[4] by 1
76: if int(C)=C and flq11; cll 'fmt2'
77: cll 'Trans Eff'; cll 'Wind/Roll Loss'; cll 'Tranny'
78: R=(H+(1-r13)H)TD[5]/B[1]G→R
79: RP+S→S; Z+T→Z; next C
80: if flq11; wtb 6,10,10
81: ret
82:
83: "BRAKE": R/A[5]→A; T→r35; if B[8]=1; sfa 10
84: if flq11; fmt 1/,64x, "BRAKE", 1/; wrt 5
85: for C=T to A[5] by 1
86: R-AT→R; if not flq10; ato +6
87: cll 'Tranny'; cll 'Wind/Roll Loss'; cll 'Trans Eff'
88: GB[1]A/D[5]-H→r1; r13r9→r2
89: r9B[5]/2r15→r2
90: cll 'Regenerative Braking'
91: fxd 5; dso U
92: RT+S→S; if int(C)=C and flq11; cll 'fmt2'
93: Z+T→Z; next C
94: if flq11; wtb 6,10,10
95: cfa 10; ret
96:
97: "I-LE": X+1→X; (A[2]+A[3]+A[4]+A[5]+A[6])X→r33
98: S+r43→r43; ret
99:

```

THIS PAGE IS BEST QUALITY PRACTICABLE
FROM COPY FURNISHED TO DDC


```

100: "Tranny":if T[10]>0;qto "GEARBOX"
101: if R=0;(T[4]*r14)T[1]*r15;0*r12;imp 5
102: cll 'D';T[2]/r12T[1]*r14
103: if r14>=T[4];T[4]*r14;imp 3
104: if r14<=T[3];T[3]*r14;imp 2
105: T[2]*D;qto "mass factor"
106: r12r14T[1]*D;qto "mass factor"
107: "GEARBOX":if R=0;0*r12;l+0
108: T[0+10]*r14
109: cll 'D';if 0=T[10] and not flq10;qto +3
110: if flq10 and 0-l>0 and r12T[1]T[0+9]<=T[9]*pi/30;0-l+0;qto -2
111: if r12T[1]T[0+10]>=T[9]*pi/30;0+l+0;qto -3
112: qto "mass factor"
113: "D":r14T[1]*r15
114: R2pi/(piB[5]/6)*r12
115: r12r15*D;ret
116: "mass factor":l+(4B[6]+B[7]r15^2)/B[1]B[5]^2+G;ret
117:
118: "Wind/Roll Loss":
119: B[1](.9(1+(R/r41)1.367e-3+(R/r41)^2*1.622e-5)/75+r5)+r20
120: (R-D[3]cos(D[4]))^2+r31
121: .563r31B[3]B[2]D[2]/(460+D[1])D[5]*r23
122: r20+r23+H
123: ret
124:
125: "Trans Eff":if T[5]=0;.9*r18;ret
126: T[6]*r18;ret
127:
128: "Battery Voltage & Resistance":
129: 2.0395exp(-.11025(1-U/C[1]))*r34
130: (.15/C[1])(1+.01772exo(3.839(1-U/C[1]))) *r36;ret
131:
132: "Max Torque Array":if flq11;dso "LOADING MAXIMUM TORQUE ARRAY"
133: 1000+C;500+r37;((380+I[2])-108)/.6975+r2
134: ((C+760)(4.6406e-4r2^2+.55)+3.1)2+V[2]
135: ((r34-r36+sqrt((r36-r34)^2-4V[2]I[2]r36/V)))/2)V+V[1]
136: if abs(V[1]-V[2])<.001;C+S[1,1];r2+S[2,1];qto +3
137: if V[1]>V[2];C+r37+C;qto -3
138: if V[1]<V[2];C-.9r37+C;r37/10+r37;qto -4
139: 2*I;for C=200int(S[1,1]/200)+200 to 6200 by 200;100+r37
140: "Arm":if (.6975r2+108+I[2])>380;((380+I[2])-108)/.6975+r2
141: ((C+760)(4.6406e-4r2^2+.55)+3.1)2+V[2]
142: "Bat":((r34-r36+sqrt((r36-r34)^2-4V[2]I[2]r36/V)))/2)V+V[1]
143: if abs(V[1]-V[2])<.01 or I[2]=380 and V[1]>V[2];qto +3
144: if V[1]>V[2];r2+r37+r2;qto -4
145: if V[1]<V[2];r2-.9r37+r2;r37/10+r37;qto -5
146: C+S[1,1];r2+S[2,1];I+1+I
147: next C;ret
148:
149: "Max Torque":300/pi+r33;2*I
150: if r33<S[1,1];((380+I[2])-108)/.6975+r2;qto +5
151: if r33>S[1,1];I+l+I;imp 0
152: if r33<S[1,I-1];I-l+I;imp 0
153: (r33-S[1,I-1])/(S[1,I]-S[1,I-1])*r3
154: S[2,I-1]+r3(S[2,I]-S[2,I-1])*r2
155: 2r2r33/r10+r0;ret
156:

```

THIS PAGE IS BEST QUALITY PRACTICABLE
FROM COPY FURNISHED TO DDC

```

157: "Battery Level":30D/π+r38
158: .6975r2+108+I[2]
159: ((r38+760)(4.6406e-4r2.56+3.1)2+V[2]
160: ((r34-9r36+√((9r36-r34)2-4V[2]I[2]r36/V)))/2)V+V[1]
161: I[2]V[2]/V[1]+9+I[1]
162: U-r27(-.334775)I[1]l.334775r35/3600+U
163: ret
164:
165: "Regenerative Braking":30D/π+r38
166: if (.6975r2+108+I[2])>380;((380+I[2])-108)/.6975+r2
167: ((r38+760)(4.6406e-4r2.56+3.1)2+V[2]
168: (-(r34+9r36)+√((r34+9r36)2-4r36(9r34-V[2]I[2]/V)))/2r36+I[1]
169: I[2]V[2]/(I[1]+9)+V[1]
170: C[1]-U+I;if I<I[1];I+I[0];imp 2
171: I[1]+I[0]
172: I[0]r35/3600+Y+Y
173: U+r27(-.334775)I[0]l.334775r35/3600+U;ret
174:
175: "PART A":sfg 11
176: for W=.9 to .1 by -.2;C[1]V+U
177: if W=.7 or W=.5;next W
178: asb "MAX. ACCELERATION"
179: qsb "ACCELERATION PATH"
180: qsb "CRUISE"
181: asb "COAST"
182: asb "BRAKE"
183: asb "IDLE"
184: next W
185: asb "Range @ Const Speed"
186: cfa 11;ret
187:

```

THIS PAGE IS BEST QUALITY PRACTICABLE
FROM COPY FURNISHED TO DDC

```

188: "MAX. ACCELERATION":fxd 2;.25+E;0+D+R+c35+r48;l+r24;sfg 6;B+Q
189: fmt 3/,53x,"SAE J227a TEST PROCEDURE",l;/wrt 6
190: fmt 50x,f5.1," Percent Charge Remaining",l;/wrt 6,100U/C[1]
191: gsb "Battery Voltage & Resistance"
192: gsb "Max Torque Array"
193: for C=0 to 62.25 by E;r41C+R;C+r47
194: cll 'Tranny';cll 'Wind/Roll Loss';cll 'Trans Eff'
195: cll 'Max Torque';HR/550+r1
196: if D=0;r2D[5]r15(1-r5)r18/B[1]B[5]+Y[1,C];0+Y[2,C];qto +11
197: (1-1/(2-r18))r0+r1+r7
198: (r0-r7+r8)550/R+r9
199: if int(C/6.25)=C/6.25;r24+l+r24
200: if flq5 and r9<r26;cll 'Grade'
201: if int(r47/6.25)=r47/6.25 and not flq5;r9+E[r24]
202: if B[13]=1;r21B[1](B[11]-Y[1,(C-E)/E]B[12]/D[5]B[10])+r19
203: if B[13]=0;r21B[1](1-B[11]+Y[1,(C-E)/E]B[12]/D[5]B[10])+r19
204: if r19<r9;r19+r9
205: r9D[5]/EB[1]+Y[1,C/E]
206: (Er41/Y[1,(C-E)/E]+r35)+Y[2,(C-E)/E]+Y[2,C/E]
207: C+Y[3,C/E]
208: if Y[1,C/E]<0;(C-E)/E+r49;qto +3
209: dsp "Time :",Y[2,C/E]," Speed :",C
210: next C
211: gsb "Grade"
212: fmt 27x,"MAXIMUM ACCELERATION";wrt 6;3+r44;l+C
213: fmt 21x,"Speed (KPH)",12x,"Time (sec)",l;/wrt 6
214: fmt 4,22x,"0 to ",f3.,12x,f7.2
215: for M=10 to 100 by 10;MF[1,1]+r4;cll 'INTERPOLATION'
216: wrt 5.4,M,r45;if (M+10)F[1,1]>Y[3,r49] and Y[3,r49]>0;qto +2
217: next M;qto +2
218: "Too Speed":fmt 23x,"Too Speed =",f6.1,"(KPH)";wrt 6,Y[3,r49]F[2,1]
219: wtb 5,10,10
220: ret
221:
222: "FORMAT I":
223: fmt 1x,"Time Speed Motor Torque Motor Drive L",4x,z;wrt 6
224: fmt "Wind L Roll L Battery Armature Battery",4x,z;wrt 6
225: fmt "Armature Motor";wrt 5
226: fmt 1x,"(sec) (KPH) (RPM) (N-M) (HP)",5x,z;wrt 6
227: fmt "(HP) (HP) (HP) Voltage Voltage Current",z
228: wrt 5;fmt 4x,"Current Efficiency";wrt 6;ret
229:
230: "FORMAT II":
231: fmt 1x,"Time Speed Motor Torque Drive L",4x,z;wrt 6
232: fmt "Wind L Roll L Battery Armature Battery",4x,z;wrt 6
233: fmt "Armature Recharge Gen.";wrt 5
234: fmt 1x,"(sec) (KPH) (RPM) (N-M)",5x,z;wrt 6
235: fmt "(HP) (HP) (HP) Voltage Voltage Current",z
236: wrt 6;fmt 4x,"Current Current Eff.",l;/wrt 6;ret
237:

```



```

238: "fmt1":Z+r50;RF[2,1]/r41+r51;30D/π+r52;2r2/8.8507+r53;r16+r54
239: (1-r18)r16+r55;r23R/550+r56;r20R/550+r57;V[1]+r58;V[2]+r59
240: I[1]+r60;I[2]+r61;100(745.7r16)/I[2]V[2]+r62
241: fmt f5.1,f10.2,f9.1,f9.2,f10.2,f9.2,x,2f10.2,2f11.1,x,3f11.1,;gto "WRT1"
242:
243: "fmt2":Z+r50;RF[2,1]/r41+r51;30D/π+r52;2r2/8.8507+r53
244: (1-r18)HR/550+r54;r23R/550+r55;r20R/550+r56;V[1]+r57;V[2]+r58
245: I[1]+r59;I[2]+r60;I[0]+r61;if V[1]=0 or I[1]=0;0+r62;jmp 2
246: 2r2r38/r10+r16;100(745.7r16)/I[2]V[2]+r62
247: fmt f5.1,f10.2,f9.1,f9.2,f10.2,f11.2,f10.2,3f11.1,x,2f11.1,f10.1
248: gto "WRT1"
249:
250: "WRT1":wrt 6,r50,r51,r52,r53,r54,r55,r56,r57,r58,r59,r60,r61,r62;ret
251:
252: "Grade":
253: if not flq6;gto +6
254: fmt 85x,"MAXIMUM GRADABILITY";wrt 6
255: fmt 78x,"Speed (KPH)          Percent Grade",/;wrt 6
256: if Y[3,(C-E)/E]<1;cfq 6;6.25+r47;ret
257: fmt 79x,"0 to ",f4.1,13x,f5.1;wrt 6,Y[3,(C-E)/E]F[2,1],100Q;cfq 6
258: 1+r48;ret
259: for M=1 to 10;100tan(asn(E[M]/B[1]))+0
260: if E[M]>0;fmt ,80x,f4.0,17x,f5.1;wrt 6,L0(M-1),0;r48+1+r48
261: next M
262: for M=1 to r43+3;wth 6,27,10;next M;ret
263:
264: "Range @ Const Speed":sfq 9;fxd 3
265: fmt 2/,53x,"RANGE AT STEADY SPEED";wrt 6
266: for O=0 to 30 by 5
267: fmt 2/,12x,"Range at constant speed ",f3.," percent grade:","/
268: wrt 6,O;B[1]sin(atn(O/100))+F
269: fmt 7x,"Speed          Range          Motor          Torque          Motor",5x,z;wrt 6
270: fmt "Wind L          Roll L",5x,z;wrt 6
271: fmt "Time          Trans.          Amp-HR          Motor",;wrt 6
272: fmt 7x,"(KPH)          (KM)          RPM          (N-M)          HP ",6x,z;wrt 6
273: fmt " HP",10x,"HP",9x,z;wrt 6
274: fmt "(hrs)          Gear          used          Efficiency",/;wrt 6
275: for M=10 to 100 by 10;MF[1,1]r41+R;0+S+E+A+Z;1+0;50+r35
276: cll 'Tranny';ccl 'Wind/Roll Loss';ccl 'Trans Eff';C[1]+U
277: (E+H)R/550+r13;(1-r18)r13+r13+r16;r16r10/2(30D/π+C)+r2
278: if r2>S[2,1];next M;next O;cfq 9;ret
279: cll 'Battery Voltage & Resistance'
280: cll 'Battery Level';if V[1]<V[2];gto +5
281: if U<0;r35/2+r35;U+U;ato -1
282: dso U100/C[1]
283: U+r;Rr35+S+S;r35+E+E;I[1]r35/3600+A+A;745.7*100*2r2C/r10I[2]V[2]+B
284: if U>.001 or V[1]-V[2]<.001;ato -5
285: if S=0;jmp 3
286: fmt 1x,2f11.2,f11.1,2f11.2,2f12.2,f11.2,f9.0,f14.2,f12.1
287: wrt 6,M,SF[2,1]/5280,C,2r2/8.8507,r16,r23R/550,r20R/550,E/3600,O,A,B
288: next M;next O;cfq 9;ret

```

DRIVING CYCLE RANGE

```

0: "PART B":sfq 7;C[1]+U;0+Y+X+S+Z+r43;fxd 0
1: if flq7;dsp " MAX. ACCELERATION";qsb "MAX. ACCELERATION"
2: if flq7;dsp " ACCELERATION PATH";qsb "ACCELERATION PATH"
3: if flq7;dsp " CRUISE";qsb "CRUISE"
4: if flq7;dsp " COAST";qsb "COAST"
5: if flq7;dsp " BRAKE";qsb "BRAKE"
6: if flq7;qsb "IDLE"
7: fmt "% LAPS =",f7.;wrt 16,X
8: fmt "% CHG. =",f7.2,1/;wrt 16,100U/C[1]
9: if flq7;qto -8
10: qto "To Metric"
11:
12: "MAX. ACCELERATION":.25+F;0+D+R+r35;l+r24;sfq 6;B+Q
13: fxd 0;dsp "NUMBER OF CYCLES COMPLETED :",X
14: qsb "Battery Voltage & Resistance"
15: qsb "Max Torque Array"
16: dsp " MAX. ACCELERATION";fxd 2
17: for C=0 to A[1]+E by E;r41C+R
18: cll 'Tranny';cll 'Wind/Roll Loss';cll 'Trans Fff'
19: cll 'Max Torque';HR/550+r1
20: if D=0;r2D[5]r15(1-r5)r19/B[1]B[5]+Y[1,C];0+Y[2,C];qto +8
21: (1-1/(2-r19))r0+r1+r7
22: (r0-r7+r3)550/R+r)
23: if B[13]=1;r21B[1](B[11]-Y[1,(C-E)/E]B[12]/D[5]B[10])+r19
24: if B[13]=0;r21B[1](1-B[11]+Y[1,(C-E)/E]B[12]/D[5]B[10])+r19
25: if r19<r9;r19+r9
26: r9D[5]/GB[1]+Y[1,C/E]
27: (Er41/Y[1,(C-E)/E]+r35)+Y[2,(C-E)/E]+Y[2,C/E]
28: C+Y[3,C/E]
29: if Y[1,C/E]<0;(C-E)/E+r49;qto +2
30: next C
31: if Y[2,A[1]/E]>A[2] or Y[3,r49]<A[1] and r49>0;cfg 7;qsb "Checkered Flag"
32: ret
33:
34: "Checkered Flag":
35: fmt 15x,"Range Driving Schedule "D" (KM):",7x,f9.2;wrt 6,r43F[2,1]/52
36: fmt 1/,15x,"Total Driving Time (hrs):",13x,f9.2,1/;wrt 6,r33/3600
37: fmt 15x,"Number of Cycles Completed :",10x,f9.2,1/;wrt 6,X
38: fmt 15x,"A-hr Gained by Regenerative Braking :",4x,f7.2,1/;wrt 6,Y
39: fmt 15x,"Percent Energy Gained by Regen. Braking :",f7.2,1/
40: wrt 6,100(1-C[1]/(C[1]+Y))
41: ret

```

TABLE III
ERAB PROGRAM VARIABLE LISTING

Simple Variables

A	Acceleration rate (m/sec^2)
B	Maximum gradeability
C	Counter
D	Motor speed (rad/sec)
E	Velocity increments used in "Maximum Acceleration"
F	Force @ drive wheels (N)
G	Mass factor
H	Total mechanical resistance (N)
I	Regenerative current (Amperes)
L	Force required for acceleration (N)
M	Gradeability routine counter, miscellaneous counter
O	Present transmission gear
Q	Gradeability (%)
R	Velocity (m/sec)
S	Distance traveled, (m)
T	Time increment (sec)
U	Ampere-hrs in battery
W	Energy Counter
X	Number of laps completed
Z	Total time to complete lap (sec)

"r" Variables

r0	Motor H.P. @ present speed
r1	Roll. H.P. + wind loss H.P. (maximum acceleration routine)
r2	Motor torque @ present speed
r3	Ratio used in interpolation routine
r4	Time (used in interpolation routine)
r5	Rolling resistance coefficient
r6	Dummy variable used in transmission edit section
r7	Sum of losses (H.P.) (maximum acceleration routine)
r8	H.P. available for acceleration (maximum acceleration routine)

"r" Variables (continued)

r9 Force @ wheel available for acceleration (N)
r10 63025 (used in H.P., torque relationships)
r11 Linear acceleration path time (acceleration path routine)
r12 Tire angular velocity (rad/sec)
r13 Wind, roll, acceleration H.P. (power calcs)
r14 Current transmission ratio
r15 Transmission ratio x final drive ratio
r16 H.P. required for acceleration
r18 Transmission efficiency
r19 Maximum tractive capability (N)
r20 Rolling resistance of tires (N)
r21 Coefficient of road adhesion
r22 Dummy variable
r23 Wind resistance (N)
r24 Counter
r25 Weight distribution factor
r26 Wheel force required for maximum gradeability (N)
r27 Battery 5 hr discharge current (Amperes)
r28 Wind velocity (m/sec)
r31 Air drag sub calculation
r33 Total time (hrs)
r34 Single cell voltage
r35 Time increment in "Battery"
r36 Internal battery resistance
r37 Convergence factor in battery
r38 Motor speed used in "current" (RPM)
r41 Conversion factor
r43 Distance counter
r44 Used in metric print out
r45 Used in metric print out
r46 Maximum gradeability
r47 Variable used in "maximum acceleration", loads E *
r48 Line counter in gradeability counter

"r" Variables (continued)

r49 Y n, r49 = data associated with maximum speed

Array Variables

Driving cycle information A(10)

- A(1) Acceleration maximum speed (kph)
- 2 Acceleration time (sec)
- 3 Cruise time (sec)
- 4 Coast time (sec)
- 5 Brake time (sec)
- 6 Idle time (sec)
- 8 Speed which linear acceleration begins
- 9 Linear acceleration delta velocity

Vehicle data B(20)

- B(1) Weight (kg)
- 2 Frontal area (m^2)
- 3 Aerodynamic drag coefficient
- 4 Rolling resistance coefficient
- 5 Tire rolling radius (cm)
- 6 Wheel moment of inertia $N\cdot m^2$
- 7 Moment inertia of motors $N\cdot m^2$
- 8 Regenerative braking flag 1 = yes, 0 = no
- 10 Wheel base (cm)
- 11 Fraction of weight on front wheels
- 12 Center of gravity height (cm)
- 13 Front or rear wheel drive, 1 = F, 0 = R

Battery data C(5)

- C(1) Ampere-hr capacity (5 hr discharge)

Ambient conditions D(8)

- D(1) Temperature ($^{\circ}C$)
- 2 Barometric Pressure (mm Hg)
- 3 Wind velocity (kph)
- 4 Wind angle (deg)
- 5 Gravity constant (m/sec^2)

Transmission data T(15)

- T(1) Final drive ratio
- 2 Motor shift speed (rad/sec)
- 3 Minimum transmission reduction
- 4 Maximum transmission reduction
- 5 Motor shift speed (RPM)
- 6 Transmission efficiency
- 9 Shift point (RPM)
- 10 Number of ratios in transmission
- 11 Ratio #1
- 12 Ratio #2
- 13 Ratio #3
- 14 Ratio #4
- 15 Ratio #5

Array Variables

F(2, 7)

F(1, 1) - Conversion from kph to miles per hour

F(1, 2) - Conversion from kg to lb

F(1, 3) - Conversion from cm to in

F(1, 4) - Conversion from N-m to in-lb

F(1, 5) - Conversion from sq. m to sq. ft

F(1, 6) - Conversion from mm to in

F(1, 7) - Conversion from °C to °F

F(2, 1) thru F(2, 7) are to convert the above from English units back to SI units.

Y(3, 0:250)

Y(1, N) : Maximum acceleration (m/sec^2)

Y(2, N) : Time increment in maximum acceleration (sec)

Y(3, N) : Velocity in maximum acceleration (m/sec)

String Variables

A\$(1) - Used for 1 letter answers

D\$(60) - Data file title

E\$(13) - Number set

F\$(5) - Used for answers

G\$(50) - Input data string

H\$(50) - Null file (is needed for I/O)

E(0:5)
E(0) } Force at wheels in 10 mph increments
E(5) }

Flags Used

Flg 1 Edit section
Flg 2 List data section
Flg 3 "Acceleration path"
Flg 4 Control pgm
Flg 5 "Acceleration path"
Flg 6 Used in gradeability
Flg 7 Used to end pgm; battery charge = 0
Flg 9 Used in "Range @ constant speed"
Flg 10 Regenerative braking flag

8.1.6 Discussion of ERAB Program by Subroutines

A brief explanation of each subroutine shown in the program flow chart and the program listing is given in this section. Exceptions are the control and data entry sections which do not play an active part in the modeling portion of the program. The variables used in the following section are described in Table IV.

TABLE IV
VARIABLE DEFINITIONS

A	Acceleration rate	(m/sec ²)
A ₁	Frontal area of test bed	(m ²)
B	Maximum gradeability	
C ₁	Road adhesion coefficient	
C ₂	Rolling resistance coefficient	
C ₃	Tire coefficient, C ₃ = .9 for radial tires	
C ₄	Aerodynamic drag coefficient	
C ₅	Fraction of weight on driving wheels	
F ₁	Rolling resistance force	(N)
F ₂	Wind resistance force	(N)
F ₃	Drive train resistance force	(N)
F ₄	Force at drive wheels	(N)
F ₅	Force at drive wheels available for acceleration	(N)
F ₆	Maximum tractive force	(N)
g	Gravity constant	(m/sec ²)
G	Mass factor	
H ₁	Height of test bed center of gravity	(cm)
I ₁	Moment of inertia of motors	(N-m ²)
I ₂	Moment of inertia of wheels	(N-m ²)
K	Weight distribution factor	
L ₁	Wheelbase length	(cm)
N	Reduction ratio between motor and wheels	
P ₁	Rolling loss power	(kw)
P ₂	Wind loss power	(kw)
P ₃	Drive train loss power	(kw)
P ₄	Power required for acceleration	(kw)
Q	Maximum gradeability at speed	(%)
R ₁	Rolling radius of tires	(cm)
ΔT	Time increment for calculations	(sec)
V	Velocity	(m/sec)
V ₁	Velocity at beginning of increment	(m/sec)
V ₂	Velocity at end of increment	(m/sec)
Δ	Speed increment	

Variable Definitions (continued)

W_1	Weight of test bed (kg)
ρ	Air density (kg/m^3)
τ	Torque at motor (N-m)
τ_{max}	Maximum motor torque (N-m)
ω	Motor angular velocity (rad/sec)

Main Body of Program

"Traction": Subroutine "wind/roll loss" is addressed to determine the rolling resistance coefficient. This in turn is used to calculate the weight distribution factor:

$$K = (C_5 L + C_2 H_1) / (L - C_1 H_1) \quad (8-1)$$

Then, maximum gradability is calculated by:

$$B = K C_1 - C_2 \quad (8-2)$$

The corresponding wheel force or maximum tractive force is calculated from:

$$F_6 = W_1 g \sin \left[\tan^{-1} (B) \right] \quad (N) \quad (8-3)$$

"Acceleration Path": All calculations are carried out within a loop, from 0 time to the specified J227a acceleration time. The time increment for calculations is a program input.

The acceleration path is specified by two inputs:

1. Speed to begin linear acceleration.
2. Linear acceleration delta velocity.

The maximum vehicle acceleration profile is calculated and stored by subroutine "Max Acceleration". The specified linear acceleration is then inserted into the maximum acceleration profile such that the final profile puts the test bed at the proper terminal speed and time. This is illustrated graphically by Figure 23.

Subroutines "Interpolation" and "Power Calcs" are called upon for acceleration rate and power requirements.

Distance traveled is summed up during this portion.

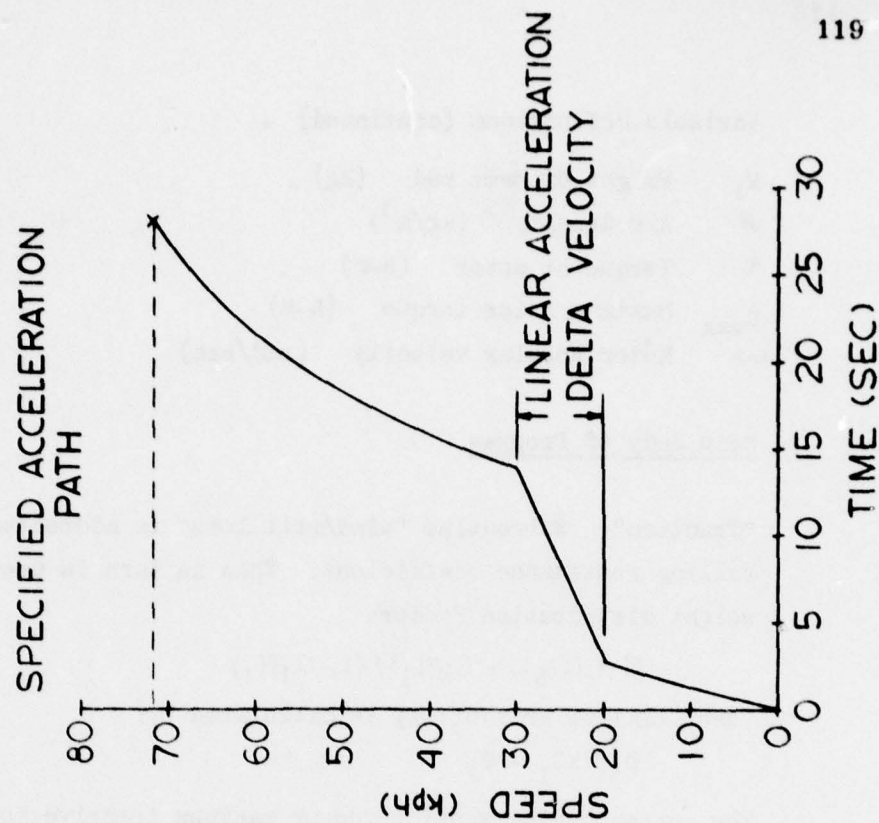
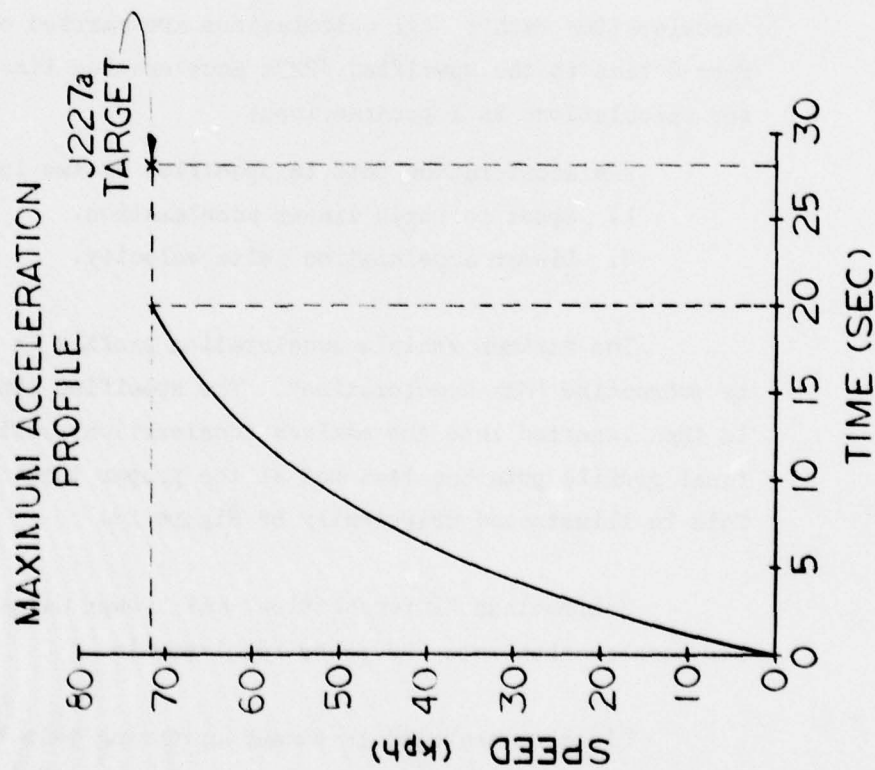
"Interpolation:" This subroutine is addressed during the "Acceleration

FIGURE 23

ACCELERATION PATH SPECIFICATIONS

Accelerate to what speed (kph)?	72
Accelerate in how much time (sec)?	28
Speed to begin linear acceleration (kph).	20
Linear acceleration delta velocity (kph).	10

Figure



Path" loop. Its function is to return the maximum acceleration and speed of the test bed at the specified time. The information is interpolated from the "Maximum Acceleration" array as a function of time.

"Power Calcs": Power calculations and battery energy level updates are carried out for each time increment of "Acceleration Path".

Horsepower required for given acceleration rate is calculated by:

$$P_4 = 1.84(10)^{-3} G W_1 A V \quad (\text{kw}) \quad (8-4)$$

Subroutines "Wind/Roll Loss", "Trans Eff", and "Tranny" are called upon for test bed power losses. Total kw required = $P_1 + P_2 + P_3 + P_4$.

The battery charge level is then updated by calling "Battery Level", knowing motor torque and speed, and the time increment.

"Cruise": The cruise portion of J227a is done at the final speed of "Acceleration Path". Horsepower requirements are calculated as in "Power Calcs":

Power required = $P_1 + P_2 + P_3$, where the variables are the same as above. "Battery Level" is called upon at the end of the subroutine to be updated. Distance traveled is calculated and added to the previous total.

"Coast": Motor horsepower and torque are set to 0, and a loop is established by incrementing time. Within the loop, the test bed losses are calculated at each time and corresponding speed. A new speed is then calculated by:

$$V_2 = V_1 - (F_1 + F_2 + F_3) \Delta T / W_1 G \quad (\text{m sec}^{-1}) \quad (8-5)$$

Distance traveled during each increment is calculated and summed.

"Brake": Braking is done by a linear deceleration from the final coast speed to a complete stop in the allotted braking time. A time incremented loop is established to find the torque available for regenerative braking at all speeds. The losses are summed as in "Coast" before the following calculation is carried out:

$$\tau = [G W A - (F_1 + F_2 + F_3)] R / 2 N \quad (\text{sec}) \quad (8-6)$$

Subroutine "Regen. Braking" is called and the battery level is updated. Distance traveled during each increment is calculated and summed.

"Idle": The number of cycles completed is updated, as is the total time spent on the driving cycle, and the total distance traveled on the driving cycle.

"Tranny": The first function of "Tranny" is to calculate the test bed motor speed. Ground speed is converted to motor speed by the following equation:

$$\omega = 100VN/R_1 \quad (\text{rad/sec}) \quad (8-7)$$

It is then determined whether a shift (a new ratio) is required by comparing the calculated motor speed to the specified shift speed. The transmission will upshift or downshift as required.

"Mass Factor": Mass factor is the effective inertia of the test bed, including both mass of the test bed and inertia of rotating parts. The following equation is utilized:

$$G = 1 + \left[(4I_1 + I_2 N^2) / W_1 g (R_1/100)^2 \right] \quad (8-8)$$

The mass factor changes with each new transmission ration.

"Wind/Roll Loss": Rolling resistance forces are calculated from:

$$C_2 = (C_3/75) (1 + 6.11 \times 10^{-4}V + 3.47 \times 10^{-6}V^2) \quad (8-9)$$

$$\text{Rolling resistance force is then: } F_1 = WC_2g \quad (N) \quad (8-10)$$

Aerodynamic drag force is calculated as follows:

$$F_2 = (1/2)\rho C_d A_1 v^2 \quad (N) \quad (8-11)$$

"Trans Eff": An efficiency or an equation for efficiency is assigned to the transmission and drive train.

"Battery Voltage & Resistance": Battery single cell voltage and internal resistance are calculated as a function of battery charge. See section 7.0 for development of equations.

"Max. Torque Array": This subroutine calculates the maximum motor torque at incremented speeds and stores this information in an array. See section 7.0 for development of equations.

"Max. Torque": Maximum torque is linearly interpolated from the "Max. Torque Array" as a function of motor speed. Motor horsepower is calculated and returned.

"Battery Level": Charge level is updated. See section 7.0 for development of equations.

"Regenerative Braking": Calculates amperage and voltage accepted by battery during regenerative braking. See section 7.0 for development of equations.

"Part A": Is control section of subroutines listed in this section; sets sequence for execution.

"Max. Acceleration": Test bed is accelerated from 0 speed to a designated speed under full motor power. Speed is incremented by .40 kph; speed, acceleration rate and elapsed time are stored in an array at each increment. Calculations are carried out in the following manner:

1. Force available at the drive wheels is calculated by:

$$F_4 = (100 T_{\max} N/R_1) - F_3 \quad (N) \quad (8-12)$$

2. This force is then compared to the maximum tractive force available (calculated in "Traction") and the lesser of these is used for further calculations.

3. Force at wheels available for acceleration is then:

$$F_5 = F_4 - F_2 - F_1 \quad (N) \quad (8-13)$$

At specific speeds, values of F_5 are stored for use in "Grade".

4. Acceleration rate is calculated:

$$A = F_5 / W_1 G \quad (m/sec^2) \quad (8-14)$$

5. Elapsed time between speed increments is now calculated:

$$\Delta T = \Delta V / A \quad (sec) \quad (8-15)$$

Time is summed up at each increment and total time to each speed is stored.

"Format I" and "Format II": Column headings for printout are formatted and printed. See section 8.1.6 for detailed information.

"fmt 1" and "fmt 2": Program calculated data is prepared and formatted for printout.

"WET 1": Program calculated data is printed.

"Grade": Maximum test bed gradeability is calculated for an incremented range of speeds. At each interval, force at wheels available for acceleration (F_5) has been stored and is now used for gradability calculations:

$$Q = 100 \tan (\sin^{-1} F_5 / W_1 g) \quad (\%) \quad (8-16)$$

If Q is greater than B (calculated in "Traction"), B is printed.

"Range at Const. Speed": This subroutine is incremented on two levels; percent grade from 0 to 30, and speeds from 10 to 100 km/hr at each grade. Power requirements from motor are calculated as shown in several other subroutines. Battery level is monitored at 50 second intervals. End of range is realized when the test bed can no longer maintain speed or the battery charge is depleted.

"Part B": Is control section of "Range under J227a".

"Checkered Flag": Compiles data at end of J227a range calculations and prints all specified output.

8.2 Mechanical Drive Train Optimization

The computer model previously described offers the capability of optimizing the test bed in several areas. The topics of special interest are: range under J227a driving cycle, range at steady speed, maximum gradeability, and maximum acceleration. To optimize in any one area may result in inadequate performance in another, therefore, a compromise must be reached. As can be seen by many of the modeling results, the proposed state-of-the-art test bed is a series of compromises.

Specific topics that were investigated by computer simulation are:

1. Selection of number of ratios in transmission.
2. Selection of transmission shift point.
3. Selection of final drive ratio.
4. Effect of increasing number of batteries.
5. Effect of acceleration path on J227a range.
6. Effects of regenerative braking.
7. Performance of a projected test bed configuration.

By a thorough study of the above parameters, many significant conclusions have been reached.

8.2.1 Selection Criterion for Transmission Configuration

At the start of the performance modeling phase of the electric test bed study, the transmission selection had been reduced to the following:

- a) 1-speed involute tooth form gear
- b) 2-speed involute tooth form gear
- c) 4-speed involute tooth form gear
- d) Infinitely variable ratio traction drive or belt drive.

Each of the transmissions were evaluated by the computer model for the following categories:

1. Acceleration performance
2. Gradeability
3. Range at steady speed
4. Range on driving cycle

8.2.2 Selection of Final Drive Ratio

The minimum reduction gear ratio or cruise gear modeled in all of the transmissions is a 1:1 ratio. This gives a common basis for final drive selection. Figure 24 shows the relationship of test bed cruise range for various final drive ratios. From this figure it can be seen that cruising range at 88 km/hr (55 mph) falls off rapidly with final drive ratios less than 5:1. This is because the motor is at low, inefficient speeds with the numerically low ratios. Further investigation shows that acceleration to cruising speed suffers with numerically high final drive ratios. Figure 25 shows this effect. The high final drive ratios force the test bed motors to work at high speeds at which they produce less torque. A 5:1 final drive ratio appears to be the best compromise between cruising range and acceleration performance; therefore, all performance modeling conducted utilized a 5:1 final drive ratio.

Figure 24

RANGE VERSUS FINAL DRIVE RATIO

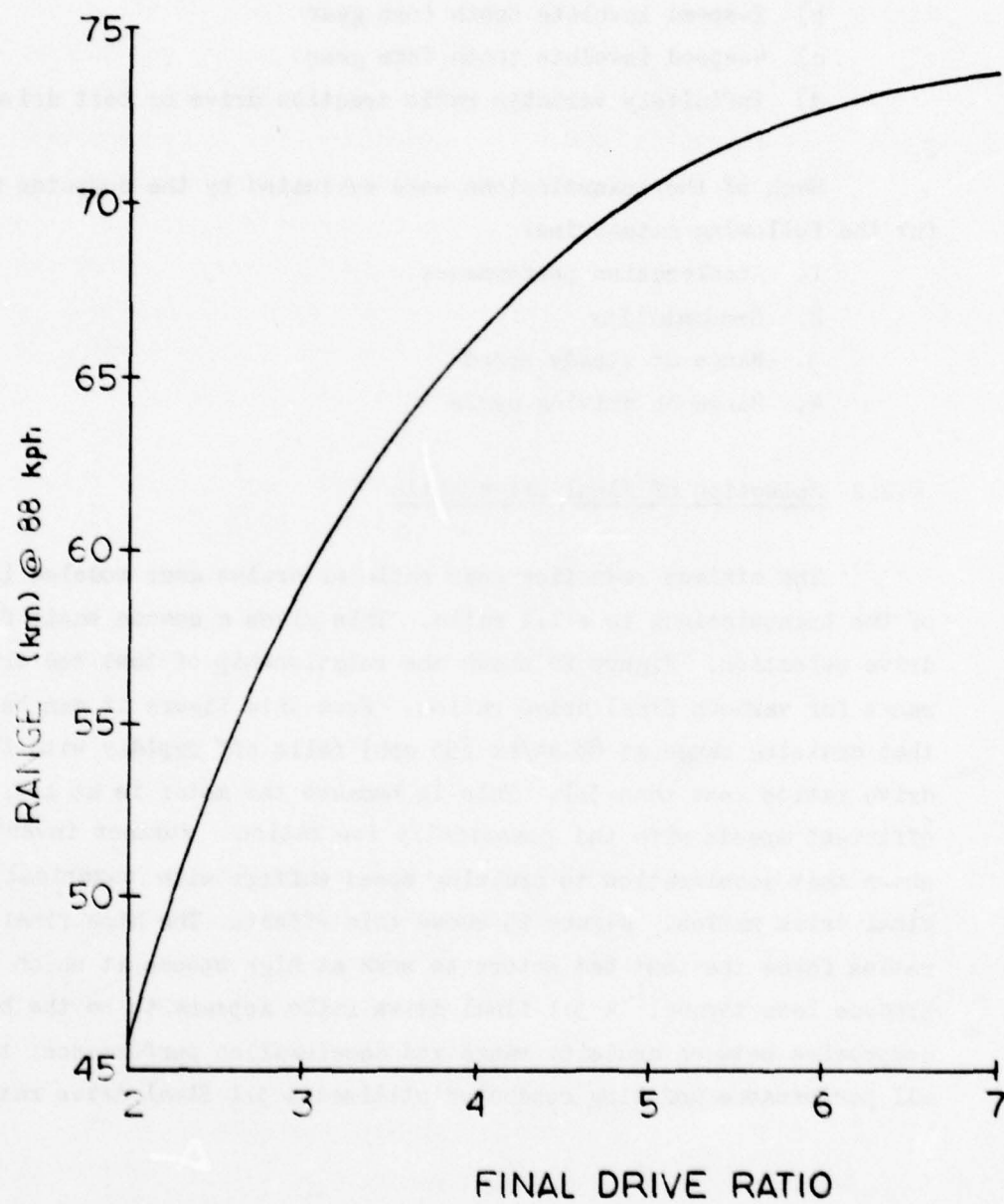
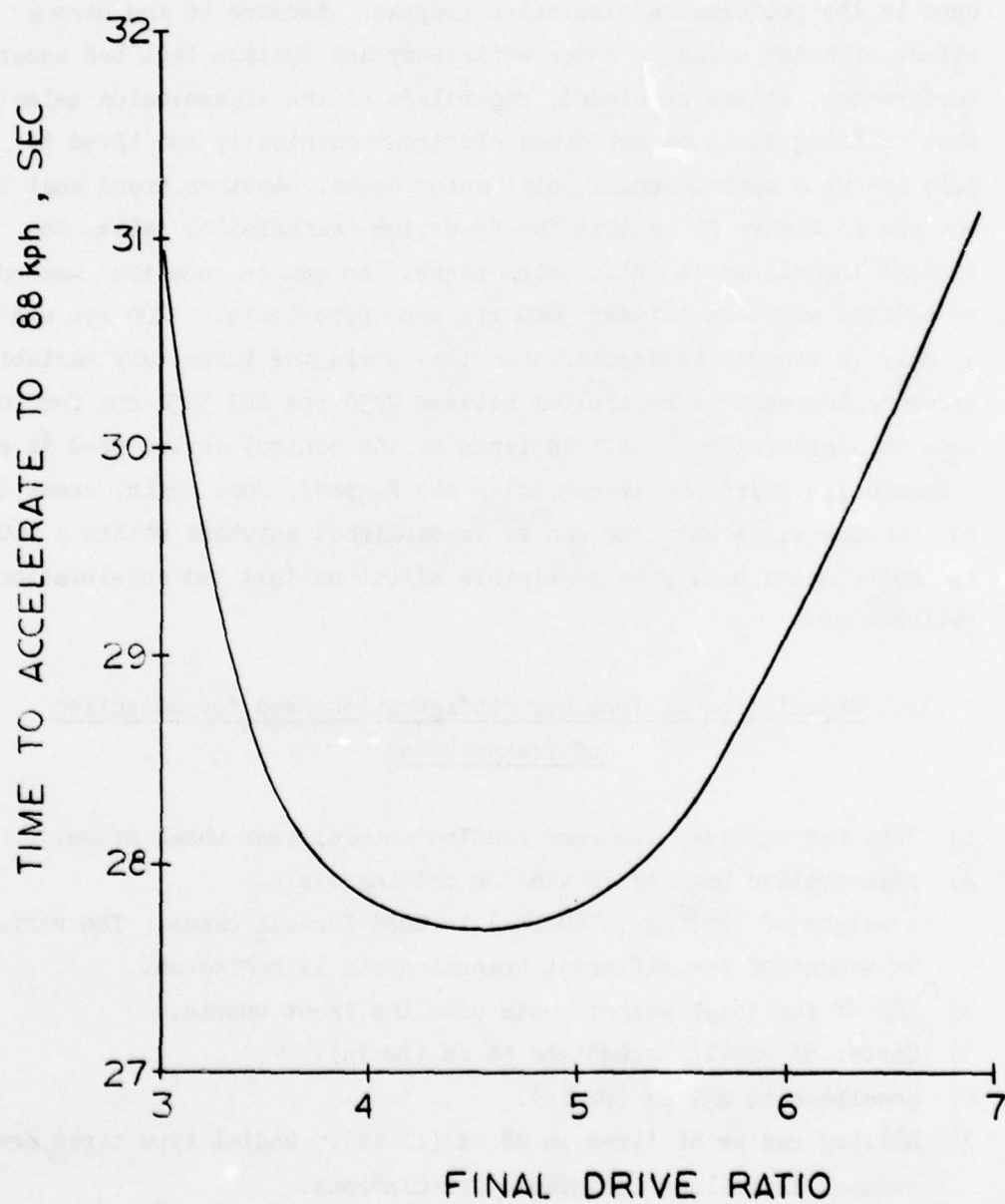


Figure 25

ACCELERATION TIME
VERSUS
FINAL DRIVE RATIO



8.2.3 Selection of Transmission Shift Point Motor Speed

Although the selection of shift point motor speed has negligible effect on test bed cruise range, it produces a significant influence on test bed acceleration time. As shown in Figure 26 the optimum shift point speed for the 2-speed is 4500 rpm while the 4-speed and infinitely variable transmissions require shifting at 3350 rpm and 3050 rpm respectively. In order to evaluate fairly each transmission type for performance capability in the test bed, the optimum shift point motor speeds were used in the performance simulation program. Because of the strong effect of motor speed on motor efficiency and optimum test bed acceleration performance, it was concluded, regardless of the transmission selected, that shifting would be performed electro-mechanically and timed to coincide with optimum shift point motor speed. Another trend that is obvious in Figure 26 is that the fewer the transmission ratios the broader the allowable shift point range. As can be seen the 2-speed could be shifted anywhere between 3600 rpm and approximately 5200 rpm and give up only .2 seconds in acceleration time while the infinitely variable transmission must be controlled between 2750 rpm and 3350 rpm for the same loss in acceleration time. In terms of the control device used to electro-mechanically shift the transmission the 2-speed, once again, seems the best choice since shifting can be accomplished anywhere within a 1600 rpm motor speed band with negligible effect on test bed acceleration performance.

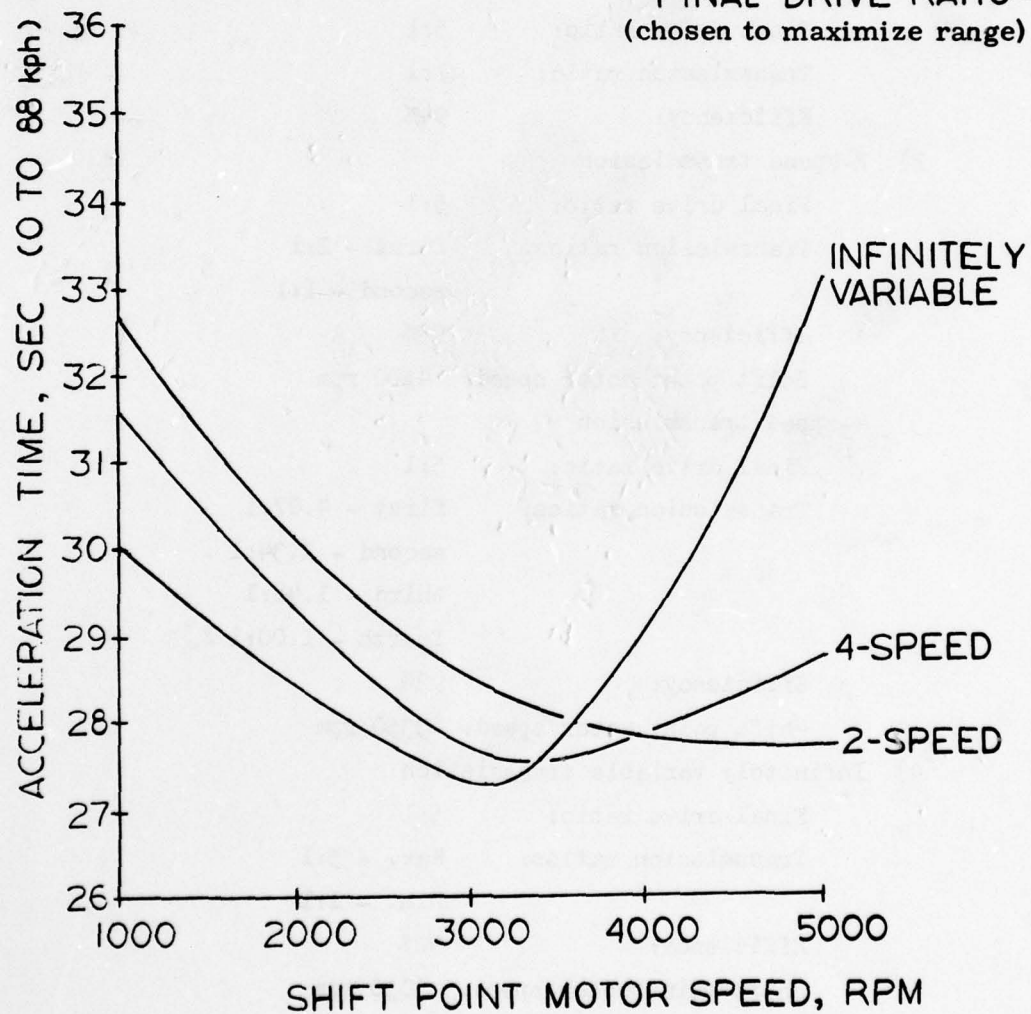
8.2.4 Description of Test Bed Configuration Used for Selection of Transmission

- 1) Test bed utilizes two rear mounted motors, rear wheel drive.
- 2) Regenerative braking is used on driving cycle.
- 3) A weight of 1245 kg (2740 lbs) is used for all cases. The variation in weight of the different transmissions is neglected.
- 4) 56% of the total weight rests over the front wheels.
- 5) Center of gravity height is 56 cm (22 in).
- 6) Wheelbase is 229 cm (90 in).
- 7) Rolling radius of tires is 28 cm (11 in). Radial type tires are assumed in rolling resistance calculations.
- 8) Moment of inertia of each wheel and tire is 4.16 N-m^2 (1500 lb-in²).

Figure 26

TEST BED ACCELERATION TIME
VERSUS
SHIFT POINT MOTOR SPEED

FINAL DRIVE RATIO = 5:1
(chosen to maximize range)



- 9) Moment of inertia of motors (total) is $.502 \text{ N-m}^2$ (175 lb-in^2).
- 10) Battery capacity is 180 A-hr for a 5 hr. discharge. There are 18 6-volt batteries wired in series, for a total nominal voltage of 108.
- 11) Frontal area is 1.67 m^2 (18 ft^2).
- 12) Aerodynamic drag coefficient is .42
- 13) Barometric pressure is 760 mm Hg.
- 14) Ambient temperature is 20°C (68°F).
- 15) All calculations are carried out at 90% initial battery charge.

8.2.5 Description of Transmissions Modeled

- 1) 1-speed, or fixed ratio

Final drive ratio:	5:1
Transmission ratio:	1:1
Efficiency:	94%
- 2) 2-speed transmission

Final drive ratio:	5:1
Transmission ratios:	first - 2:1
	second - 1:1
Efficiency:	93%
Shift point motor speed:	4500 rpm
- 3) 4-speed transmission

Final drive ratio:	5:1
Transmission ratios:	first - 4.07:1
	second - 2.34:1
	third - 1.48:1
	fourth - 1.00:1
Efficiency:	92%
Shift point motor speed:	3350 rpm
- 4) Infinitely variable transmission

Final drive ratio:	5:1
Transmission ratios:	Max. - 5:1
	Min. - 1:1
Efficiency:	92%
Shift point motor speed:	3050 rpm

8.2.6 Results of Transmission Modeling

Figure 27 shows the test bed range variations for the transmissions while driving J227a schedule "D". Clearly the 4-speed and infinitely variable show an advantage over the 1 and 2-speed transmissions. This advantage is a 12% range increase over the 1-speed and a 6% increase over the 2-speed.

Figure 28 demonstrates again that the 2, 4, and infinitely variable transmissions perform similarly. Calculated acceleration times to 88 km/hr are within one second of each other while the 1-speed transmission is 18% slower than any of the others.

Range at steady speed is effected by transmission type at low cruising speeds. Figure 29 shows the difference in range between the four types. The overlap regions of the 2-speed and 4-speed curves can be attributed to the different gear ratios changing at various motor speeds. The plot shows there is little difference between the transmission types, but the 2-speed appears to be the best choice at low speeds. It should be noted that at speeds above 50 kph the different range curves become nearly indistinguishable.

Figure 30 illustrates the advantages offered by multiple speed transmissions in test bed gradeability. The 1-speed is clearly inadequate in this category. The 2-speed falls somewhat short of the 4-speed and infinitely variable transmission in maximum gradeability, but is more than adequate for commuter driving cycle use.

In the above mentioned criteria for transmission selection, the 2-speed, 4-speed, and infinitely variable speed are all acceptable. The 1-speed falls short in all areas and is not a good choice for the test bed. Since the final choice in transmissions must be based on not only performance but reliability, package size, and weight, the custom design 2-speed involute tooth form transmission is considered the optimum overall choice for use in the test bed.

The 4-speed transmission is a second choice due to its increased size and additional complexity. The infinitely variable belt drive or traction drive offer good potential but at this time the reliability of such units is not known.

Figure 27

RANGE UNDER J227a SCHEDULE "D"
FOR VARIOUS TRANSMISSION TYPES

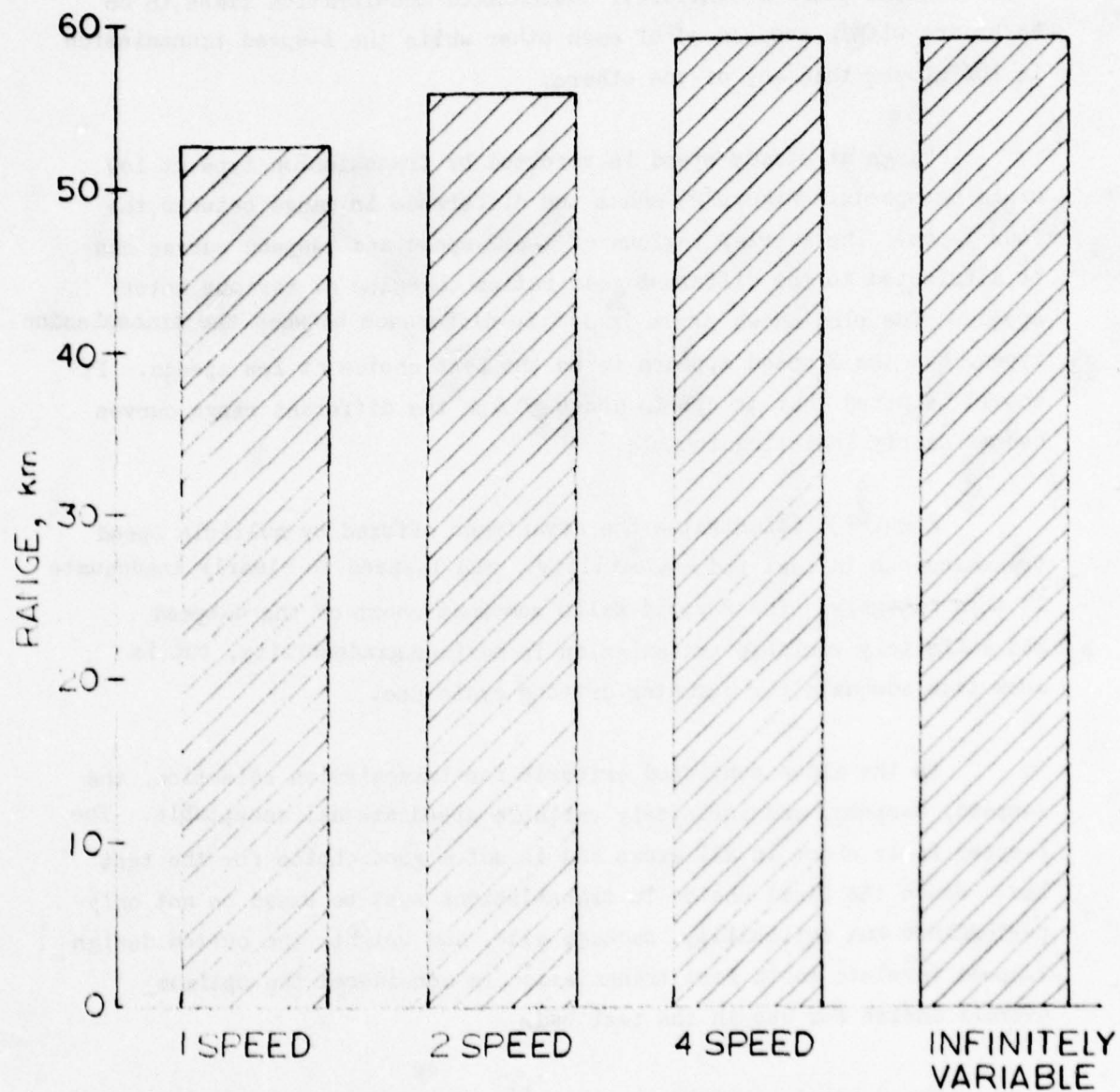


Figure 28

ACCELERATION TIME FROM 0 TO 88 kph
FOR VARIOUS TRANSMISSION TYPES

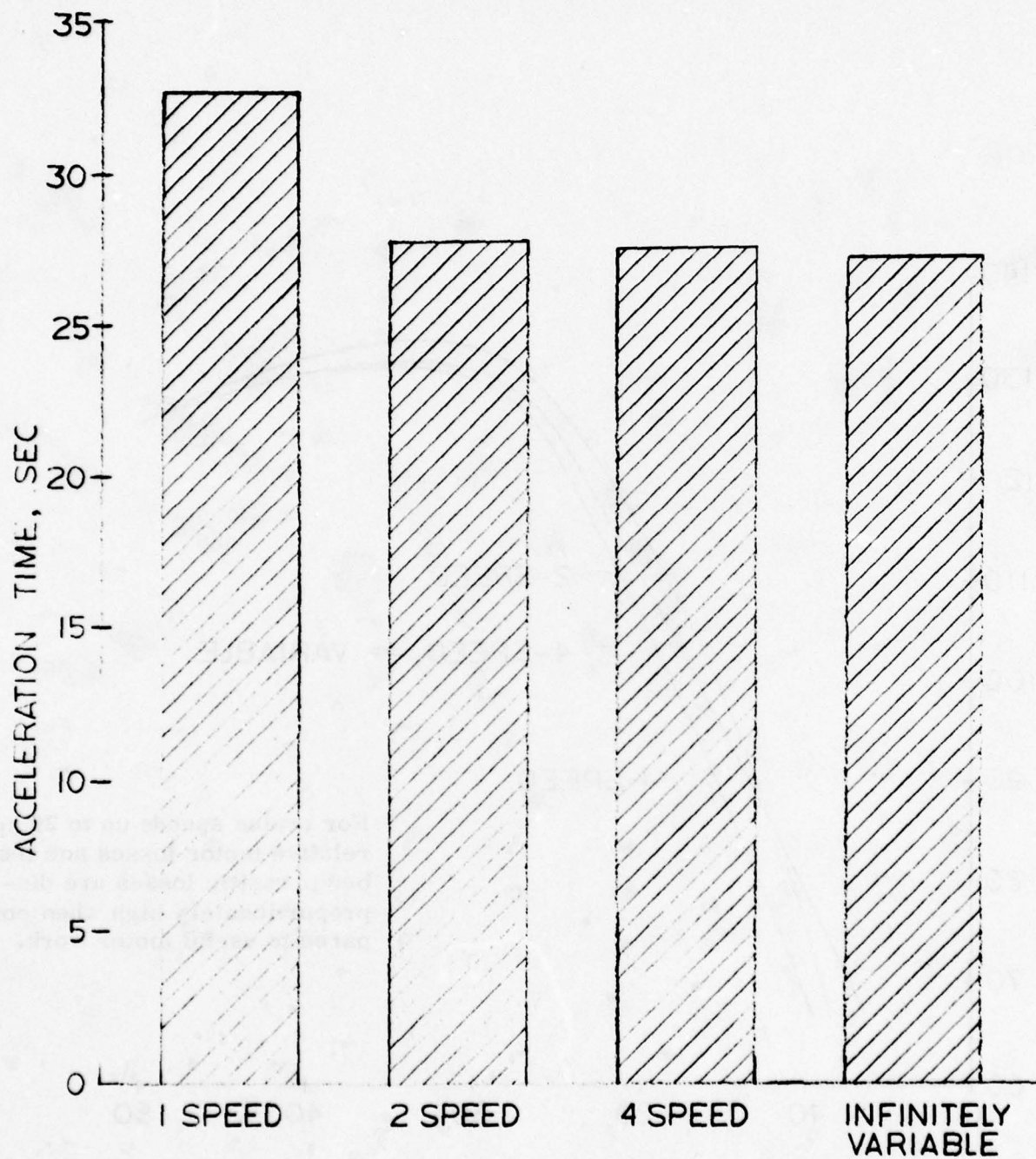


Figure 29
CRUISING RANGE VERSUS SPEED

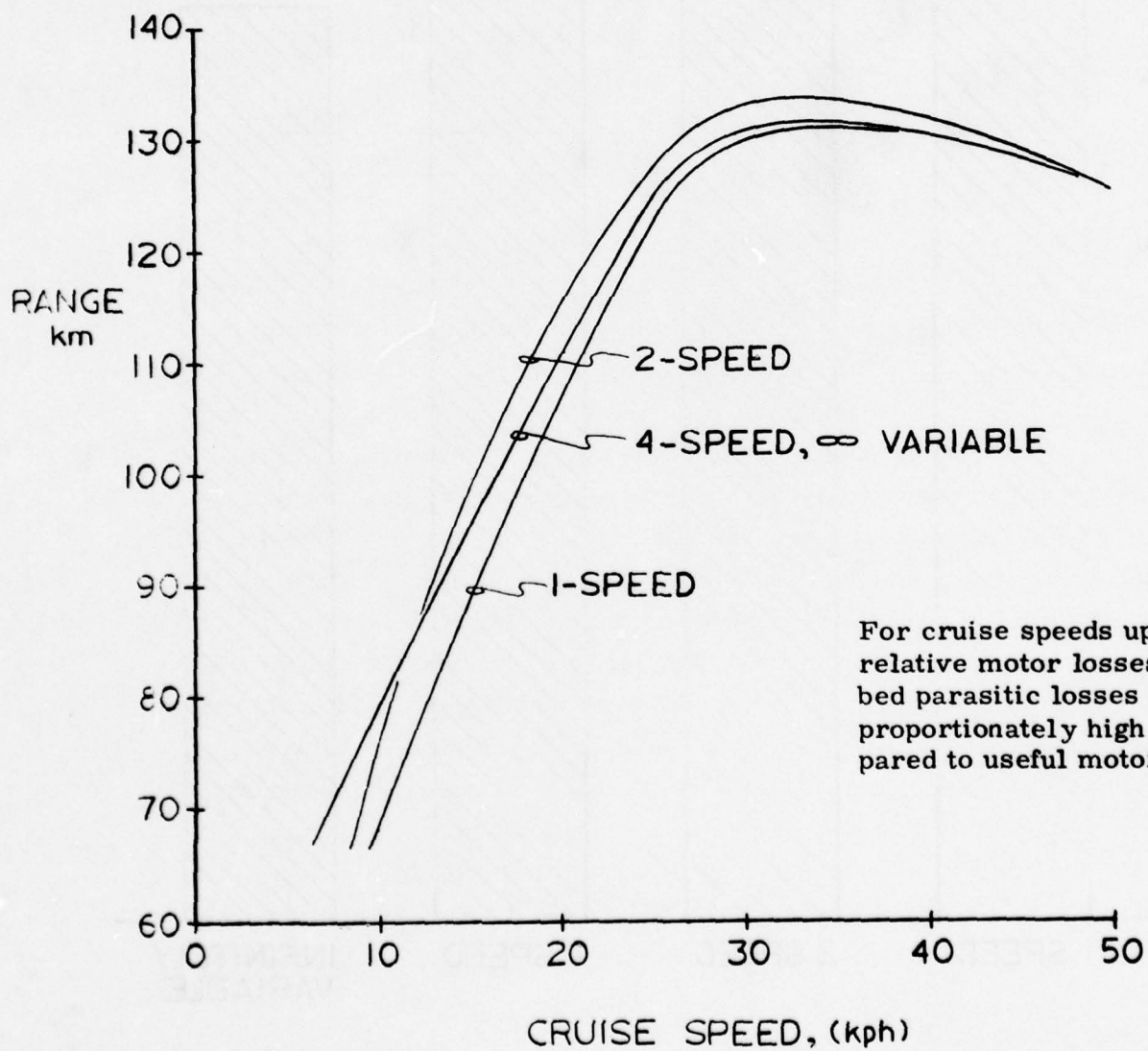
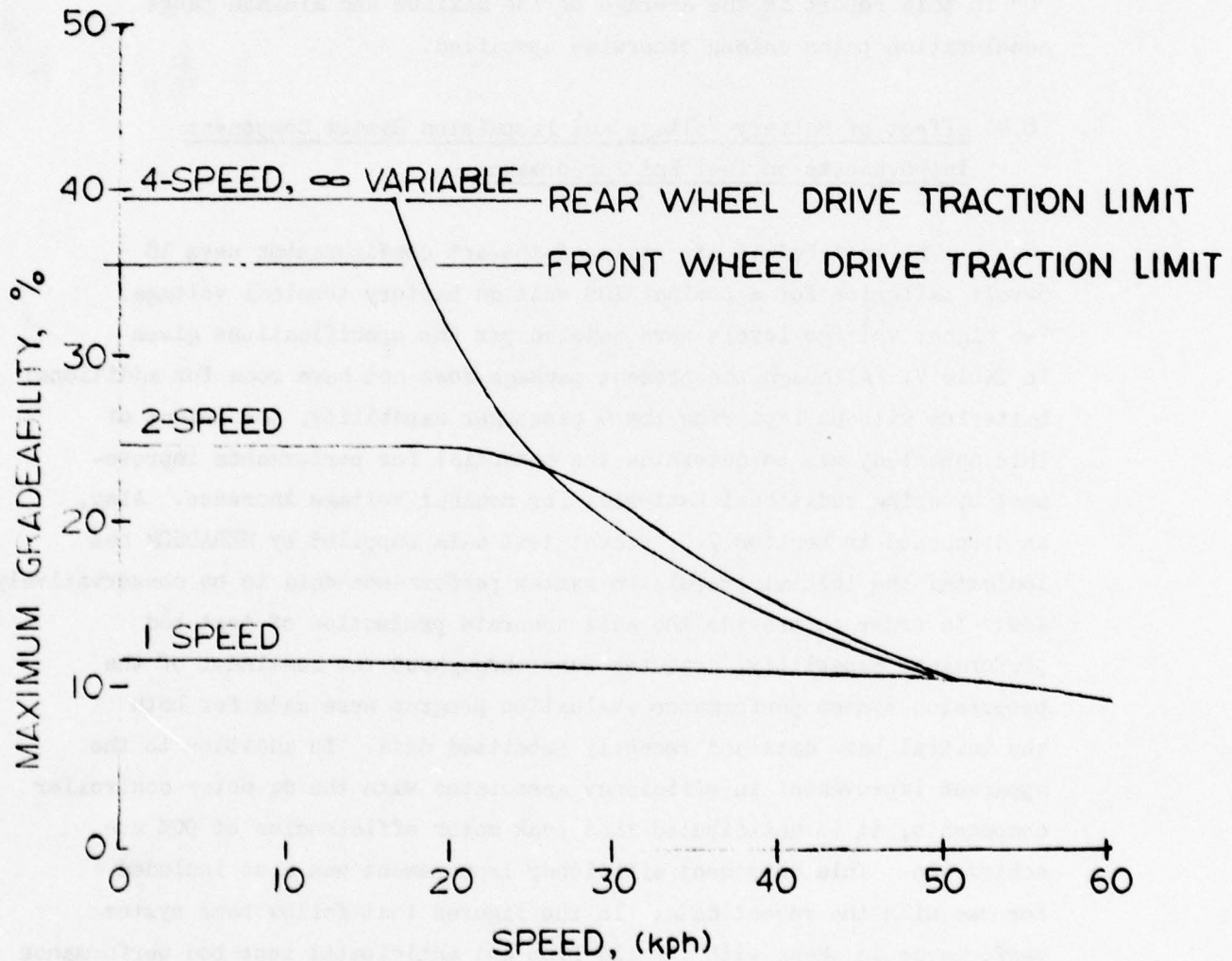


Figure 30

MAXIMUM GRADEABILITY VERSUS SPEED



8.3 Effect of Acceleration Path on Driving Cycle Range

For the 2-speed test bed described, the range under J227a schedule "D" varied as much as 7% with different acceleration paths. Figure 31 shows the two extreme cases; path "A" producing the maximum range and path "B" resulting in the minimum. The net effect of acceleration path on range is shown by Figure 32.

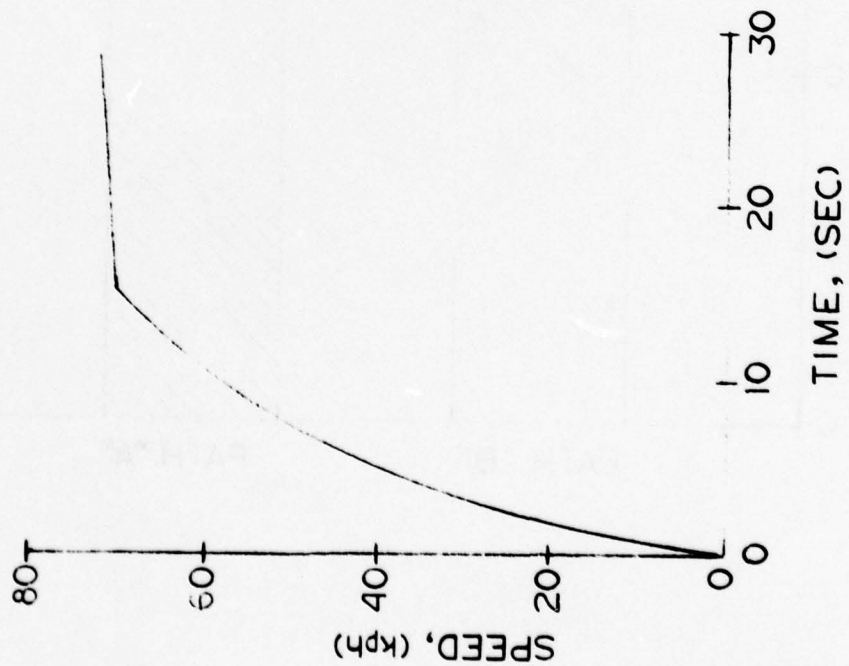
It should be noted that the acceleration paths illustrated by Figure 31 would be virtually impossible to duplicate in the test bed. The purpose here was to show extent of range variation possible as a result of choice of acceleration path. Stated test bed range under schedule "D" in this report is the average of the maximum and minimum range acceleration paths unless otherwise specified.

8.4 Effect of Battery Voltage and Propulsion System Component Improvements on Test Bed Performance

The test bed in its state-of-the-art configuration uses 18 6-volt batteries for a nominal 108 volt dc battery terminal voltage. Two higher voltage levels were modeled per the specifications given in Table V. Although the present package does not have room for additional batteries without impairing the 4 passenger capability, the intent of this sub-study was to determine the potential for performance improvement by using additional batteries for nominal voltage increase. Also, as discussed in section 7.0, recent test data supplied by MERADCOM has indicated the initial propulsion system performance data to be conservatively low. In order to provide the most accurate projection of test bed performance capability, computer runs throughout the remainder of the propulsion system performance evaluation program were made for both the initial base data and recently submitted data. In addition to the apparent improvement in efficiency associated with the dc motor controller components, it is anticipated that peak motor efficiencies of 90% are achievable. This component efficiency improvement was also included for use with the recent data. In the figures that follow base system performance is shown with a solid line and anticipated test bed performance

Figure 31

ACCELERATION PATH "A"



ACCELERATION PATH "B"

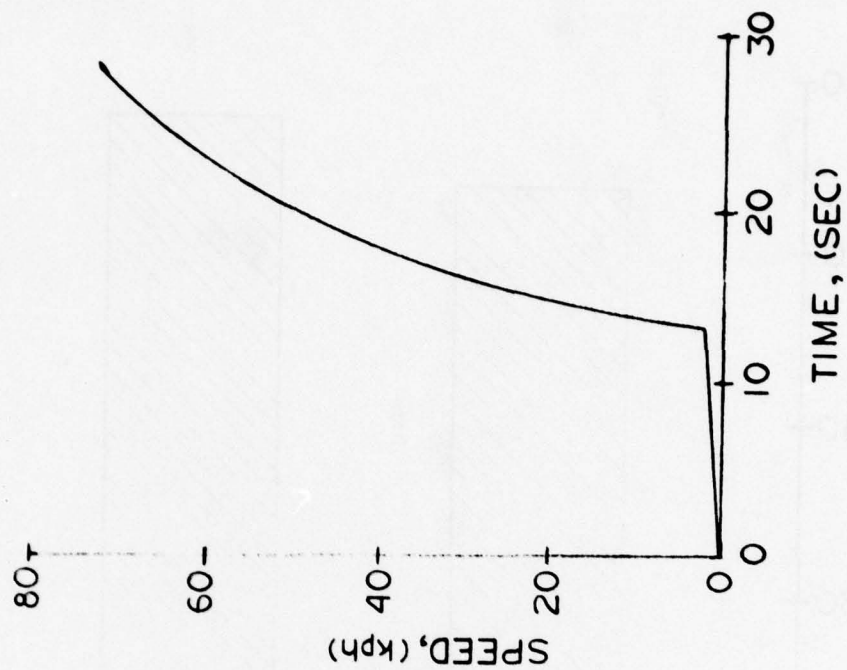


Figure 32
SCHEDULE "D" RANGE
VERSUS
ACCELERATION PATH

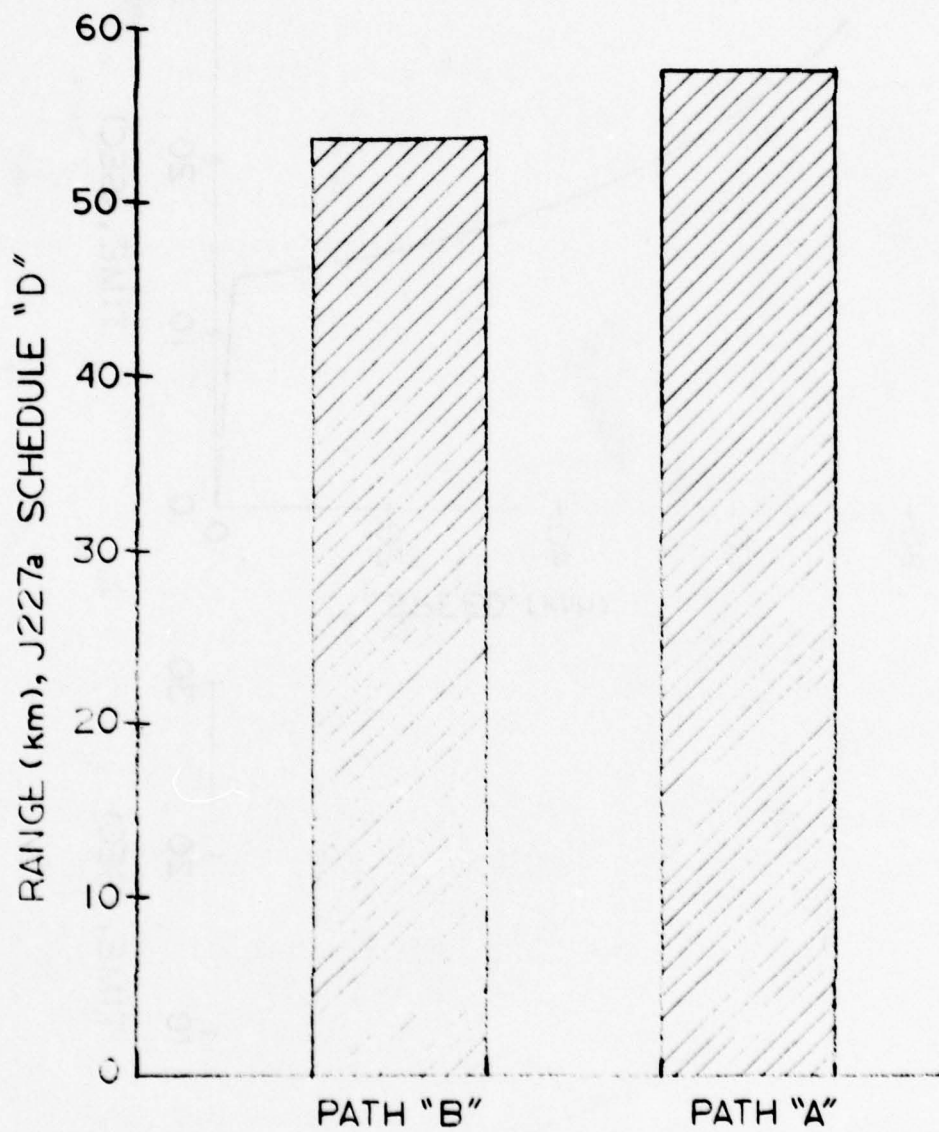


TABLE V
TEST BED SPECIFICATIONS
WITH ADDITIONAL BATTERIES

	108V	120V*	132V*
Number of Batteries	18	20	22
Amp-hr Rating (5 hr)	180	180	180
Test Bed Weight (Kg)	1245	1301	1357

* Other specifications are the same as described in section 1.3. A 2-speed transmission is used.

levels indicated by the recent MERADCOM data and expected motor efficiency improvement is shown with broken lines.

Figure 33 shows the increase in schedule "D" range with additional voltage. The 120 volt battery system offers a 6% range increase over the 108 volt system and the 132 volt offers a 13% increase. Figure 34 shows similar increases in cruise range with greater voltages. At 88 km/hr cruise speed, the range is up 11% for the 120 volt system and 24% for the 132 volt system. Acceleration times are decreased as voltage increases and is shown in Figure 35.

By increasing the number of batteries from 18 to 22, the present test bed range and acceleration performance can be substantially increased. While the use of the 108 volt system has provided a base for test bed drive train performance evaluation and optimization, it appears reasonable from a performance standpoint to increase the battery voltage to 132 volts.

8.5 Effectiveness of Regenerative Braking

Figure 36 shows the calculated effects of regenerative braking on test bed range for J227a schedules "C" and "D". The test bed in these cases is the 2-speed configuration previously described. Note that the test bed benefits more from regenerative braking when driving schedule "C" than schedule "D". The calculated increase in range is 11.4% for schedule "C" and only 5.9% for schedule "D". This can be attributed to the shorter distance of the "C" cycle; thus the test bed completes more cycles and has correspondingly more recuperative opportunities.

8.6 Performance of Advanced Test Bed

The configuration for an advanced test bed using lead-acid batteries is described in Table VI, along with the proposed state-of-the-art test bed. The specifications are identical in all areas except: total weight, weight distribution, center of gravity height, and aerodynamic drag coefficient. It is felt that these are the prime areas that could be improved with a special design test bed.

Figure 33

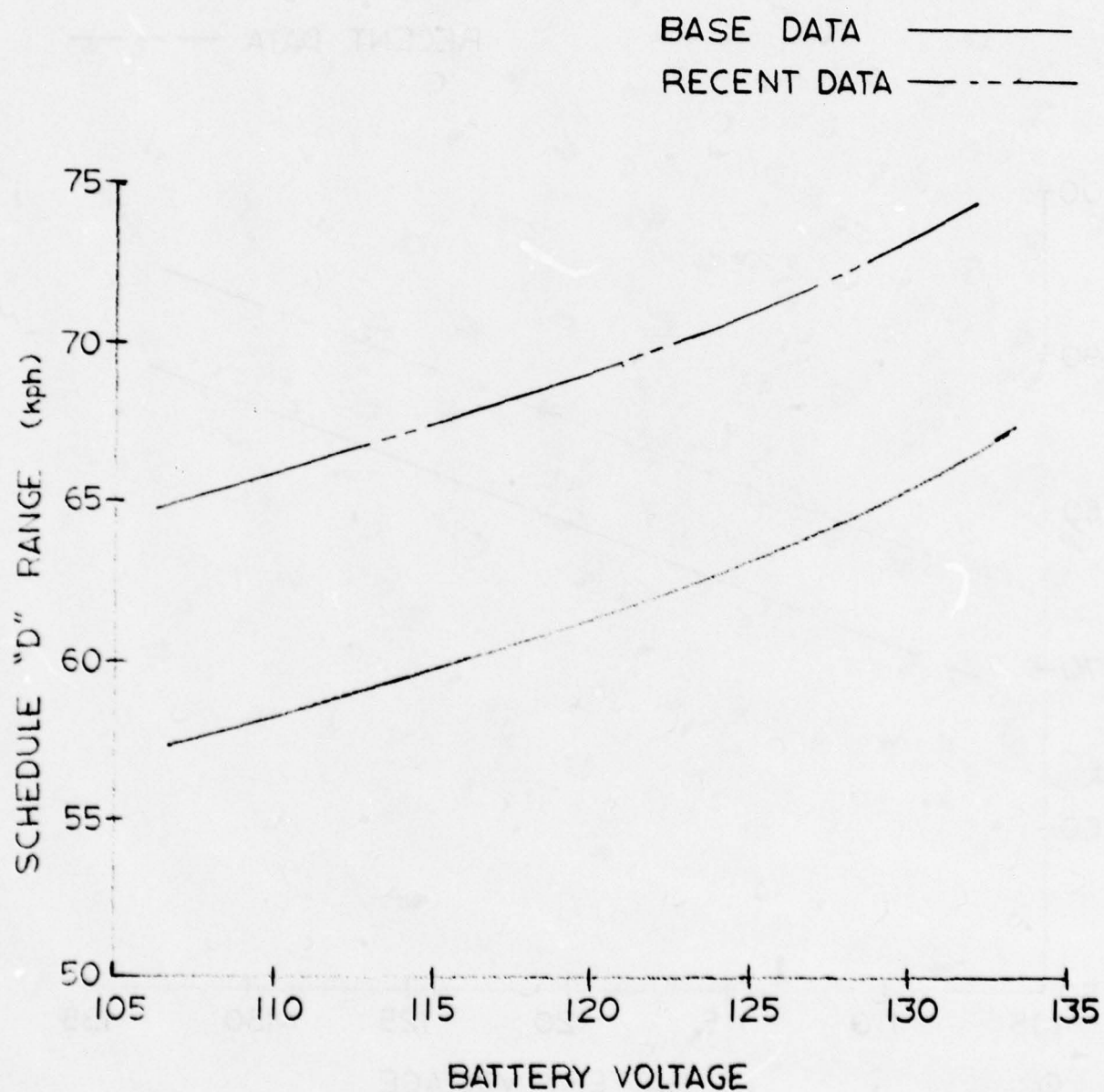
SCHEDULE "D" RANGE VERSUS
TEST BED BATTERY VOLTAGE

Figure 34
RANGE AT CONSTANT 88 kph
VERSUS
TEST BED BATTERY VOLTAGE

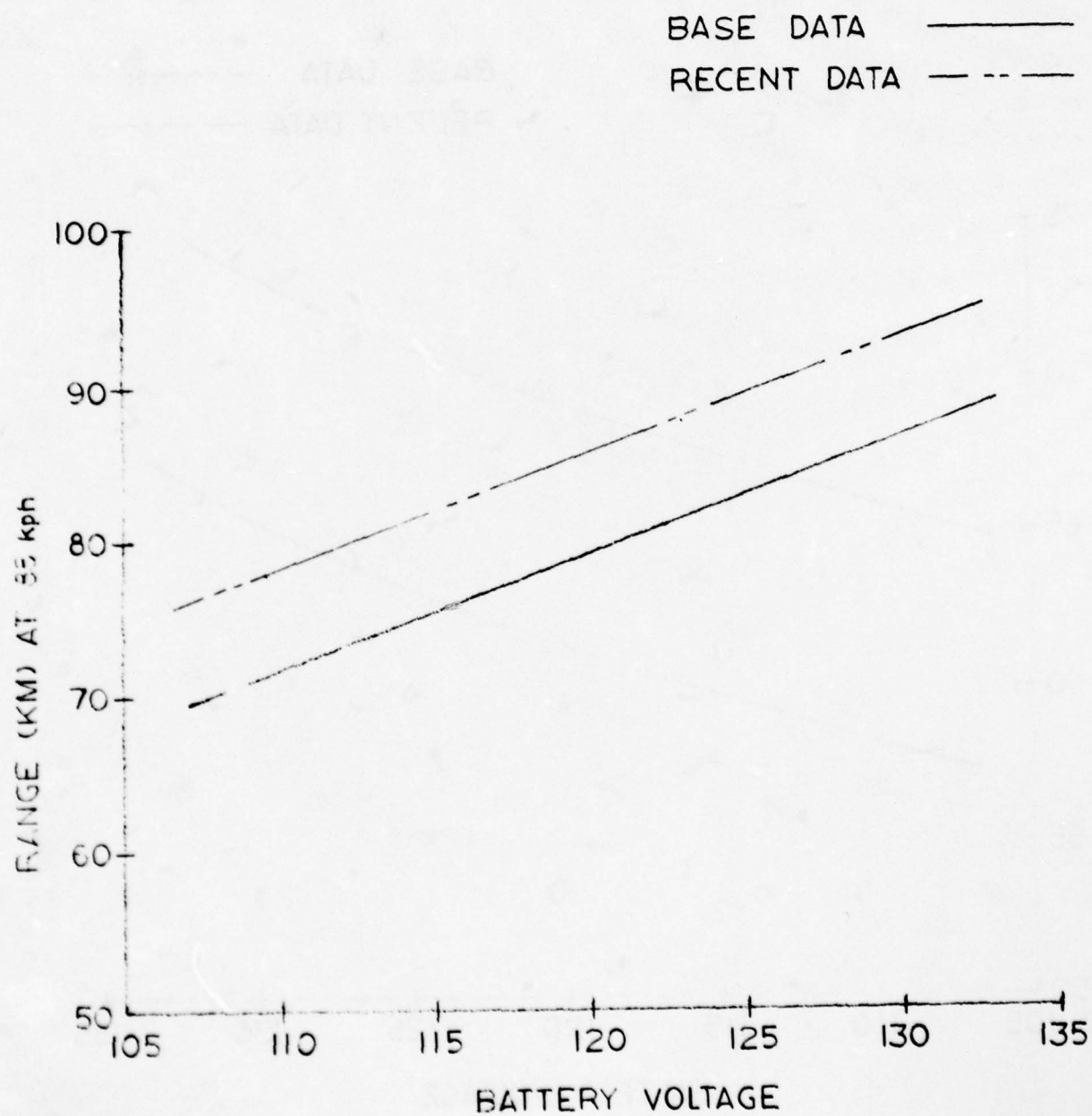


Figure 35

TEST BED ACCELERATION TIME
VERSUS BATTERY VOLTAGE

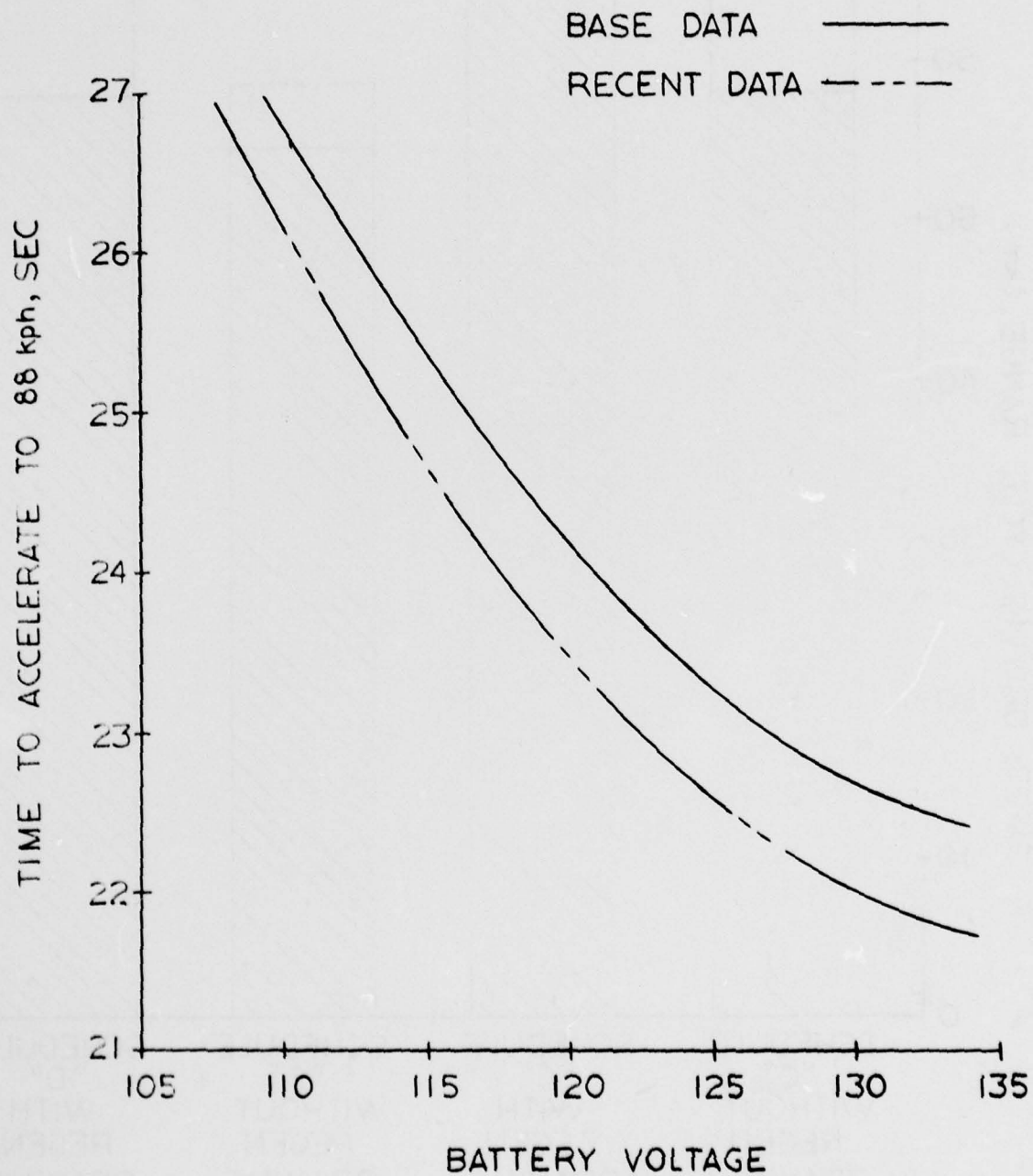


Figure 36

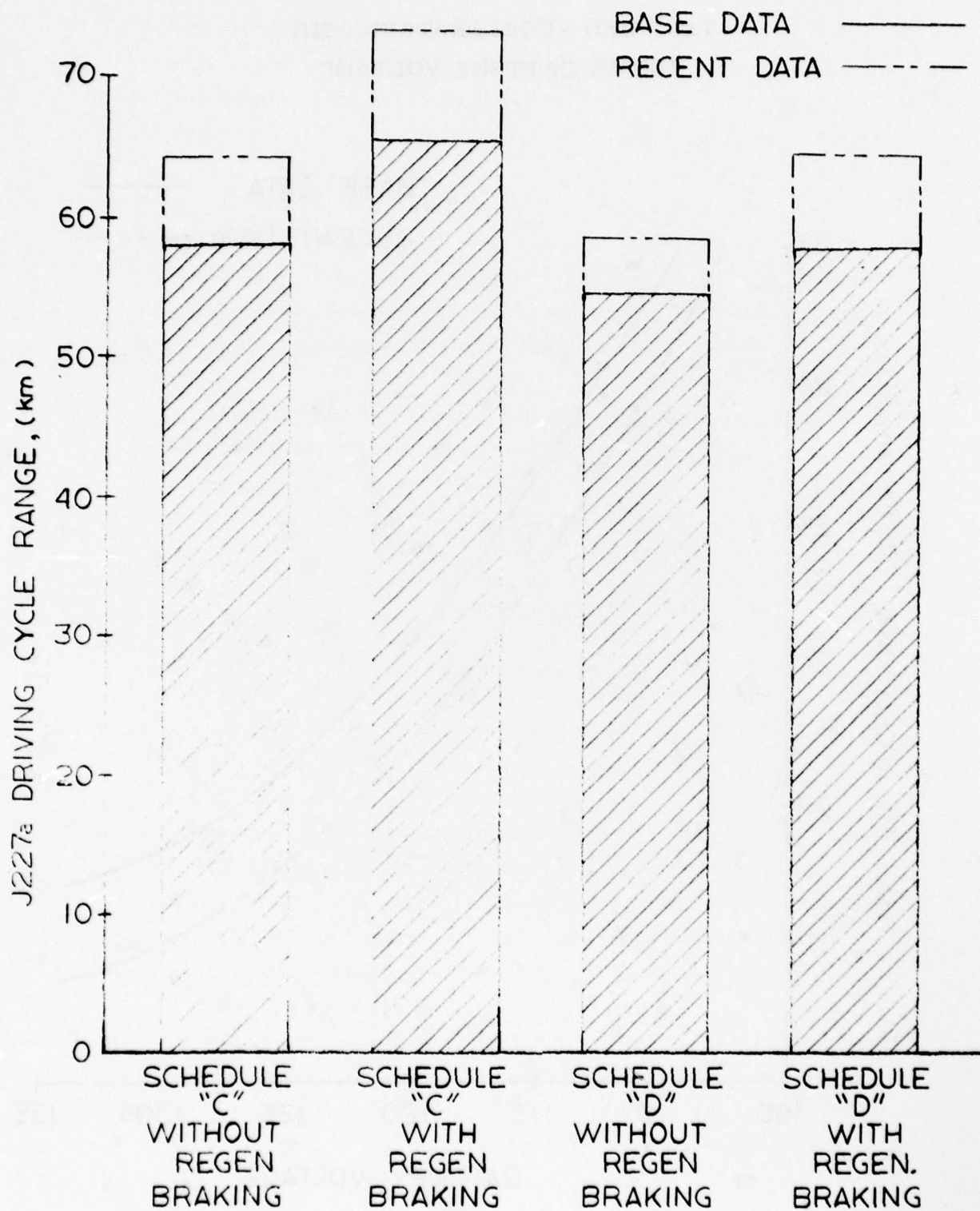
EFFECTS OF REGENERATIVE BRAKING ON DRIVING
CYCLE RANGE FOR SCHEDULES "C" AND "D"

TABLE VI
COMPARATIVE PROJECTED TEST BED SPECIFICATIONS

Specifications	State-of-the-Art Test Bed	Projected Test Bed
Motor and drive wheel location	Rear	Rear
Total weight (kg)	1245	1032
Percent of weight on front wheels	56	50
Center of gravity height (cm)	56	50
Wheelbase (cm)	228.6	228.6
Rolling radius of tires (cm)	28	28
Moment of inertia of wheels ($N\cdot m^2$)	4.16	4.16
Moment of inertia of motors ($N\cdot m^2$)	.502	.502
Battery amp-hour capacity 5-hr discharge	180	180
Number of Batteries	18	18
Operating voltage	108	108
Frontal area (m^2)	1.67	1.67
Aerodynamic drag coefficient	.42	.36
Final drive ratio	5.0:1	5.0:1
Transmission type	2-speed	2-speed
Motor shift speed (rpm)	4500	4500

Weight reduction offers the largest benefit in range and performance. This can be achieved by extensive use of light-weight materials - aluminum alloys and high strength plastics - both of which current technology offers. By the use of a central "tunnel" for battery placement, the space efficiency and weight could be improved. The central tunnel concept offers other benefits - a lower center of gravity and more even weight distribution - both important to handling characteristics.

It should be noted that weight reduction increases the battery energy to test bed weight ratios, as does the approach taken in section 8.4, which was to increase the number of batteries while maintaining the heavier test bed. In terms of design effectiveness, weight reduction is the preferred method of increasing range and performance.

Aerodynamic drag losses become significant at cruising speeds; approximately 58% of the motor power is used in overcoming the air resistance at 88 km/hr. The frontal area of the test bed is 1.67 m^2 , which is quite low, and it is felt that little improvement is possible in a 4-passenger vehicle. The drag coefficient is a respectable .42, but with a special design body it is possible to lower this value to approximately .36.

Figures 37 through 40 show the increased performance potential of the advanced configuration test bed. The reductions in weight and drag coefficient offer a significant improvement in all areas of performance.

Upon completion of the electric test bed performance computer simulation, several key conclusions have been reached:

- 1) A 2-speed solenoid shifted, involute tooth form transmission is best suited to the state-of-the-art test bed.
- 2) Range on schedule "D" driving cycle can vary as much as 7%, depending on acceleration paths.
- 3) Regenerative braking increases range on schedule "D" by 5.9%. Schedule C range is enhanced by 11.4%.
- 4) Increasing the number of batteries to 132 volt dc nominal terminal voltage improves all performance parameters proportionately greater than the increase in battery voltage.

Figure 37

ACCELERATION TIME TO 88 kph FOR STATE-OF-
THE-ART AND PROJECTED ELECTRIC TEST BED

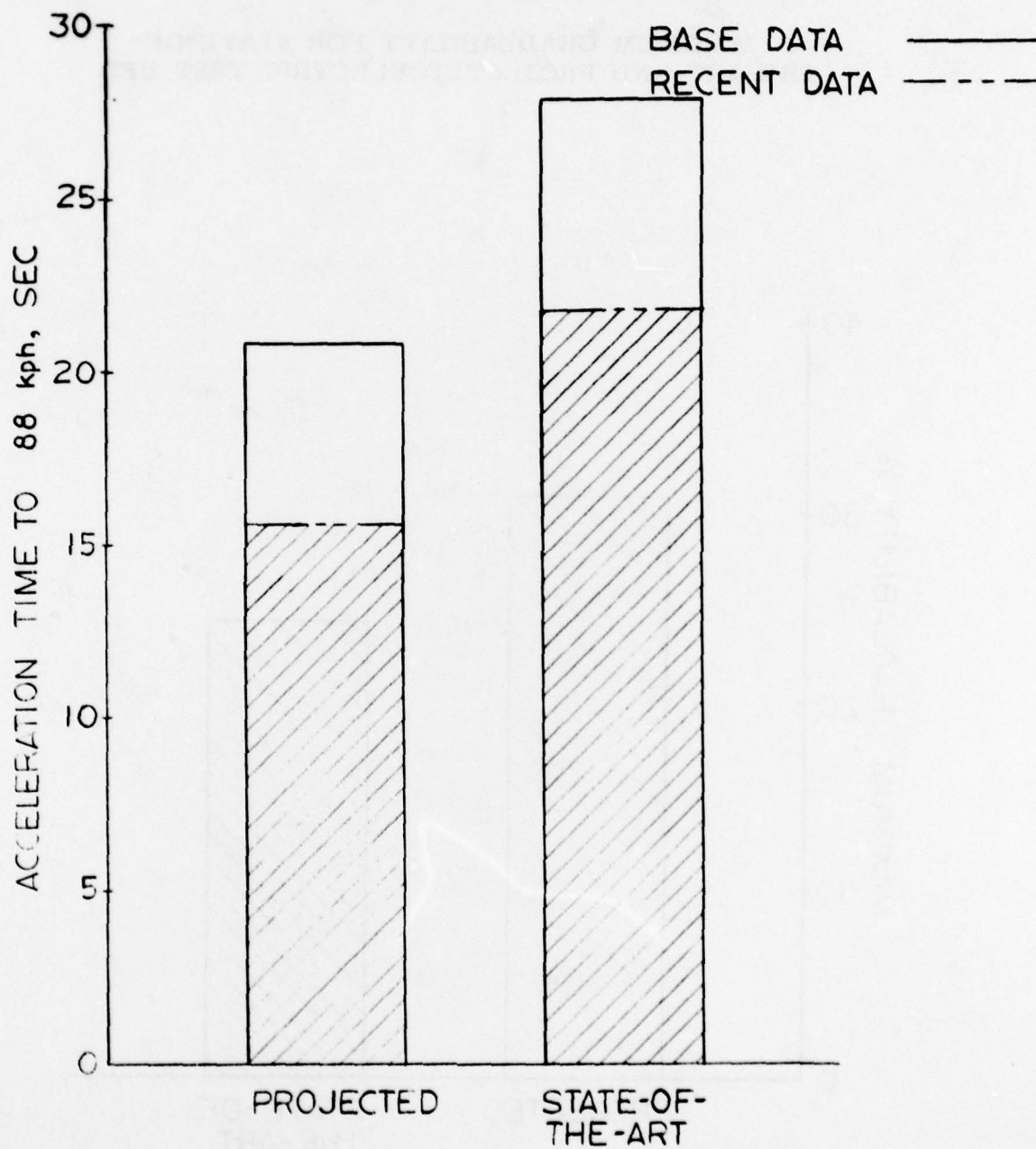


Figure 38

MAXIMUM GRADEABILITY FOR STATE-OF-
THE-ART AND PROJECTED ELECTRIC TEST BED

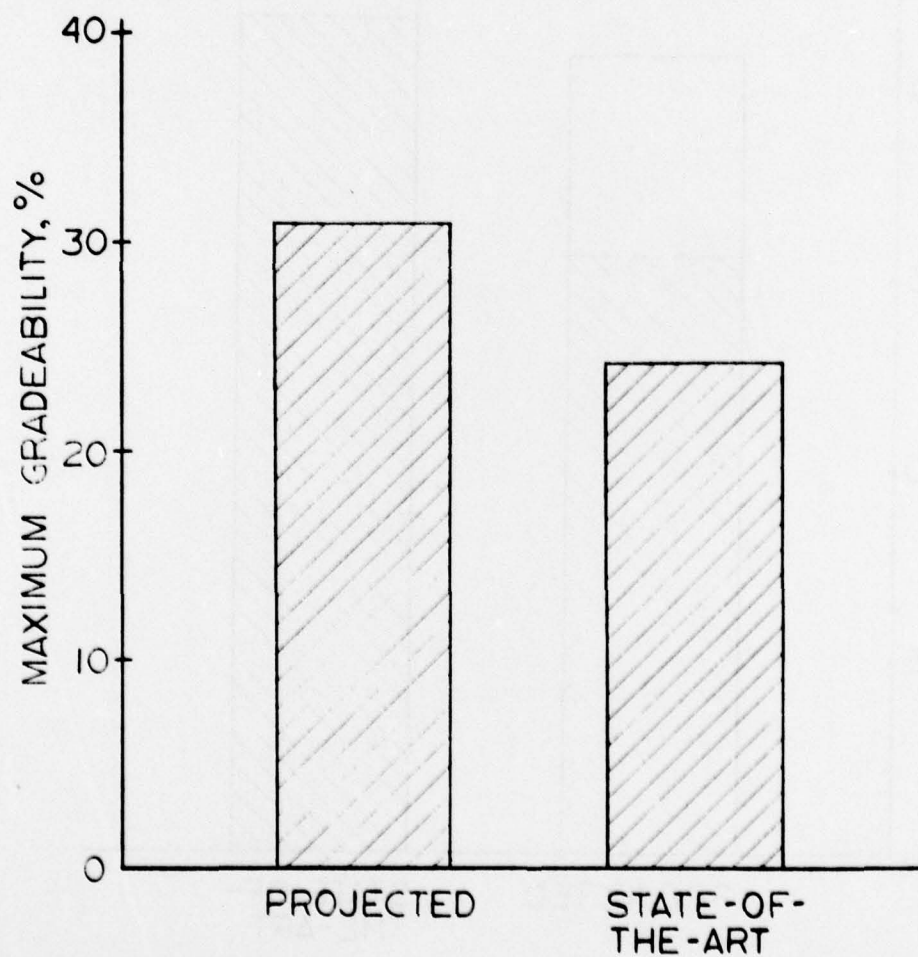


Figure 39

RANGE UNDER J227a SCHEDULE "D" FOR
STATE-OF-THE-ART AND PROJECTED ELECTRIC TEST BED

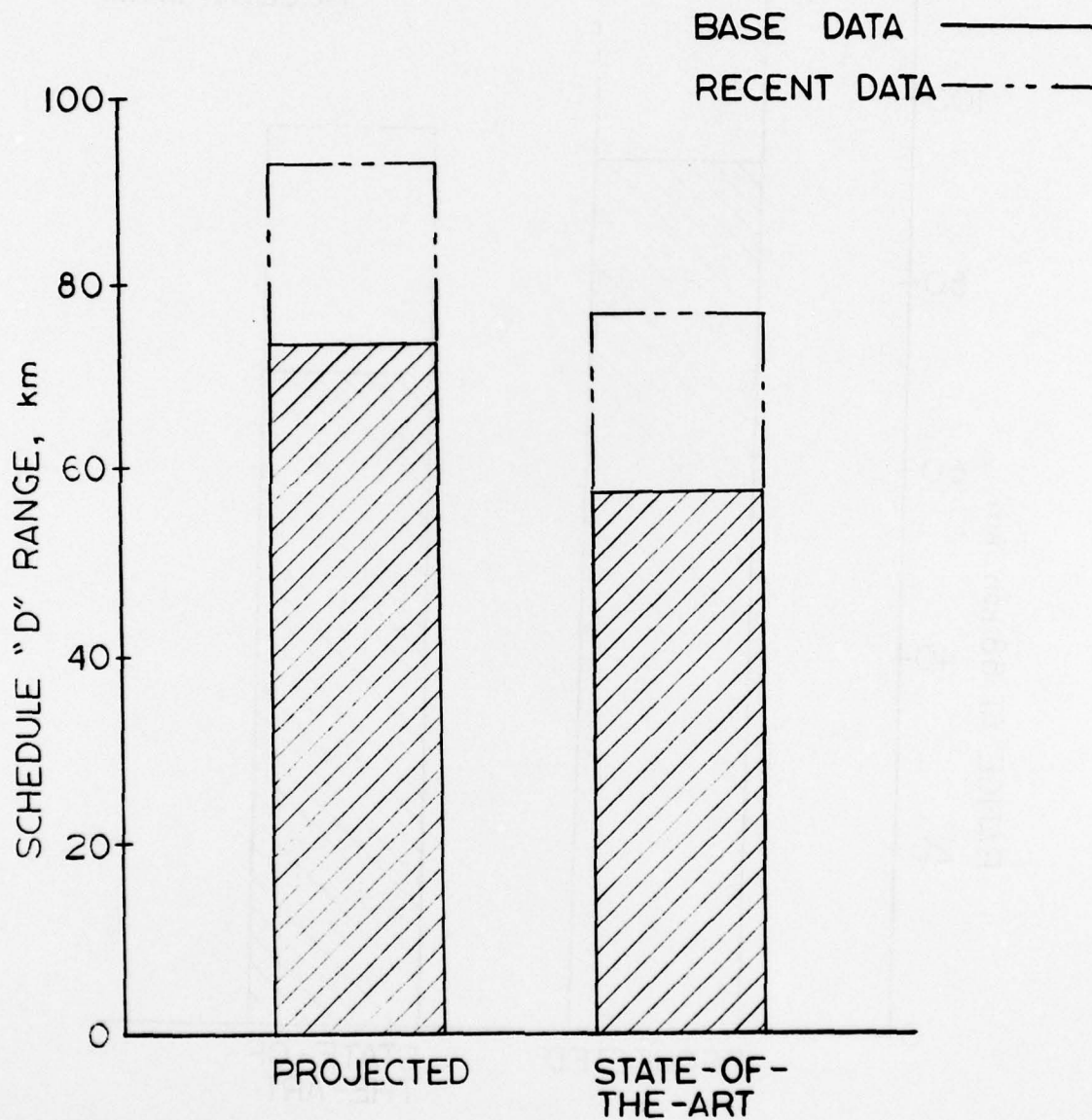
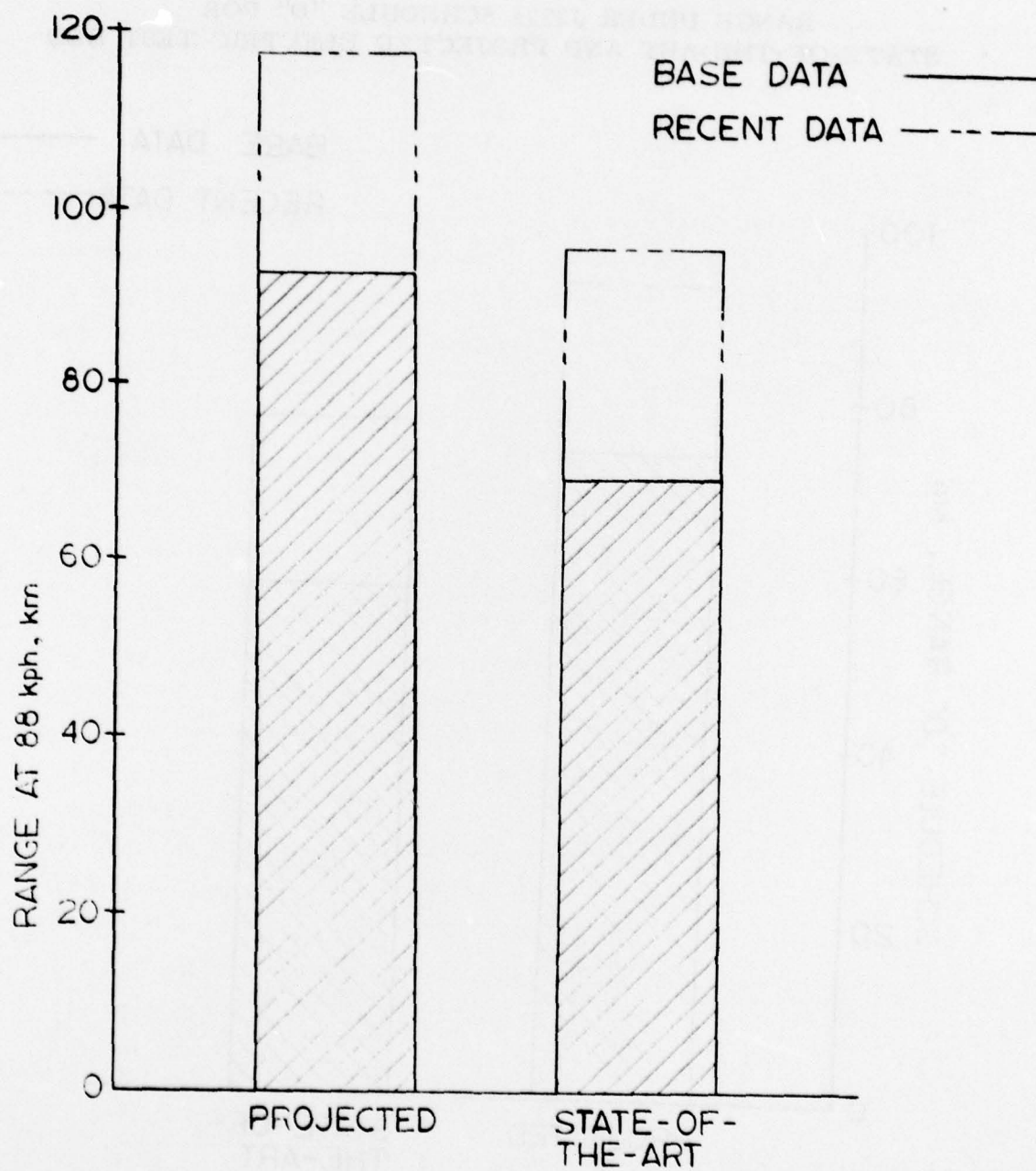


Figure 40

RANGE AT 88 kph FOR STATE-OF-
THE-ART AND PROJECTED ELECTRIC TEST BED



- 5) An advanced configuration test bed using lead-acid batteries offers substantial performance improvements and up to 30% more range under schedule "D" than the state-of-the-art test bed.

9.0 TEST BED MECHANICAL CONFIGURATION

The test bed will utilize only state-of-the-art mechanical components. High capacity drum brakes will be used in conjunction with a regenerative braking system. Proportionality of the dual braking system will be established through the microprocessor. Drum brakes are preferred to disc brakes since parasitic losses are reduced with drum brakes and a self-energizing design will alleviate the need for the vacuum boost pump system needed to reduce the high brake pedal effort characteristic of disc brakes.

The suspension system will consist of a de Dion type drive axle arrangement for maximum camber control and lateral stability while the non-driving wheels will be carried by an independent coil or torsion spring and trailing link arrangement. Both front and rear battery tray assemblies will be carried by the respective suspension support members rather than the body structure. This design rationale will result in a light-weight body structure which will tend to minimize test bed curb weight. Occupant safety will be maximized by retention of energy absorbing bumpers, side intrusion guard beams, et cetera. The rear wheel drive configuration is once again preferred due to the available frontal volume for energy absorbing materials. Safety interlocks will also be provided to prevent access to any electrical components while the test bed is in the "power on" mode.

It is anticipated that routine service would be at an absolute minimum since only the batteries would have to be checked for proper level at periodic intervals. Sealed grease cup suspension joints and long life synthetic lubricants in the transmission would virtually eliminate the need for "grease jobs" and "oil changes". The need for battery fluid level check would be indicated on the instrument panel. Two fluid reservoirs, one in front and one in the rear, will automatically

provide the batteries with the correct cell fluid level for periods of up to several months. "Topping off" will consist only of refilling the conveniently located reservoir. The same reservoir fill system will be used to sense battery "out-gassing" during the recharge mode for optimum control of charge rate and charge cycle termination. The battery recharge methodology is discussed extensively elsewhere (11).

10.0 TEST BED INSTRUMENTATION AND ACCESSORIES

The state-of-the-art test bed configuration will initially utilize commercially available instrumentation. This includes, as a minimum, a solid state battery charge level indicator along with a series of system status lights such as those depicted in Figure 41. A cable driven speedometer and directional turn signal indicators should also be provided. Power for accessories in the state-of-the-art test bed should be obtained from a 500 watt dc chopper voltage converter. The voltage converter will provide power to the test bed lighting system, windshield wiper, heater/defroster blower motors and propulsion motor cooling blowers.

As the MERADCOM microprocessor power requirements become better understood, accessory power including the 12 volt dc power supply will be obtained from the propulsion system batteries thru a 500 watt dc switched converter circuit. It has also been confirmed by MERADCOM that the microprocessor can be used to provide the test bed operator with time of day, trip distance, and elapsed trip time information when requested on an LED display that would otherwise display test bed speed, as shown in Figure 42. Additionally, a first generation program has been developed which reads the instantaneous battery charge on a meter and corrects the apparent battery charge level for ambient temperature change, battery history and other variables. This will provide the test bed operator with a more correct assessment of available energy from the battery.

11.0 CONCLUSIONS

As a result of the test bed/MERADCOM dc propulsion system optimization process, two configurations appear to be reasonable choices from a

p. 154

Figure 41
CONVENTIONAL INSTRUMENT PANEL

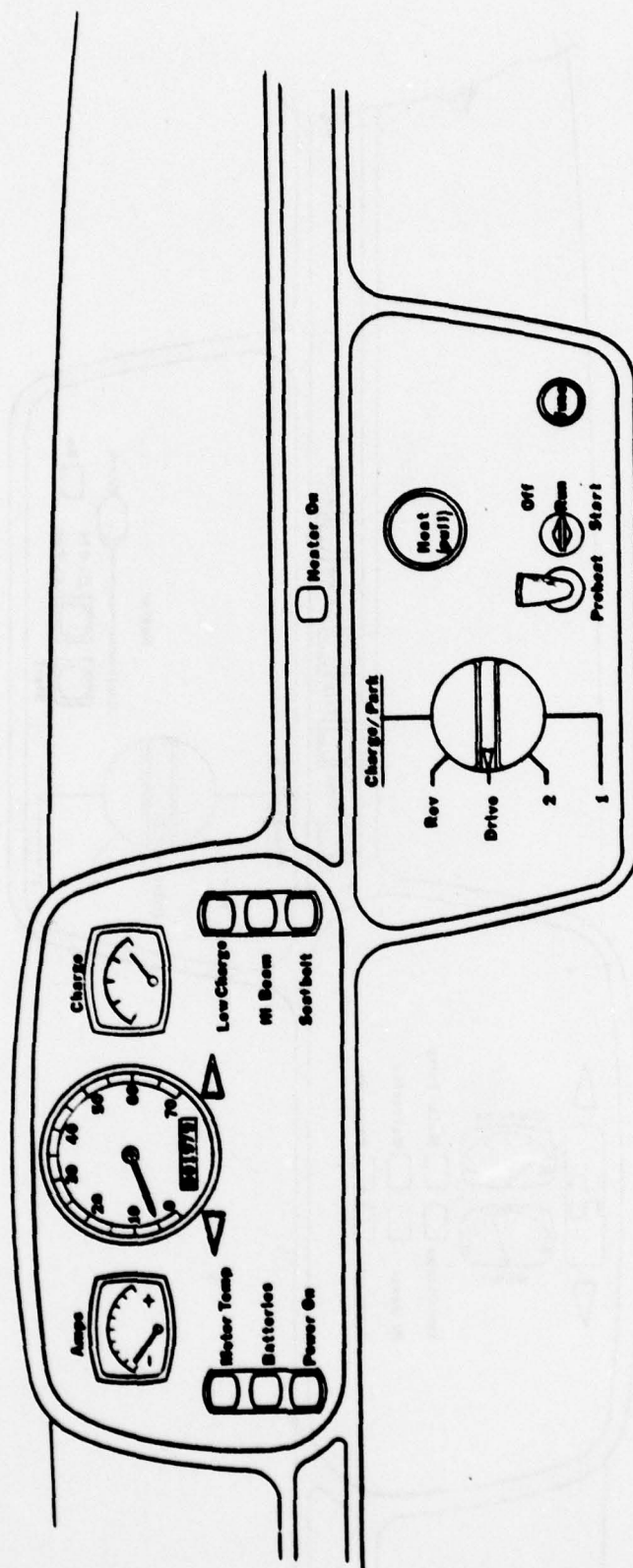
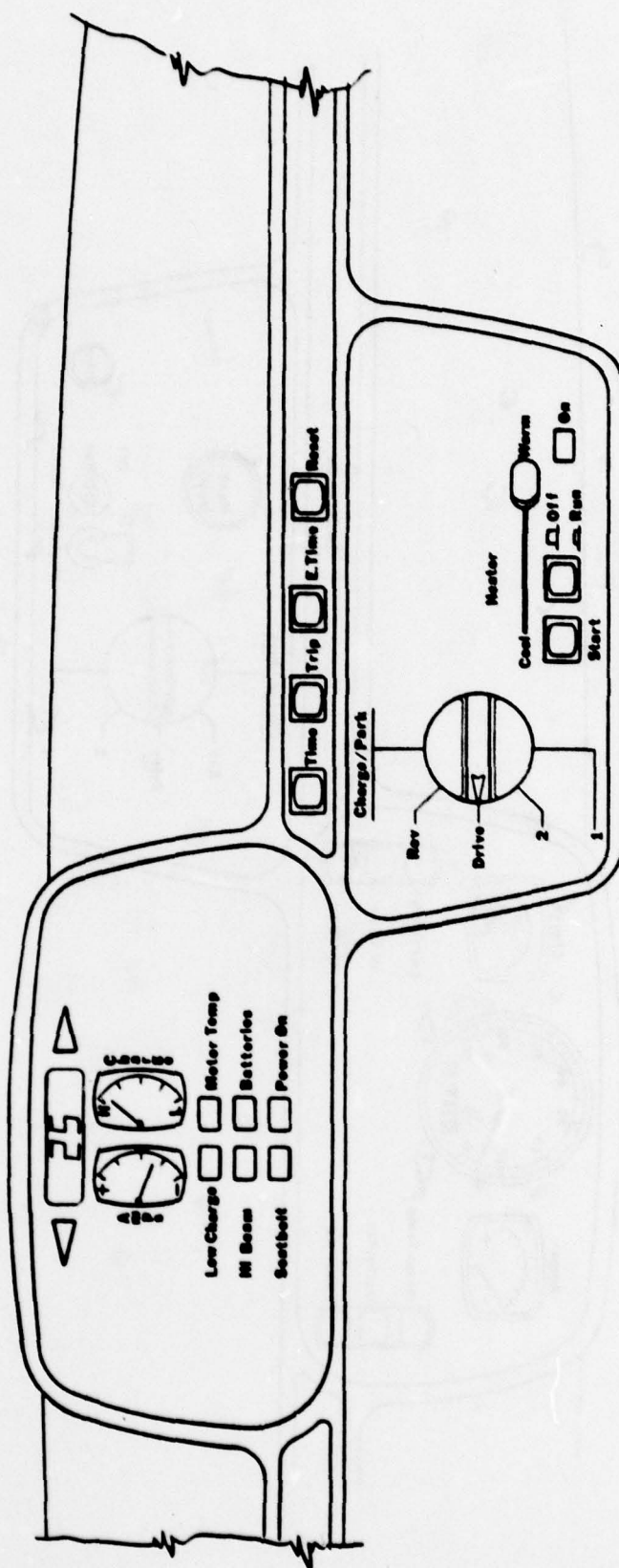


Figure 42
MICROCOMPUTER/LED INSTRUMENT PANEL



→ performance standpoint. The fundamental differences in the two test beds lie in the placement of the driver axle and electric propulsion system components. The rear wheel drive configuration is considered the optimum primarily due to a slight performance advantage. Highlights of both configurations are listed below.

- . Two speed involute tooth form electro-mechanically shifted transmission, 10:1 primary drive ratio and 5:1 final drive ratio;
- . High capacity drum brakes with regenerative brake coupling;
- . de Dion drive axle suspension with independent coil or torsion spring suspension on non-drive wheels (battery trays integral with suspension support frame);
- . Radial construction tires;
- . Four occupant interior capacity; ✓
- . 229-239 centimeter wheel base;
- . Virtually no requirement for routine maintenance;
- . Conventional occupant safety equipment retained;
- . Performance capability exceeds the requirements of the SAE J227a schedule "D" driving cycle with either 108 volt dc or 132 volt dc electric propulsion systems. ↙

The design optimization process was conducted in such a manner so as to produce the best possible mechanical component configuration for the MERADCOM dc propulsion system in a state-of-the-art test bed. As industry provides improved batteries, tires, and lighter weight and more aerodynamic body forms, the range and performance of "next generation" test beds utilizing the optimized dc propulsion system drive train can be expected to improve proportionately.

LIST OF REFERENCES

- 1 U.S. Department of Transportation/Federal Highway Administration, Nationwide Personal Transportation Study - Automobile Occupancy, Report No. 1, April, 1972.
- 2 Taborack, Jaroslav J., Mechanics of Vehicles, Machine Design.
- 3 Division of Transportation Energy Conservation, Determination of the Effectiveness and Feasibility of Regenerative Braking Systems on Electric and Other Automobiles, Volume II, Design Study and Final Report, UCRL/W52306-02, February, 1978.
- 4 Department of Energy Electric and Hybrid Vehicle, EHV/Quarterly Report, DOE/CS-0026/2, Volume 2, No. 2, May, 1978.
- 5 Kamada, K., I. Okazaki, T. Takagki, New Lead-Acid Batteries for Electric Vehicles and Approach to their Evaluation Method, Japan Storage Battery Co., Ltd., Kyoto, Japan.
- 6 Reimers, Eberhart, The IHTS: A New Building Block For Power Conditioners, IEEE 1972 PFESC Record, pp 89-95.
- 7 Reimers, Eberhart, Design Analysis of Multiphase DC Chopper Motor Drive, IEEE Transactions on Industry Applications, Vol. 1A-8, No. 2, March/April 1972, pp 136-144.
- 8 Reimers, Eberhart, Application of Two Phase DC Chopper Motor Drive, IEEE 1972 IAS Conference Record, pp 803-811. Transactions on Industry Applications May/June 1973, pp 803-811.
- 9 Reimers, Eberhart, "The Integrated Power Switch", co-author P.P. Balthasar, IEEE Transactions on Industry Applications, Vol. 1A-12, No. 2, March/April 1976.
- 10 J. Willihnganz, C & D Batteries Charging Lead-Acid Storage Batteries Electro Chemical Society, Cleveland, 1971 meeting.
- 11 Battery Methodology Recharge Report Under Preparation by MERADCOM Project Officer, Eberhart Reimers.

Distribution List

<u>ADDRESSEE</u>	<u>NUMBER</u>
<u>Department of Defense</u>	
Technical Library DDR & E The Pentagon, Room 3E1039 Washington, DC 20301	1
Director, Technical Information Defense Advanced Research Projects Agency 1400 Wilson Boulevard Arlington, VA 22209	1
Defense Documentation Center Cameron Station Alexandria, Virginia 22314	12
<u>Department of the Army</u>	
Dr. Charles H. Church Chief, Advanced Concepts Team USADCSRDA, DANA-ARZ The Pentagon, Room 3E-361 Washington, DC 20301	1
Director, Tank Automotive Science Laboratory ATTN: Colonel Herbert H. Dobbs USATARAACOM, DRDTA-RGT Warren, MI 48090	2
<u>Department of Energy</u>	
Mr. Edward Beyma Transportation Energy Conservation Division Department of Energy 20 Massachusetts Avenue, NW Washington, DC 20545	5
<u>USAFERAACOM</u>	
Commander ATTN: Special Assistant for R & D USAFERAACOM, DRDRL-ZK Fort Belvoir, VA 22060	1

USAMERADCOM (Continued)NUMBER

Commander:
ATTN: Special Assistant for Materiel Assessment
USAMERADCOM, DRDME-ZC
Fort Belvoir, VA 22060

1

Commander
ATTN: Office of Patent Counsel
USAMERADCOM, DRDME-L
Fort Belvoir, VA 22060

1

Commander
Electrotechnology Laboratory
USAMERADCOM, DRDME-E
Fort Belvoir, VA 22060

1

Commander
ATTN: Electrical Equipment Division
USAMERADCOM, DRDME-EA
Fort Belvoir, VA 22060

12

Commander
ATTN: Technical Library
USAMERADCOM, DRDME-WC
Fort Belvoir, VA 22060

2